Università degli Studi di Ferrara

DOTTORATO DI RICERCA IN
FARMACOLOGIA E ONCOLOGIA MOLECOLARE

CICLO XXVII

COORDINATORE Prof. Antonio Cuneo

Altered motor phenotype and dopamine transmission associated with mutations of the parkinsonian gene LRRK2

Settore Scientifico Disciplinare BIO/14

Dottorando
Dott. Longo Francesco

Tutore
Prof. Morari Michele

Anni 2012/2014

SUMMARY

INTRODUCTION

LRRK2: a protein implicated in Parkinson's Disease

Protein organization

The leucine-rich repeat kinase 2 (LRRK2, PARK8) gene on chromosome 12 contains 51 exons and encodes a large multifunctional and multidomain protein containing 2527 amino acids. LRRK2 is a ubiquitous, mainly cytosolic, protein with a molecular weight of approximately 285 kDa, predominantly existing in a dimeric conformation *in vivo* with different points of interaction through each individual monomer (Greggio et al., 2008). According to sequence analysis, LRRK2 shows a central catalytic domain with GTPase and kinase activities. However, the N-terminal portion presents protein-protein interaction domains such as the armadillo (residues 180-660), ankyrin (residues 690-860) and the namesake leucine-rich repeats (LRRs; residues 985-1274) domains, whereas the C-terminal terminus hosts the structural repeat motif WD40 (residues 2142-2498; Fig.1).

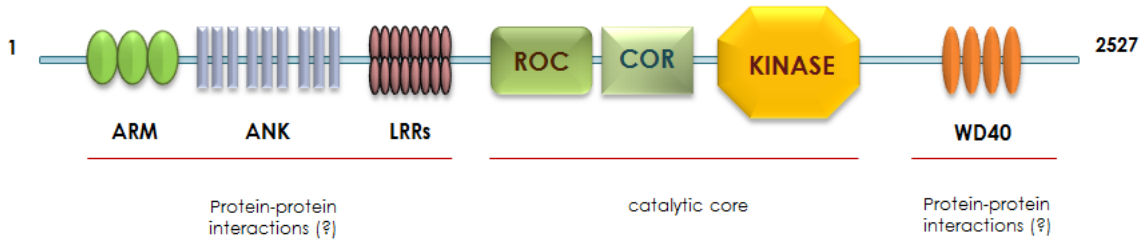

Fig. 1. Schematic representation of LRRK2 protein linear structure.

Catalytic domains. LRRK2 encodes two different enzymatic activities: kinase and GTPase. The central region of the protein includes the Ras of complex protein (ROC) GTPase protein domain with the adjacent C-terminal of Roc domain (COR) in conjunction with a kinase domain. Considering LRRK2 in the context of evolutionarily related protein kinases, LRRK2 originates from a different source and bears a quite different sequence from the origin (Marin, 2006; 2008). LRRK2 belongs to the TKL subfamily of human protein kinases (Manning et al., 2002), whose members show sequence similarity to both serine/threonine and tyrosine kinases. According to sequence similarity, its kinase domain shares homology with mixed-lineage kinases (MLKs) which are members of the mitogen activated protein kinase (MAPK) family (Jameel et al., 2009) However, more recent data indicate that the LRRK2 kinase domain mostly resembles the receptor-interacting protein kinase (RIPK) family (West et al., 2005), that plays a crucial role in cellular stress. The

presence of ROC and COR domains makes LRRK2 a member of a superfamily of proteins, named ROCO, that includes at least three other human proteins: LRRK1, DAPK1 and MASL1 (Marin, 2008). The human proteins LRRK2 and LRRK1 belong to a subgroup of ROCO proteins that always have an N-terminal LRR and a C-terminal kinase domain in addition to the ROC-COR tandem. This pair of domains is conserved throughout evolution, suggesting their functional interdependence. According to the model of the homologous domain in prokaryote *C. tepidum*, the COR domain (residues 1524-1837) is composed of nine α-helices and six β-sheets that are linked by a loop exposed to the solvent (Gotthardt et al., 2008). Interestingly, the prediction for human COR differs from the *C. tepidum* primarily in its C-terminal half, an area responsible for dimerization, thus suggesting that in human LRRK2, dimerization occurrs through its ROC domain. Indeed, the monomeric structure of the ROC domain (residues 1335-1515) comprises five α-helices and six β-sheets that are linked by loops, and the dimer form is stabilized through hydrogen bindings and hydrophobic interactions. The surface of the dimer presents only one functional ligand-binding unit, showing unique nucleotide and Mg^{2+} binding sites with contributions from both monomers (Deng et al., 2008). In vitro studies have shown that LRRK2 can bind GTP through the GTPase domain via a phosphate-binding motif (P-loop) region, and that it can hydrolyze GTP involving a catalytic Switch II motif that is critical for GTPase activity. A high-resolution kinase domain model, recently obtained from the homolog ROCO4, has been proposed as a platform for understanding the human LRRK2 kinase domain (residues 1183-2134) that is formed by seven α-helices and six β-sheets linked by loops, which are exposed to the solvent (Gilsbach et al., 2012). LRRK2 represents an unusual protein in which two distinct enzymatic domains within a single polypeptide chain interacts to regulate activity. In particular, the kinase activity is stimulated upon GTP binding to ROC, and it is reasonable to suppose that ROC regulates kinase activity by changing its conformations (active/inactive). Thus, a loss of GTP binding or an increased turnover of GTP to GDP should result in lowered kinase activity (Deng et al., 2008). Moreover, several studies demonstrated that LRRK2 self-regulation is a mechanism for controlling its kinase activity, which is mediated, in part, by its GTPase domain and homodimerization. Similar to MAPKKKs, which are regulated by small GTPases, LRRK2 kinase activity might be regulated by its own GTPase domain in an intrinsic manner (Lee et al., 2012a).

Repeat domains. Various investigators have identified four domains composed of structural repeat motifs likely to be involved in regulation and localization of LRRK2. The presence of these particular domains occurring in 14% of all prokaryotic and eukariotic

proteins (Marcotte et al., 1999), suggests that LRRK2, in addition to its predicted protein kinase and GTPase activities, acts as a scaffold in different multiprotein signaling complex pathways. Although the presence of the armadillo repeats (ARM) domain in the N-terminus of the protein has been questioned, recent studies concluded that LRRK2 contains ARM-like repeats domain. This domain is formed by 21 α-helices grouped to form supercoil, and are linked by loops to form a curved structure (Cardona et al., 2014; Marin, 2008). The following domain, in order from N- to C-terminus, is the ankyrin repeats (ANK) domain, found in diverse bacterial and eukaryotic proteins. It is compared to cytoskeletal erythrocyte ankyrin characterized by two antiparallel α-helices followed by a loop to form a gently curved structure. According to the various models proposed by different groups, the LRRs domain is located N-terminal to the ROC domain and is composed of 14 repeats. The first 13 repeats share the LRR consensus sequence found in LRR proteins interacting with Ras, whereas the 14th repeat deviates from this consensus. These 14 repeats are grouped into two modules and each LRR subunit contributes to form a curved β-sheets linked by a large loop (Cardona et al., 2014).

Located at the C-terminal end of the protein, the predicted WD40 domain of LRRK2 comprises seven repeats formed by 30 β-sheets linked by loops to form a circular bladed propeller-like structure (Cardona et al., 2014). Although WD40 has been identified in many proteins with different functions as well as proteins involved in the cytoskeletal assembly, vesicle formation and trafficking, or in proteins with enzymatic activity, the structure of this domain is well conserved and represents the most common repeat domain found in the human protein. Different studies also demonstrated that WD40 is crucial for LRRK2 physiological and pathological activities, playing an important role in the synaptic vesicular network of LRRK2 (Piccoli et al., 2011).

Dimerization and autophosphorylation

Studies using ROCO proteins from lower organisms indicate that LRRK2 predominantly exists in a dimeric conformation, and dimerization occurs in the ROC-COR bi-domain (Deng et al., 2008; Greggio et al., 2008), even though different other points of interaction through each individual monomer have been found. In particular, when the ROC domain was used as a bait in a yeast two-hybrid system, it bound to the N-terminus of LRRK2, the C-terminus of the LRR domain, the N-terminus of the ROC domain, and the C-terminus of the WD40 domain (Greggio et al., 2008). Interestingly, the deletion of the ROC domain is not sufficient to prevent dimerization, suggesting additional interaction regions within

LRRK2. Since a N-terminal deletion of the ANK and LRR domains does not reduce dimerization, whereas a WD40 truncated-LRRK2 could not dimerize, ROC and WD40 domains seems to be critical for LRRK2 dimerization. Dimer formation is a common phenomenon among protein kinases and can help to mediate different auto-regulation and downstream signaling pathways. In addition, allosteric regulation is mediated by homodimerization in a number of serine-threonine kinases including mitogen-activated protein (MAP) kinases, p38, c-Jun N-terminal kinase (JNK), and their upstream kinases (Leung and Lassam, 2001; Ohren et al., 2004). Despite LRRK2 monomeric form is the predominant species in cells and might have kinase activity, experimental evidence suggests that LRRK2 exists and functions as a dimer with autophosphorylation of the full-lenght protein occurring as an intramolecular (*cis*) event (Berger et al., 2010; Greggio et al., 2008). It was demonstrated that the autophosphorylation sites such as Thr1410, Thr1491 and Thr1503 are located mainly within the ROC domain (Gloeckner et al., 2010; Greggio et al., 2009; Kamikawaji et al., 2009; Pungaliya et al., 2010) where GTPase activity of LRRK2 is localized. In this scenario, autophosphorylation could represent an intramolecular post-translational modification that regulates the GTPase activity suggesting that the kinase activity acts as an internal modulator of the ROC domain and consequently of signal transmission. Moreover GTPase activity may be also be regulated through the recruitment of other cellular proteins (Gotthardt et al., 2008).

Mutations

The complete open reading frame of LRRK2 codes for a 2527 amino acid protein and as for many other large genes, a number of known variants can be found along the coding sequence. To date, more than 100 amino acid substitutions have been reported in human LRRK2 (Rubio et al., 2012), many of which are not currently linked to any disease. Some polymorphisms have been related to different pathologies such as leprosy (Zhang et al., 2009) or cancer (Hassin-Baer et al., 2009) and, possibly, inflammatory bowel disease (Barrett et al., 2008), whereas others are linked to neurodegenerative disease or represent an important risk factor (Paisan-Ruiz et al., 2013; Paisan-Ruiz et al., 2008). In 2004, two independent groups (Paisan-Ruiz et al., 2004; Zimprich et al., 2004) showed, for the first time, that mutations of LRRK2 were linked to dominantly inherited Parkinson's disease (PD), corroborating a previous study which identified PARK8 as a new locus associated with PD within large Japanese family (Funayama et al., 2002). This initial discovery had a significant impact on the functional characterization of LRRK2, shedding light on disease-causing mutations in this protein, and on the genetics of PD (Fig. 2).

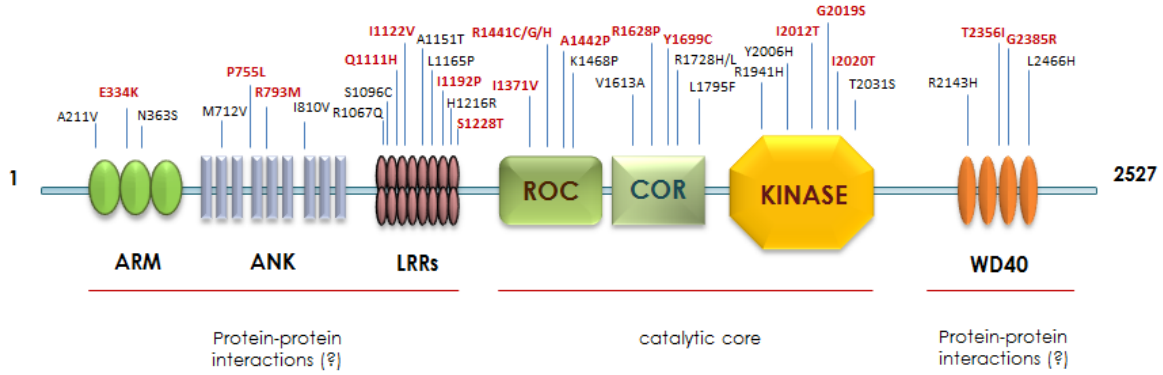

Fig. 2. Distribution of the PD-related substitutions in relation to the functional domains of LRRK2. The mutations described as pathogenic are in red.

Of note, six missense mutations that include the p.N1437H, p.R1441C/G/H, p.Y1699C, p.S1761R, p.G2019S, and p.I2020T substitutions, clearly segregate with disease and are clustered within the enzymatic core of the protein (Cookson, 2010; Mata et al., 2006). In particular, the substitution of a glycine with a serine in position 2019 (G2019S) is located in the activation loop of the kinase domain at the conserved Mg^{2+}-binding motif (Goldwurm et al., 2005) and represents the most common PD-related mutation. The G2019S substitution induces a stabilization of the enzyme in the active form leading to an increased kinase activity in vitro (Greggio et al., 2006; Jaleel et al., 2007; West et al., 2005) and in vivo (Sheng et al., 2012). This mutation facilitates substrates access without an enhancement of substrate affinity (West et al., 2005). The other pathogenic mutation located within the kinase domain is represented by I2020T but how it affects protein function is still debated. Some studies reported that this mutation results in an increased kinase activity (Gloeckner et al., 2006; Kamikawaji et al., 2013), even though such increase is less marked than that caused by G2019S, while other groups revealed an unchanged or a decreased function (Jaleel et al., 2007; Nichols et al., 2010). Furthermore, structure model analysis suggested that G2019S introduces a phosphorylation site (most mutations introduce a S or a T) or stabilizes an active form by hydrogen bonds, whereas the introduction of an extra hydrogen bond by I2020T could stabilize the inactive form of the kinase domain (Gilsbach et al., 2012). The second most common LRRK2 mutation, R1441C, together with two other variations of the same codon (R1441G and R1441H), has been found in the ROC/GTPase domain and is located at the interface of the ROC and COR domains (Lewis et al., 2007; Li et al., 2007). At the functional level, the R1441 mutations causes an increase of the affinity of LRRK2 for GTP which results in a reduced

GTPase activity, and, as a consequence, in a decrease in GTP hydrolysis (Liao et al., 2014). The ROC mutations lead to longer lasting activation of LRRK2 compared to the wild-type protein, due to the persistent GTP-bound form. However, the three mutations cause the loss of a positive charge (arginine) and affect the domain surface causing misfolding of ROC domain (Gotthardt et al., 2008). According to structure analysis, all three substitutions have an effect on protein stability, whereas only R1441C/G affects its function. In particular, the R1441H mutation induces an important effect on the tertiary structure of LRRK2 that impairs dimerization (Cardona et al., 2014). As for the R1441 mutation, also the substitution of tyrosine with cytosine at the 1699 residue located on the outer surface of the COR domain leads to a reduction in GTPase activity via alteration of the ROC and COR domains interaction (Daniels et al., 2011). Outside of the ROC/COR/Kinase enzymatic core of LRRK2, several groups have shown different amino acid variants, although most of them do not show any association with PD (Cardona et al., 2014). The identification of mutations within the WD40 and the LLR domains, together with the evidence that these domains are involved in protein-protein interactions, prompted several groups to analyze the role and the modifications occurring in these domains. At the C-terminus of the protein, the G2385R substitution lies on the surface of one of the propeller blades of the WD40 domain (Mata et al., 2006) and shows a clear genetic association with PD although its effects are controversial (Fung et al., 2006; Tan et al., 2007). Some reports showed that G2385R decreases kinase activity both in vitro and in vivo (Jaleel et al., 2007; Rudenko et al., 2012) whereas others did not find any significant difference compared to the wild-type protein (Nichols et al., 2010; West et al., 2007). However, it has recently been reported that the G2385R variant, which destabilizes LRRK2 structure, only has a mild impact on LRRK2 functional properties in the cell (Piccoli et al., 2011). On one hand, it increases the binding to Hsp90 (heat-shock protein of 90 kDa) which plays a role in maintaining LRRK2 stability (Rudenko et al., 2012). On the other hand, it decreases LRRK2 ability to bind 14-3-3 proteins, a family of conserved regulatory molecules expressed in all eukaryotic cells, able to bind a multitude of functionally diverse signaling proteins, including kinases, phosphatases, and transmembrane receptors (Fu et al., 2000). A number of variants have also been described at the N-terminus of the protein. Although three different variants are located within the ARM domain, only one of them (E334K), affecting the electrostatic surface and charging distribution in this domain, has been described as a likely PD-associated mutation (Cardona et al., 2014). Potentially pathogenic variants have been described into the ANK domain. In particular, the R793M mutation, exposed on the surface of the helix 2 of the

putative ankyrine repeat 4, alters the structural integrity and, consequently, the protein-protein interaction properties of LRRK2 (Mills et al., 2012). Inside the LLR repeats domain, four substitution (Q1111H, I1122V, I1192V and S1228T) are considered to be pathogenic. These amino acid substitutions, described by different groups, have been shown to alter the domain stability affecting the interaction with other proteins without altering protein function (Cardona et al., 2014).

Parkinson's Disease and LRRK2-associated phenotype: the clinical scenario

Parkinson's Disease overview

In the last two decades there has been a substantial evolution of the classical view of the second most common progressive neurological disorder in aging populations. PD (OMIM 168600) affects 1.5 % of the population over 60 years of age, with an incidence of 17–93 in 100 000 individuals per year, rising with age (Lees, 2009).

For many years, after James Parkinson's clinical description of the shaking palsy in 1817, the presence of a genetic component of PD has been debated, until Polymeropoulos and colleagues (Polymeropoulos et al., 1997) identified, in 1997, a pathogenic missense mutation in the α-synuclein gene (SNCA) of an Italian kindred where PD was inherited in autosomal-dominant fashion. This initial identification, followed by the finding that mutations in the same gene was associated with familial PD and work as a risk factor in sporadic PD as well (Cookson, 2010), had a significant impact on our understanding of the pathology. Indeed, the inherited and sporadic PD have common pathogenic mechanisms. Substantial evidence from postmortem human brains defined important neuropathological hallmarks of PD. Traditionally, PD has been considered a sporadic disorder pathologically characterized by the selective and progressive loss of dopaminergic neurons in the substantia nigra pars compacta (SNpc) with consequent depletion of dopamine (DA) in striatum and in other projection areas. Moreover, in the surviving neurons, α-synuclein is the main component of filamentous assemblies termed Lewy bodies (LBs) and Lewy neurites, where it accumulates in an aggregate form (Spillantini et al., 1997; Weintraub et al., 2008). Even though the mechanism behind LBs formation remains debated, further immunoreactivity studies have identified additional proteins such as ubiquitin, αB-Crystallin, Hsp70, Hsp40 as key components of LBs (Auluck et al., 2002; Pountney et al., 2005). Of note, recent evidence now suggests the possibility that α-synuclein acts as a prion-like protein for spreading PD, propagating from neuron to neuron (Olanow and

Brundin, 2013). Nonetheless, whether LBs are neurotoxic or represent a protective neuronal response is currently debated (Cookson, 2009; McNaught and Olanow, 2006).
The typical clinical presentation of PD includes akinesia, bradykinesia, rigidity and resting tremor, which are related predominantly to the progressive neurodegeneration of DA cells. However, several studies have established that non-dopaminergic and non-motor symptoms are common, occurring across all stages of PD. Symptoms like hyposmia, constipation, depression, apathy, psychosis, cognition impairment and sleep disorders are sometimes present before diagnosis, and are often poorly recognized and inadequately treated, leading to severe disability, impaired quality of life, and shorter life expectancy (Chaudhuri and Schapira, 2009). A variety of different types of studies indicate that the onset of PD is so gradual that it is often difficult to pinpoint in an individual patient when the disease first emerges. The variable course of the disorder once the motor symptoms develop depends on the age at symptom onset, with an older age causing a more rapid disease course. Although Braak's suggestion that the disease process may start peripherally and spread to the olfactory pathways has given support to the possibility that autonomic symptoms may be considered as clinical correlates of LBs deposition in these regions, when and where the neuropathological process begins remains debated (Gaig and Tolosa, 2009).

Clinical treatment. Despite the research in neuroprotection continues to grow, and many cellular targets are being investigated, the possibility to pharmacologically stop or slow the progression of neurodegeneration remains elusive. To date no proven neuroprotective treatment is available for PD, and clinical approach is mainly focused on DA replacement in order to ameliorate motor symptoms and improve the quality of life and life expectancy (Goetz and Pal, 2014). Currently, L-DOPA represents the most effective symptomatic treatment of PD since its introduction over 40 years ago (Cotzias, 1969). Being a prodrug, L-DOPA is inactive until it crosses the blood-brain barrier (BBB), and is decarboxylated to DA by aromatic amino acid decarboxylase (AADC) in surviving nigrostriatal dopaminergic neuron and, in advanced disease stages, striatal serotonin terminals. Because L-DOPA can be metabolized to DA also in the periphery, leading to significant gastrointestinal adverse drug reactions, peripherally restrained AADC inhibitors, such as benserazide or carbidopa are combined to L-DOPA to prevent its peripheral breakdown (Fahn, 2008).
Unfortunately, the response to L-DOPA changes with the progression of the disease and side-effects also emerge over time. As L-DOPA dosage increases over time, dyskinesias

(abnormal involuntary movements) and motor fluctuations become more common in patients within a few years of therapy (Fabbrini et al., 2007). Furthermore, no treatment for preventing or eliminating dyskinesias exists, and the mechanisms underlying this motor disturbance are still poorly understood.

It is important to note that although L-DOPA remains the gold standard of symptomatic therapy of PD, other pharmacological agents are currently used. Monotherapy with dopamine agonists, which directly stimulate DA receptors, represents the logical choice to rescue the impairment in DA transmission in early PD. In addition, non-ergolinic compound (i.e. pramipexole and ropinirole), together with catechol-O-methyl transferase (COMT) inhibitors and MAO-B inhibitors (that both inhibit DA metabolism) can also be used safely in more advanced phases of the disease, in conjunction with L-DOPA, to reduce motor fluctuations and dyskinesias (Rascol et al., 2005). When motor fluctuations and dyskinesia develop, or medical therapy fails to control symptoms adequately, surgical interventions for advanced PD represent a valid option (Weiss et al., 2010). These interventions include brain invasive procedures such as deep brain stimulation (DBS) of the subthalamics nucleus (STN) or globus pallidus internus (GPi), pallidotomy and thalamotomy (Nijhawan et al., 2009; Odekerken et al., 2013; Okun and Vitek, 2004).

Recently, a number of "non-pharmacological" strategies have emerged as alternative therapeutic approaches for PD, although most of them did not develop beyond the preclinical stage (Kordower, 2015). Gene transfer using viral vectors can provide long-term expression of therapeutic proteins in vivo. To date, different therapeutic approaches with adeno-associated virus (AAV) or lentiviral vectors, were undertaken to promote neuroprotection (by delivery of the neurotrophic factor neurturin), to enhance conversion of L-DOPA to DA (by delivery of AADC), and to modulate basal ganglia activity (by delivery of glutamic acid decarboxylase)(Mittermeyer et al., 2012; Muramatsu, 2010; Palfi et al., 2014). Finally, emerging evidence that differential expression of endogenous regulatory small RNAs, known as microRNAs (miRNAs), might play key regulatory roles in neurodegeneration, provides new therapeutic targets, opening a new avenues in PD therapy (Harraz et al., 2011).

Genetics of Parkinson's Disease

In the last two decades, using classic linkage analysis, genome-wide association studies and exome sequencing, 18 chromosomal loci (PARK1–18; Table 1) have been associated with familial PD (Lesage and Brice, 2012). To date, critical reviews argue that grouping different PD forms by pathology allow to better understand pathogenesis, nevertheless

most accepted classification show that gene variations causing PD are grouped in 2 categories: dominantly and recessively inherited mutations.

Autosomal dominant PD genes. Although mutations in LRRK2, represent the most common cause of autosomal dominant PD (up to 10% of all familial forms) (Bonifati, 2014), at least three other genes (SNCA, VPS35, EIF4EG1) have been conclusively established to cause PD in the same autosomal dominant manner. The above mentioned α-synuclein is a 14 kDa protein localized to presynaptic terminals, in the nucleus, in the cytosol, in the mitochondria-associated membrane and in the endoplasmic reticulum (Guardia-Laguarta et al., 2014). The normal function of α-synuclein remains poorly understood and the precise mechanisms by which it leads to toxicity and cell death are also unclear. Substantial evidence suggests that α-syn function is related to its capacity to interact directly with particularly highly curved membranes phospholipids such as vesicles, playing a role in vesicle trafficking during exocytosis (Snead and Eliezer, 2014). Mutations in the SNCA gene (PARK1 locus), oxidative stress and post-translational modifications lead α-synuclein to adopt an oligomeric and/or fibrillary conformation that induces toxicity through several mechanism. These species could impair mitochondrial structure and complex activity (Devi et al., 2008), as well as disrupt ER-Golgi vesicular transport, which results in toxic ER stress and impairs the efficiency of some protein degradation mechanisms acting as negative regulator of DA release (Abeliovich et al., 2000).

Recently, the identification of the D620N variation on the Vacuolar Protein Sorting 35 (VPS35) gene has been shown to cause late-onset L-DOPA-responsive autosomal dominant parkinsonism which is reminiscent of sporadic PD (Trinh and Farrer, 2013). The frequency of mutation carriers is low and estimated to represent about 0.1% of the PD population. This gene encodes a subunit of the retromer system which mediates intracellular retrograde transport of endosomes to the trans-Golgi network (TGN). How mutant VPS35 causes PD is presently unknown, even though several lines of evidence indicate that mutant VPS35 may cause neurodegeneration via a gain-of-function mechanism with a dominant-negative effect on retromer assembly (Trinh and Farrer, 2013). In particular, Vps35 D620N mutants appear to disrupt the cargo sorting function of retromer, causing a deficit in retromer-dependent trafficking of CI-M6PR (cation-independent mannose-6-phosphate Receptor) and its ligand cathepsin D, likely arising from the generation and redistribution of enlarged endosome compartments that retain retromer (Follett et al., 2014).

Traditional linkage methods have recently identified the R1205H mutation in the EIF4G1 (eukaryotic translation initiation factor 4-gamma 1) gene as an infrequent cause of dominantly inherited PD, with an estimated frequency between 0.02–0.2% in the PD population (Chartier-Harlin et al., 2011). Of note, the eIF4G1 protein is regulated by phosphorylation of eIF4E-binding proteins (4E-BP) through the mammalian target of rapamycin (mTOR) pathway (Ramirez-Valle et al., 2008), and represents a multisubunit translation initiation complex involved in mRNA translation processes that regulates cell survival in response to stress (Chartier-Harlin et al., 2011). Interestingly, several lines of evidence point to a crucial involvement of the translation initiation process in PD. Indeed, it has been shown that LRRK2 interacts with eIF4E and directly phosphorylates 4E-BP at the postsynaptic site in vitro (Lee et al., 2012b). Furthermore the mTOR pathway and 4E-BP phosphorylation are strictly linked to PD. Activation of 4E-BP by rapamycin, or its transgenic overexpression, prevent DA neuron loss in Drosophila models (Tain et al., 2009) and are associated with L-DOPA-induced dyskinesia (Santini et al., 2009). Finally, in a very recent study, OA Ross and colleagues established a link between VPS35 and EIF4G1 in α-synuclein-related neurodegeneration using a yeast model (Ross et al., 2015).

Table 1. Summary of genes and loci associated with PD.

Locus	Gene	Chromosomal location	Inheritance	Type of parkinsonism
PARK1/PARK4	*SNCA*	4q21	AD + risk	LOPD/EOPD
PARK2	*Parkin*	6q25-q27	AR	EOPD
PARK3	Unknown	2p13	AD	LOPD
PARK5	*UCHL1*	4p14	AD	LOPD
PARK6	*PINK1*	1p36	AR	EOPD
PARK7	*DJ-1*	1p36	AR	EOPD
PARK8	*LRRK2*	12q12	AD	LOPD
PARK9	*ATP13 A2*	1p26	AR	EOPD
PARK10	Unknown	1p32	Unknown	LOPD
PARK11	*GIGYF2*	2q37	AD	LOPD
PARK12	Unknown	Xq21-25	X-linked	LOPD
PARK13	*HTRA2*	2p12	AD	LOPD
PARK14	*PLA2G6*	22q13	AR	EOPD
PARK15	*FBXO7*	22q12-q13	AR	EOPD
PARK16	Unknown	1q32	Risk	LOPD
PARK17	*GAK*	4p16	Risk	LOPD
PARK18	*HLA*	6p21	Risk	LOPD
-	*EIF4GI*	3q27	AD	LOPD
-	*GBA*	Iq21	Risk	LOPD
-	*MAPT*	17q21	Risk	LOPD
-	*BST1*	4q15	Risk	LOPD

Abbreviations: AD, autosomal dominant; AR, autosomal recessive; EOPD, early-onset PD; LOPD, late-onset PD

Autosomal recessive PD genes. Mutations, including point mutations and large rearrangements, leading to deletions or multiplications, in each of the following three genes, *Parkin* (PARK2), *PINK1* (*PTEN induced putative kinase 1;* PARK6) and *DJ-1* (PARK7) have been identified worldwide.

Mutations in PARK2 alone account for almost 50% of early-onset familial recessive PD cases and are compatible with ∼15% of sporadic PD forms (Bonifati, 2014). Over a hundred mutations in PARK2 have been reported, which include homozygous or heterozygous point mutations but also deletions and duplications. The encoded protein, Parkin, belongs to the ubiquitin E3 ligases family and interacts with ubiquitin-conjugating enzymes (E2s) to catalyze the attachment of ubiquitin to protein targets (Shimura et al., 2000), thus tagging these proteins for destruction by the proteasome. In addition, Parkin is involved in mitochondrial maintenance, and mutations within this gene might be associated

with changes of mitochondrial autophagy and neuronal dysfunction (Park et al., 2009). Patients carrying Parkin mutations present L-DOPA-responsive PD, frequently accompanied by motor fluctuations and dyskinesias that often develop early in the course of treatment (Periquet et al., 2001). However, rarely LBs have been detected, although neural loss in nigrostriatal pathway is usually severe, suggesting pathogenic differences between the autosomal recessive and the classical forms of PD. Nonetheless, the first patient with pathogenic PINK1 mutations and LBs-positive pathology was recently reported (Bonifati, 2014).

Mutations in the PINK1 and DJ-1 gene are less common, accounting for ~1–8%, and 1–2% of early-onset PD cases, respectively (Bonifati, 2014). The protein encoded by PINK1 is located in the mitochondrial membranes and is involved in the mitochondrial response to cellular and oxidative stress (Valente et al., 2004a). It is clear that PINK1, by acting upstream of parkin, is involved in the elimination of damaged mitochondria, and might protect neurons against mitochondrial dysfunction and proteasome-induced apoptosis (Bonifati, 2014). The clinical phenotype is similar to that caused by mutations in Parkin, with a slow disease progression and rare additional psychiatric disturbances, particularly anxiety and depression (Valente et al., 2004b).

Interestingly DJ-1 is also likely to be involved in mitochondrial physiology; in fact it represents a sensor for oxidative stress and may mediate neuroprotection. In the presence of oxidative stress, DJ-1 has been shown to translocate to the mitochondria and exert a protective effect (Canet-Aviles et al., 2004). In particular, the L166P mutation leads to a less stable protein and to the reduction of antioxidative activity, implicating a loss-of-function mechanism (Moore et al., 2003). Finally, similar to the other recessive PD forms, the clinical picture includes an early onset, good response to L-DOPA, and slow progression. By analysis of these genes, it has come most clearly that repair of damaged mitochondria represents a common physiological function, but how these proteins are involved is not yet clear.

Of note, other more rare recessively inherited forms of PD have been identified. Mutations in the ATP13A2 (ATPase type 13A2), PLA2G6 (phospholipase A2, group VI) and FBXO7 (F-box only protein 7) genes cause an atypical PD-associated phenotype that is distinguished from the other three aforementioned forms by an earlier (juvenile) onset, partial or less sustained response to L-DOPA, and atypical clinical features such as upper motor neuron signs, pyramidal signs, dystonia, supranuclear gaze palsy, myoclonus and cognitive decline (Bonifati, 2014).

LRRK2-associated phenotype

The majority of clinical reports on LRRK2 PD patients consistently indicate that their clinical phenotype is not distinguishable from the idiopathic form (Healy et al., 2008; Paisan-Ruiz, 2009). PD patients carrying LRRK2 pathogenic mutations have been identified in more than 40 populations worldwide. In addition, variable degrees of population-specificity have been shown, indicating that ethnicity is an important factor that influences diagnosis (Paisan-Ruiz, 2009). Notably, penetrance of LRRK2 mutations is almost complete and age-dependent, with an increase between 17% to 85% from 50 to 70 years of age, and some G2019S mutation carriers exhibiting the disease after 80 years of age (San Luciano et al., 2010). The most frequent LRRK2 mutation, G2019S, shows incomplete penetrance and this might explain why this mutation is detectable in patients with familial PD but also in some with sporadic PD, suggesting that genetic and/or environmental factors may associate with LRRK2 to trigger dopaminergic neurodegeneration (Hulihan et al., 2008). This variant is frequent in PD patients from southern Europe, in particular in Portuguese (16%), Spanish and Italian populations. However, the highest incidence has been reported in Nord African Arabs (42%) and in Ashkenazi Jewish (28%) (Paisan-Ruiz et al., 2013). Moreover, G2019S is associated with a specific haplotype present in all subjects, suggesting that the mutation was transmitted by a single ancient founder across European population (Kachergus et al., 2005). Given the high frequency of the G2019S mutation, the clinical phenotype of LRRK2 patients is mostly associated with this mutation. Several studies consider tremor as the initial and predominant symptom of LRRK2 carriers but, in a recent study, tremor incidence was lower in patients with G2019S PD than idiopathic PD (Trinh et al., 2014). Overall, the G2019S mutation is often associated with the classical motor triad characterized by bradykinesia, rigidity and asymmetrical tremor, by a good response to L-DOPA and a slow and benign disease progression (Paisan-Ruiz, 2009). In addition, postural instability and dystonia have been reported, although dystonia may only appear due to a complication of both medical and surgical treatment (Healy et al., 2008). The impact on the susceptibility to develop L-DOPA-induced dyskinesias (LID) is also debated: some groups found it to be more frequent in G2019S carriers than idiopathic PD (Lesage et al., 2008), whereas others showed no difference, even though the time elapsed from L-DOPA treatment onset to LID appearance was significant longer in LRRK2 compared to non-LRRK2 carriers (Healy et al., 2008). Compared to sporadic PD patients, LRRK2 carriers present a lower risk of cognitive decline and psychiatric features (Alcalay et al., 2010); on the other hand, higher frequency of depression, anxiety and irritability have been reported. Interestingly, Shanker

and colleagues reported a trend for a greater risk of premorbid mood disorders in LRRK2 patients compared to gene-negative patients, assuming that mood disorder susceptibility genes may modify LRRK2 mutation penetrance. Of note, numerous reports identified different degrees of cognitive alterations in a number of healthy asymptomatic G2019S carriers that could represent a hopeful way to investigate early markers for pre-symptomatic PD (Thaler et al., 2012).

The distribution in age at onset and the clinical features are similar in LRRK2 R1441C patients and idiopathic or LRRK2 G2019S PD patients. Moreover G2385R carrier patients demonstrate clinical features similar to non-carrier patients, indicating that mutations in different LRRK2 domains lead to similar clinical phenotypes. Lastly, patients carrying the Y1699C mutation show unilateral leg tremors at onset, foot dystonia and then bradykinesia, rigidity, and postural instability with good responsitivity to L-DOPA (Haugarvoll et al., 2008).

Neuropathology of LRRK2 mutation carriers

The pathological features of patients with LRRK2 mutations are strikingly heterogeneous. Postmortem analysis from more than 30 LRRK2 mutation carriers displayed dopaminergic neuronal loss and gliosis in the SN, although the same mutations can cause quite different neuropathology, and LBs or Lewy neurites are not present in all cases (Wider et al., 2010). The G2019S phenotype is often characterized by the presence of α-synuclein–immune-positive LBs and, although other postmortem findings, such as tau-positive or ubiquitin-immunoreactive inclusions, have been found, this mutation does not always manifest as synucleinopathy or LBs disease (Ruffmann et al., 2012). Rather than distinct processes, these pathological endpoints may share the same primary cause, assuming that LRRK2 and tau/ α -synuclein crosstalk along a common neurotoxicity pathway (Rajput et al., 2006). However, the exact relationship between α–synuclein and LRRK2 is unclear as postmortem localization studies have produced conflicting results (Sharma et al., 2011). Due to the growing interest in the potential interaction of these proteins in the pathogenesis of PD, a very recent study from Guerreiro group, using diverse and more rigorous techniques, showed that endogenous LRRK2 and α-synuclein interact in cells, mouse and human brain tissue. Their data show that the G2019S mutation does not alter the ability of LRRK2 to interact with α-synuclein in HEK-293 cells, indicating that the kinase domain, and hence the phosphorylation capacity of LRRK2, does not play a major role in its interaction with α-synuclein (Guerreiro et al., 2013). Interestingly, in cell models, an increase in LRRK2 expression is associated with elevation of α-synuclein mRNA

(Carballo-Carbajal et al., 2010). These features are consistent with reports that the levels of LRRK2, rather than its mutations, regulate the progression of neuropathology induced by PD-related α-synuclein mutants (Lin et al., 2009). Furthermore, despite the poor specificity of the different LRRK2 antibodies (Davies et al., 2013), a number of studies in human brain tissues showed the co-localization of LRRK2 with α-synuclein-immunoreactive LBs (Guerreiro et al., 2013),. Of note, analysis of LRRK2 mRNA expression in post-mortem brain tissue from control, idiopathic PD (IPD) cases and G2019S-positive PD cases showed, in addition to a widespread neuronal localization and weak levels in SN, significant reductions in non-nigral regions (cerebellum, amygdala, frontal cortex and cingulate gyrus) of IPD brain (Sharma et al., 2011). In this scenario, further work is required to explain the contrast between the increased levels of LRRK2 in PD brain regions with pathological accumulation of α-synuclein and the pathogenic role of LRRK2 outside nigral neurons.

The most striking variability was observed in R1441 mutation carriers. DA neuron loss and gliosis in the SN, without α-synuclein-positive inclusions, have been reported in the only case examined with the R1441G substitution (Marti-Masso et al., 2009), even though some autopsies from R1441C carriers showed various neuropathological patterns. Indeed, data from four patients revealed that one case did not show synuclein and tau pathology, two cases had LBs and Lewy's neurites (LNs), and the remaining one showed neurofibrillary tangles (NFT) without either LBs or LNs (Wszolek et al., 1997). However, no pathology reports are available for p.R1441H substitution carriers. Finally, similar finding have been reported for the I2020T and Y1699C mutations that showed tau, LBs and ubiquitin-positive cytoplasmic and nuclear inclusions (Ujiie et al., 2012).

Understanding the mechanisms that lead to dopaminergic loss in LRRK2 patients represents the unresolved challenge in the LRRK2 field. The clinical and pathological heterogeneity of LRRK2 mutation carriers, together with the widespread expression of LRRK2, supported the idea that this protein interacts with other molecules in the affected neuronal populations, and this may play an important role in the accumulation and aggregation of unfolded proteins. As extensively suggested, LRRK2 interacts with other proteins which also form protein complexes (Cookson, 2010; Greggio et al., 2011), likely acting upstream of them. Moreover, additional genetic and environmental risk factors determine the type of pathology that develops in a given individual. For example, mutation of the genes encoding α-synuclein and tau, SNCA and microtubule associated protein tau (MAPT) respectively, could be the obvious candidate to influence pathogenesis, directly or indirectly interacting with the protein LRRK2. Likewise, different environmental factors

such as pesticides and head trauma might lead LRRK2 either towards tau or α-synuclein pathology (Li et al., 2014). To date, the physiological and pathophysiological consequences of LRRK2 mutation remain largely unknown. Investigators have largely attempted to validate LRRK2 protein interactors by using a LRRK2- dependent phosphorylation readout, but until now all attempts have failed.

LRRK2: protein interaction network and pathogenic mechanisms

Expression

LRRK2 is found at high levels in several organs, such as liver, lung, kidney, heart, spleen, intestine and lymph nodes (Galter et al., 2006; Giasson et al., 2006; Hakimi et al., 2011), while is poorly expressed in the mammalian brain relative to most well-characterized protein kinases. Despite the lack of sensitive and specific antibodies (Davies et al., 2013), the neuroanatomical localization of LRRK2 in the brain showed a striking relation between LRRK2 gene expression and the nigrostriatal DA system affected in PD. In situ hybridization studies on LRRK2 mRNA in the mouse brain revealed that expression is highest in the cortex, moderate in striatum, olfactory tubercle, hippocampus and cerebellum, and lowest in SNpc (Biskup et al., 2006; Melrose et al., 2006).

Within the brain, LRRK2 is abundantly expressed in neurons, but it can also be detected at lower levels in astrocytes and microglia where its expression can be induced by inflammatory stimuli (Giesert et al., 2013; Paisan-Ruiz, 2009). In the cortex, striatum, and SNpc, the pattern of LRRK2 expression differs within distinct neuronal subpopulations . Throughout the striatum, in both rats and mice, LRRK2 expression appeared to be restricted to medium spiny neurons, with low to undetectable expression in larger interneurons. This is also confirmed by the overlapping of DARPP-32 and LRRK2 staining in neuronal perikarya. In the last years, the expression of LRRK2 in SNpc has been object of intensive studies. Diverse studies failed to detected protein levels, while others, after having developed more specific anti-LRRK2 polyclonal antibodies, described LRRK2 protein expression in the mouse and human SNpc, (Biskup et al., 2006; Greggio et al., 2006; Melrose et al., 2007). Interestingly, although any LRRK2 signal using similar staining conditions has been found in rat SNpc dopaminergic neurons, minimal LRRK2-immunoreactivity has been showed in the substantia nigra pars reticulata (SNpr) in both rats and mice (West et al., 2014). At a subcellular level, in striatal and cortical neurons, LRRK2 is localized throughout the cytoplasm of neuronal perikarya and dendritic

processes where it is associated with vesicular and intracellular membranous structures (i.e. mitochondria, endosomes, lysosomes, multivesicular bodies, lipid rafts, microtubule-associated transport vesicles, synaptosomes, Golgi complex, and endoplasmic reticulum), with the microtubule network and other membrane-bound organelles (Alegre-Abarrategui et al., 2009; Biskup et al., 2006). The synaptic localization of LRRK2 represents a contentious issue. In particular, some studies found that LRRK2 expression does not overlap with presynaptic markers, including synaptotagmin-1 (a large protein able to bind Ca2+ and involved in the presynaptic vesicle membrane fusion) in striatal and cortical neurons, but has close association with TH-positive projections, suggesting a predominantly postsynaptic localization in the striatum (West et al., 2014). Instead, others investigators suggest that the association of LRRK2 with cytoskeletal elements hints a possible role in vesicular transport, protein trafficking and presynaptic vesicle endo/exocytosis (Belluzzi et al., 2012) as well as in membrane and protein turnover, including the lysosomal degradation pathway. The LRRK2 association with outer mitochondrial membrane in rodents may suggest a causal role in PD, where mitochondrial function is impaired. Interestingly, mitochondria undergo frequent fission and fusion events especially before a cell undergoes apoptosis, and these processes are regulated by molecular machinery that includes dynamin-related GTPases and WD40 repeat-containing proteins. Therefore, LRRK2 might potentially serve as a scaffold during mitochondrial fission and fusion (Li and Beal, 2005).

Interaction network and cellular function

LRRK2 protein distribution within various cell compartments might reflect a functional role in multiple cellular pathways (Fig.3). The physiological cellular function of LRRK2 is not clear despite strong evolutionary conservation of this class of protein. Some evidence suggests a role in cytoskeleton organization, translation regulation, autophagy-lysosomal pathways, neurite outgrowth, vesicular trafficking, neurotransmitter release and immunoregulation, but as mentioned above, little is known about the physiological interactors and/or regulators of LRRK2, and a few substrates for its domains have been described.

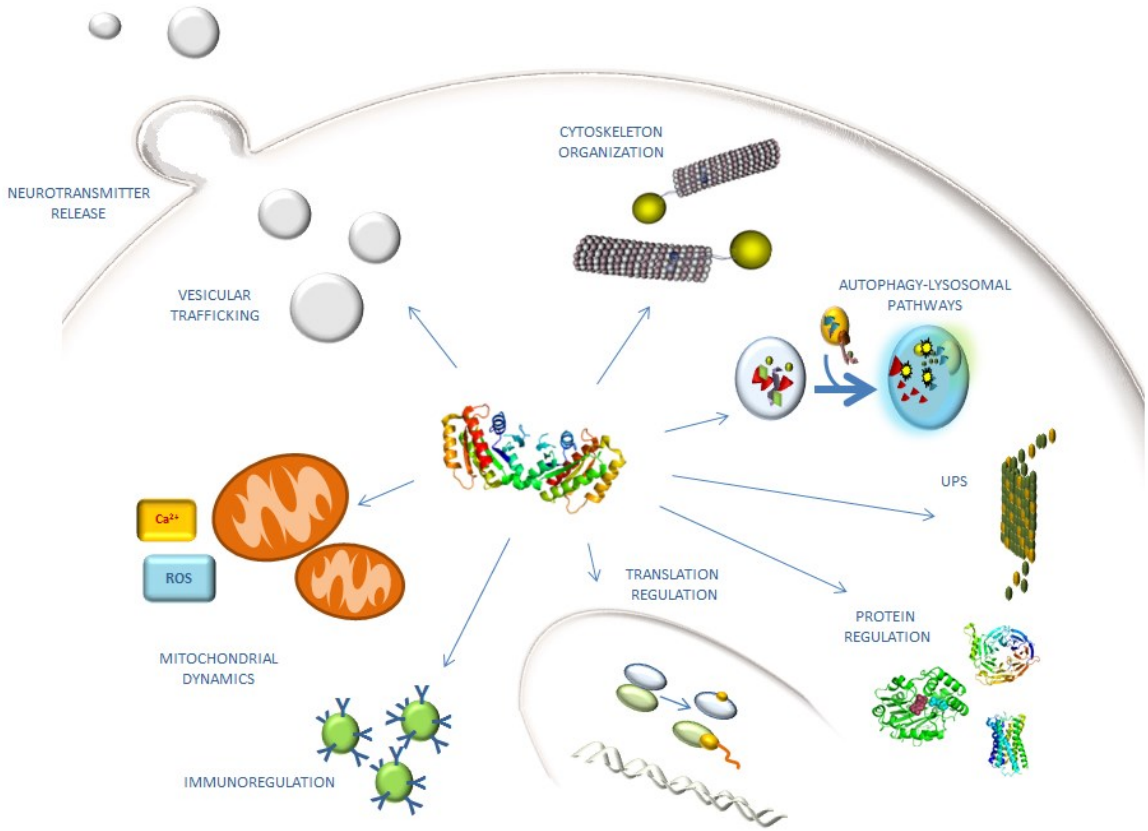

Fig. 3. LRRK2 involvement in cellular mechanisms.

Cytoskeletal regulation. Ultrastructural analysis supports LRRK2 interaction with cytoskeletal proteins including tubulin, tubulin-associated tau and actin. A very recent study, in line with previous evidence, demonstrated a specific, direct interaction of LRRK2 with three different β-tubulin isoforms, which is mediated by the LRRK2 ROC domain and the β-tubulin C-terminus. This interaction is dependent on guanidine nucleotide binding and modulated by ROC domain autophosphorylation. The R1441G mutation seems to disrupt this interaction, possibly by affecting tubulin acetylation. Conversely, embryonic fibroblasts (MEFs) obtained from LRRK2 knock-out mice show increased tubulin acetylation. Interestingly, Gillardon and collaborators found that recombinant human LRRK2 phosphorylates β-tubulin, and phosphorylation levels are three-fold enhanced in the presence of the G2019S mutation, with the consequential increase of microtubule polymerization (Gillardon, 2009). In addition, LRRK2 co-localizes with highly dynamic cytoskeletal structures in dopaminergic cells, and LRRK2 overexpression and mutation impact upon the morphology of growth cones (Law et al., 2014).

Moesin, a component of the ERM (ezrin/radixin/ moesin) family has been identified as one of the cytoskeletal LRRK2 kinase target (Parisiadou et al., 2009). These proteins play an important role in the regulation of the membrane structure and its organization by anchoring the actin cytoskeleton to the plasma membrane. Although moesin is likely to be only an efficient in vitro substrate for LRRK2, it allows the development of efficient model substrate peptides, called LRRKtide and Nictide, derived from ERK sequence, which helped improve the analysis of LRRK2 kinase activity *in vitro* (Jaleel et al., 2007). However, LRRK2 also plays a role in actin dynamics, interacting with actin isoforms and with the actin-associated proteins that contribute to filament assembly, organization and maintenance. A number of studies show that LRRK2 mutations lead to the accumulation of polymerized actin as well as phosphorylated ERM, and that these effects are reversed in LRRK2 knockout neurons (Parisiadou et al., 2009). Pathogenic mutations influence the interaction between LRRK2 and microtubules: some studies indicate that G2019S and R1441G/H reduce LRRK2- β-tubulin interaction (Law et al., 2014), while others an increased affinity (Kett et al., 2012). Taken together, these data suggest a role for LRRK2 in the regulation of cytoskeletal dynamics with implications for the pathogenesis of PD.
Furthermore, the suggestion that LRRK2 can directly phosphorylate tubulin-associated tau is corroborated from the evidence that tau phosphorylation is reduced in LRRK2 knock-out mice (Kawakami et al., 2012). In addition, the G2019S and I2020T mutations increase tau-phosphorylation, influencing the tau's affinity for microtubules protein and promoting its aggregation (Melrose et al., 2010).

Protein regulation and Autophagy. LRRK2 has been proposed to physically interact with 14-3-3 proteins, upon phosphorylation at residues S910 and S935 at the N-terminus of the leucine-rich repeats (Dzamko et al., 2010; Nichols et al., 2010). The 14-3-3 proteins represent a family of conserved regulatory molecules that usually assemble into either homo- or heterodimers and, in their dimeric form, bind to two phosphorylated residues which can come from the same target protein, or from two separate binding partners. These proteins have the ability to protect important regulatory sites from dephosphorylation, or to mediate dimerization of two distinct target proteins. Dzamko and colleagues showed that pathogenic LRRK2 mutations disrupt the binding between 14-3-3 and LRRK2: as a consequence, LRRK2 levels are decreased and LRKK2 is accumulated in non-cytosolic pools. How 14-3-3 interaction influences LRRK2 function or its cytoplasmic localization has not been clarified yet. It has been shown that this interaction does not control LRRK2 protein kinase activity, as mutations of Ser910 and/or Ser935 do not influence LRRK2

catalytic activity or dimer formation of wild type LRRK2. However, Ser910/Ser935 phosphorylation and 14-3-3 binding is markedly reduced in mouse tissues derived from homozygous R1441C knock-in mice that display impaired dopaminergic neurotransmission (Dzamko et al., 2010; Nichols et al., 2010; Tong et al., 2009). A very recent study describes an additional residue in the ROC domain involved in the regulation of the 14-3-3 binding to LRRK2. Binding of phospho-Ser1444 residue to 14-3-3 impairs LRRK2 kinase activity, and phosphorylation is abolished by pathogenic mutations in the ROC domain, even though whether this results in altered cytosolic localization of LRRK2 has not been determined yet (Muda et al., 2014). In addition, the Ser910, Ser935 and Ser1444 residues are not phosphorylated by LRRK2 itself, but rather by multiple kinases, including cAMP-dependent protein kinase (PKA). This kinase is one of key regulators in signal transduction in the brain; it is activated in response to increasing concentrations of cAMP and phosphorylates a vast number of protein kinases, including the MAPKKK c-Raf. Furthermore, PKA facilitates synaptic transmission and assumes an important function as a regulator of DA synthesis. In this context, LRRK2 kinase activity could be modulated by PKA-mediated binding of 14-3-3, suggesting that PKA acts as an upstream kinase for LRRK2 (Muda et al., 2014).

Interaction between the LRRK2 ROC-COR domain with the DVL (dishevelled) phosphoproteins family (DVL1-3) has been reported. DVLs represent key regulators of Wnt (Wingless/Int) signalling pathway, which is important for axon guidance, synapse formation and neuronal maintenance. Indeed, they can mediate the activation of small GTPases with structural similarity to the LRRK2 ROC domain. In this context, DVLs may influence LRRK2 GTPase activity, and ROC-COR domain mutations modulating LRRK2-DVL interactions indirectly influence kinase activity (Sancho et al., 2009). In addition, LRRK2 has been reported to interact with various small GTPases including Rac1 (Chan et al., 2011), rab5b (Shin et al., 2008), and rab7 (Dodson et al., 2012).

Accumulating evidence suggests that LRRK2 interacts with heat shock protein 90 (Hsp90) in vitro and in vivo, and that inhibition of Hsp90 disrupts this association, followed by LRRK2 degradation and increased cell viability. Hsp90 is a molecular chaperone essential for activating many signaling proteins and for regulating their stability in the eukaryotic cell. Moreover, Hsp90 contributes to the stabilization, activation, and/or translocation of client protein kinases, such as Src family tyrosine kinase and serine/threonine protein kinases, such as LRRK2. The binding of Hsp90 to LRRK2 seems to reflect protein instability, indeed the inhibition of Hsp90 chaperone function dramatically decreases the stability of LRRK2 in cell lines and primary neuronal cultures via a proteasome-mediated

degradation mechanism. Hsp90 could be a target for suppressing the accumulation of PD-related LRRK2 mutants and their pathogenic activity in neurons. Indeed, treatment of neurons with a Hsp90 inhibitor rescued the axon growth retardation defect caused by overexpression of the LRRK2 G2019S mutation (Wang et al., 2008). Furthermore, Hsp90 shows greater affinity for G2385R LRRK2 than the wild-type form, and its inhibition leads to the association of mutant LRRK2 with high molecular mass native fractions, that probably represent proteasome degradation products. Of note the G2385R mutation within the WD40 domain, which represents a risk factor of PD, causes a partial loss ofkinase activity by reducing phosphorylation at Ser910/Ser935 sites, and a concomitant diminished ability to bind 14-3-3 proteins (Rudenko et al., 2012).

Moreover, LRRK2 was found to interact with the C-terminus of Hsp70-interacting protein (CHIP), an E3 ubiquitin ligase that significantly reduces the cellular levels of LRRK2 by ubiquitination and proteasome-dependent degradation, leading to lowered LRRK2 protein levels (Ding and Goldberg, 2009). Binding to LRRK2 occurs between the charged domain and the ROC domain of LRRK2, or between the TPR domain of CHIP and the N-terminal region of LRRK2.Since the TPR domain of CHIP is well-known to bind to Hsp90, it is likely that a portion of the LRRK2-Hsp90 complex will also be associated with CHIP. Interestingly, because it has been reported that LRRK2 binds to the E3 ubiquitin ligase Parkin, enhancing its auto-ubiquitination activity, and that CHIP also forms a complex with Parkin enhancing its ubiquitin ligase activity, it is possible that the reported interaction between LRRK2 and Parkin is mediated by CHIP (Ding and Goldberg, 2009). It has been proposed that the ability of CHIP to degrade potentially neurotoxic misfolded, damaged or mutated proteins might diminish with age. In this contest diminished CHIP-mediated degradation of LRRK2 in aged or stressed neurons may contribute to sporadic PD as well as familial PD in patients bearing LRRK2 mutations.

In either case, current data indicate that LRRK2 protein levels nicely correlate with neuronal toxicity. The interaction with Hsp70 targets LRRK2 to the lysosomal membrane for chaperone-mediated degradation thus representing a mechanism to control protein levels, (Skibinski et al., 2014). Recently, Beilina and colleagues, using protein–protein interaction arrays, identified BCL2-associated athanogene 5, Rab7L1 (RAB7, member RAS oncogene family-like 1), and Cyclin-G–associated kinase, as binding partners of LRRK2. These proteins form a complex that promotes clearance of Golgi-derived vesicles through the autophagy–lysosome system both in vitro and in vivo, although the impact of these interactions on LRRK2 levels and chaperone-mediated autophagy remains unknown (Beilina et al., 2014). Interestingly, additional studies have investigated the interaction

between LRRK2 and mitogen-activated kinases (MAPKs), such as extracellular signal-regulated kinase (ERK), Jun N-terminal kinase (JNK) and p38. LRRK2 induces the phosphorylation of MAPK/ERK kinases (MEK), while the G2019S mutation promotes autophagy in cells via the MEK/ERK pathway (Liou et al., 2008).

Effect on protein translation. Evidence has been provided that LRRK2 is involved in one of the many established signaling cascades, including the mTOR and ERK pathway, and protein translation in general has been suggested to be instrumental to LRRK2 effects in fly models. In particular, both human LRRK2 and the Drosophila orthologue of LRRK2 phosphorylate eukaryotic initiation factor 4E (eIF4E)-binding protein (4E-BP), a negative regulator of eIF4E-mediated protein translation and a key mediator of various stress responses. 4E-BP is a target of mammalian target of rapamycin (mTOR), which is of interest in research on aging since recent evidence suggests that in diverse species, deletion of mTOR signalling components or treatment with the mTOR inhibitor, rapamycin, can extend lifespan. It has long been recognized that a key regulator of eIF4E function is the phosphorylation-induced release of 4E-BP from eIF4E. Although LRRK2 stimulates eIF4E-mediated protein translation both in vivo and in vitro, it attenuates resistance to oxidative stress and survival of DA neurons in Drosophila. The chronic inactivation of 4E-BP by pathogenic LRRK2 mutations might lead to deregulation of protein translation, likely resulting in age-dependent loss of DA neurons (Imai et al., 2008). mTOR signaling may link LRRK2 with aging, despite the fact that experiments have shown that 4E-BP is a relatively poor substrate for highly purified LRRK2.

Because recent genome-wide association studies (GWAS) revealed that the LRRK2 locus represents a genetic risk factor for sporadic PD (Satake et al., 2009), the potential alteration of LRRK2 expression in the etiology of sporadic PD is of outmost interest. To this purpose a number of studies have highlighted a role for LRRK2 in microRNA (miRNA) regulation. miRNAs are evolutionarily conserved small non-protein-coding transcripts that bind to partially complementary sites in the 3′-untranslated region (3′-UTR) of target messenger RNAs (mRNAs), and thereby control the translation of their target gene. A number of miRNAs have been associated with neuronal development, synaptic plasticity, memory formation and neurodegenerative diseases in the nervous system through their regulation of the translation of targeted genes (Hebert and De Strooper, 2009). Cho and colleagues, reported that the levels of LRRK2 were enhanced whereas those of miRNA-205 (miR-205) were decreased in the frontal cortex of sporadic PD patients (Cho et al., 2013). Since LRRK2 mRNA levels (i.e. LRRK2 expression) remained unchanged, a potential post-

transcriptional modification of the LRRK2 protein expression in the sporadic PD brain was suggested. Interestingly, miR-205 reduced LRRK2 levels in cell lines and primary neuron cultures, through targeting its binding site in the 3′-UTR of LRRK2 gene. In addition, introduction of miR-205 prevented the neurite outgrowth defects in the neurons expressing a PD-related LRRK2 R1441G mutant. In this context, the downregulation of miR-205 may play a role in the pathogenic elevation of LRRK2 protein in the sporadic PD brain (Cho et al., 2013). These findings support previous data in which LRRK2, through its kinase domain, was shown to control the production and the regulation of let-7 and miR-184, (Gehrke et al., 2010). Unfortunately, at this stage little is known about the alteration in LRRK2 function during the aging process, and no specific post-translational modifications associated with aging are known, as it is undetermined how people carrying LRRK2 mutations develop disease as adults.

Relationship to mitochondria. Mitochondrial dysfunction is widely recognized as a trigger of PD, and LRRK2 has been found to be involved in different mitochondrial events, including mitochondrial dynamics and morphology, mitochondrial calcium buffering, ROS production and mitochondrial membrane potential maintenance. In vitro studies on primary cultures of cortical neurons found that LRRK2 colocalizes with the mitochondrial marker Cyto C and partially with the fission Dynamin like protein 1 (DLP1). Interestingly, LRRK2 G2019S overexpression in cortical neurons increases DLP-1 activity and promotes mitochondrial fission, suggesting that LRRK2 is likely to be involved in mitochondrial fission/fusion dynamics (Niu et al., 2012). In addition, cellular transfection with LRRK2 WT and LRRK2 G2019S could induce mitochondrial fragmentation and consequent cell death (Iaccarino et al., 2007). A reduction of mitochondrial membrane potential and intracellular ATP levels, accompanied by mitochondrial elongation, have been reported in skin biopsies from human LRRK2 G2019S carriers (Mortiboys et al., 2010). This is in accordance with the study of Papkovskaia and colleagues (Papkovskaia et al., 2012) that pointed to a kinase-dependent mechanism. Moreover, LRRK2 mutants are involved in the modulation of the peroxiredoxin3 activity. This enzyme, located within mitochondria, acts as antioxidant and is phosphorylated by LRRK2 (Angeles et al., 2011). Reduced cell survival and mitochondrial dysfunction, such as increased sensitivity to rotenone-mediated complex I inhibition (Ng et al., 2009), have been also shown in Drosophila flies carrying LRRK2 mutants, whereas WT LRRK2, seems to attenuate H_2O_2-induced oxidative stress, suggesting a protective role for LRRK2 (Liou et al., 2008). Mutations in LRRK2 could affect mitochondrial function by increasing the vulnerability to oxidative stress. Induced

pluripotent stem cells (iPSCs) derived from fibroblast of G2019S LRRK2 carriers show higher levels of mitochondrial DNA (mtDNA) damage than cells from control subjects, and are characterized by a reduced mitochondrial respiration and motility (Papkovskaia et al., 2012).

LRRK2 and vesicle trafficking. Given the synaptic expression of LRRK2 and its association with the membranous structures involved in vesicular release, including endoplasmic reticulum, Golgi apparatus, cytoskeleton, lipid raft and synaptic vesicles (Migheli et al., 2013), it is not surprising that LRRK2 is involved in vesicle trafficking and neurotransmitter release (Tong et al., 2009). Of note, the activated form of LRRK2 (LRRK2 dimer) is substantially enriched at the membrane of cells expressing endogenous or exogenous LRRK2, and the membrane-associated fraction of LRRK2 possesses greater kinase activity than cytosolic LRRK2, suggesting intense catalytic role at this site (Berger et al., 2010). Several studies show that LRRK2 acts at the synaptic site, interacting with a high number of pre-synaptic proteins including NSF (*N-ethylmaleimide-sensitive fusion factor)*, AP-2 (*adapter protein 2*), SV2A (*synapticvescicle protein 2A*), synapsin 1A, syntaxin 1, clathrin (Piccoli et al., 2011), Rab5 and actin (Meixner et al., 2011). Shin and colleagues reported that the interaction between LRRK2 and Rab5 is involved in the modulation of synaptic vesicle endocytosis (Shin et al., 2008). Recently in vivo and in vitro studies revealed the interaction between LRRK2 and ArfGAP1 (*ADP-ribosylation factor GTPase-activating protein 1*). ArfGAP1 is able to promote the GTPase activity of Arf1 (*ADP-ribosylation factor 1*), a small protein involved in maintaining the morphology of the Golgi apparatus and the extrusion of vesicular proteins to the endoplasmic reticulum (Donaldson and Radhakrishna, 2001).

LRRK2 interacts with actin filaments and microtubules involved in vesicular transport and trafficking, regulating ERM phosphorylation *via* kinase activity and actin polymerization (Parisiadou et al., 2009). Interestingly, Cirnaru and coworkers (Cirnaru et al., 2014) showed a reduction of the interaction between LRRK2 and synaptic vesicles and a simultaneous enhancement of the affinity between actin and synapsin, after inhibition of kinase function.

LRRK2 interacts with SV2A, a neuronal protein involved in Ca^{2+}-dependent exocytosis (Chang and Sudhof, 2009). SV2A interacts with synaptotagmin, a Ca^{2+} sensor protein in the membrane of the pre-synaptic axon terminal that interacts with the SNARE complex (*Soluble NSF Attachment Protein Receptor*) under Ca^{2+}-free conditions and translocates to the lipid membrane when is bound to Ca^{2+} . The interaction of SV2A with Synaptotagmin

is negatively modulated by Ca^{2+} and positively modulated by SV2A phosphorylation. LRRK2 likely phosphorylates SV2A, thus increasing the bound fraction of Synaptotagmin and promoting vesicle fusion with the presynaptic membrane. In addition, LRRK2 interacts with NSF, a protein involved in the dissociation of the SNARE complex (Tong et al., 2009). LRRK2 was shown to interact via phosphorylation of the AP2/clathrin/dynamin-1 complex (Piccoli et al., 2011), and all these proteins participate in the first event of endocytosis of synaptic vesicles. Another possible target of LRRK2 may be the clathrin chains and the AP2 complex: the kinase domain likely modulates the binding to the membrane (Fingerhut et al., 2001). LRRK2 might therefore regulate the endocytosis acting on the phosphorylation status of these interactors. A recent study on the structure of the presynaptic site reveals that LRRK2 silencing leads to a spatial redistribution of vesicles in terms of distance from the presynaptic membrane, alters recycling dynamics and increases vesicle kinetics, thereby proving that LRRK2 plays a role in this mechanism (Piccoli et al., 2011). Finally, LRRK2 phosphorylates endofilline A (EndoA), a conserved protein that is critically involved in synaptic vesicle endocytosis. In vitro experiments demonstrated that LRRK2-mediated EndoA phosphorylation affects membrane tubulation and association. This phosphorylation modulates the endocytosis of synaptic membrane in vivo, blocking the separation of synaptic proteins from the membrane (Matta et al., 2012). These features suggest that LRRK2 facilitates efficient vesicle formation in synapses, through its kinase activity.

Of note, because LRRK2 levels are particularly low in nigral dopaminergic neurons as compared with their high expression in striatal medium-sized spiny projection neurons (MSNs) (Mandemakers et al., 2012), the possibility that LRRK2 plays an important role on the postsynaptic side has been hypothesized. Interestingly, recent studies show that LRRK2 interacts with PKA, which mediates important signaling pathways critical for neuron function, in MSNs. At the postsynaptic side, PKA signaling is activated by DA acting via D1 DA receptors. In addition, PKA regulates glutamatergic transmission by modulating channel properties through direct phosphorylation, and its activity is modulated by A kinase anchoring proteins (AKAPs), which recruit PKA to distinct locations placing kinase close to their appropriate substrates. LRRK2 is considered to be an AKAP-like regulator of the subcellular distribution of a PKA subunit, PKARIIβ, which is particularly abundant in MSNs. In particular LRRK2 seem to acts as a negative modulator of PKA in the MSNs during synaptogenesis and in response to DA receptor activation (Parisiadou et al., 2014).

LRRK2: animal models

In the last decade, under the impulse of the discovery of LRRK2 and its role in PD, cellular and animal models have been developed that provided important insights into the pathobiology of LRRK2, representing a fundamental tool to identify and validate the molecular and cellular mechanisms underlying a genetically-linked disease. Traditionally, animal models of PD have been generated using substances able to mimic the dysfunction of nigrostriatal transmission by blocking DA release and DA receptors (reserpine and neuroleptics; functional models) or by destroying DA neurons (neurotoxins 6-OHDA; (Ungerstedt et al., 1974) or MPTP (Langston and Ballard, 1983) ; neurodegeneration models) (Dauer and Przedborski, 2003). These pharmacological models have had enormous value in helping understand the consequences of nigrostriatal dopaminergic cell loss, in developing neuroprotective approaches and testing symptomatic/neuroprotective therapies. Unfortunately, these models replicate only partly the neuropathological features of human PD and have limited predictivity value. Moreover, the growing demand of understanding the pathophysiological mechanisms of familial PD would remain unfulfilled using these models.

Numerous new models of PD based on genetic manipulation have been generated over the last ten years (Daniel and Moore, 2014; Melrose et al., 2006). Intense efforts have focused on the generation of LRRK2 animal models, although these have proved somewhat limited in terms of recapitulating the whole phenotype of human PD (Beal, 2010). Nonetheless, all current LRRK2 models present unique differences and offer different advantages. Some LRRK2 models display different LRRK2-related phenotypes in terms of motor deficits, cytopathology, changes in dopaminergic neurotransmission, whereas other models, such as worms,flies certain transgenic rodent models, and rodent viral models show sustained dopaminergic neurodegeneration upon overexpression of human G2019S LRRK2 mutation (Daniel and Moore, 2014). To note, rodent models represent the most important tool to understand the pathological function of LRRK2 because genomic analysis reveal that Drosophila and C. elegans do not contain true orthologs of human LRRK2, and the absence of basal ganglia circuitry in invertebrates together with their short life span make them imperfect models for studying PD. For these reasons, different rodent models have been developed.

LRRK2 knockout models

To study the role of LRRK2 in the brain, different groups analyzed the impact of genetic deletion of LRRK2. Different approaches have been used to generate LRRK2 knockout (KO) models, including deletion of different exons or promoters, and as a consequence, different results have been obtained. LRRK2 KO mice obtained through deletion of the kinase domain (exon 40) or the GTPase domain (exon 2; exon 1 and exon 29-30) encoding regions, display an intact nigrostriatal dopaminergic pathway up to 2 years of age. Moreover, mice are viable, fertile, do not display motor deficits and do not exhibit altered sensitivity to MPTP-induced neurotoxicity. In addition, neuropathological features including α-synuclein accumulation or aggregation in the brain, ubiquitin accumulation, gliosis or altered neuronal structure, are absent in LRRK2 KO mice (Andres-Mateos et al., 2009; Tong et al., 2010). Conversely, a recent study (Hinkle et al., 2012) shows that the deletion of exon 41, that encodes the activation hinge of the kinase domain, induces abnormal exploratory activity in 20-month-old LRRK2 KO mice, without affecting the nigrostriatal dopaminergic pathway. Of note, different independent groups showed a relationship between LRRK2 removal and age-dependent kidney and lung abnormalities, including reduced size due to increased apoptosis, enhanced autophagic activity, altered morphology with prominent α-synuclein and ubiquitin accumulation (Herzig et al., 2011; Tong et al., 2012). Furthermore, although proliferation and survival of neural precursors is not altered in LRRK2 KO mice, and the loss of LRRK2 has no effect on the spine dynamics in MSNs (Hinkle et al., 2012), the immature neuroblasts show enhanced dendritic branching and complexity while the density of mossy fibers projecting from the dentate gyrus to the hippocampal CA3 region is increased (Paus et al., 2013). This suggests a regulatory role for LRRK2 in adult neurogenesis.

LRRK2 transgenic models

The generation of inducible transgenic mice overexpressing human LRRK2 under transcriptional control of a tetracycline operator (TetO)-regulated promoter, crossed with transgenic mice expressing a Tet transactivator (tTA) from the CamKIIa promoter (Parisiadou et al., 2009), provide interesting evidence for the pathological interaction of LRRK2 and α-synuclein in PD. Despite no signs of neurodegeneration, but only altered microtubule organization and Golgi fragmentation, were detected in these transgenic lines, the overexpression of WT or G2019S LRRK2 accelerated the progression of A53T α-synuclein-mediated neuropathology (Lin et al., 2009). Unfortunately, to date no consistent

evidence can explain whether LRRK2 increases α-synuclein neuronal damage and why the pathological interaction of these two proteins is restricted to specific neuronal populations.
Recently, a new transgenic line has been generated, in which the expression of G2019S and R1441C LRRK2 has been obtained under the transcriptional control of a hybrid CMV-enhanced human platelet derived growth factor β-chain promoter (CMVe- PDGFb) (Ramonet et al., 2011). Interestingly, although no alteration in locomotive activity or in DA striatal levels and re-uptake were detected, the overexpression of G2019S LRRK2 induced a progressive degeneration of nigrostriatal dopaminergic neurons in mice. Conversely, R1441C LRRK2 transgenic mice exhibited an impairment in locomotor activity and a reduction in catecholamine levels in the cerebral cortex. In addition, the overexpression of G2019S or R1441C LRRK2 induced the accumulation of autophagic vacuoles and damaged mitochondria in the brains of aged mice, and increased tau phosphorylation without changing ubiquitin or α-synuclein levels (Ramonet et al., 2011). Interestingly, the expression of I2020T LRRK2 under the control of another promoter (CMV),displayed a transient impairment of locomotor activity, reduced striatal dopamine levels, fragmented Golgi apparatus, and an elevated degree of tubulin polymerization associated with reduced neurite length (Maekawa et al., 2012). Zhou and coworkers generated constitutive and inducible lines of transgenic rats expressing G2019S LRRK2 (Zhou et al., 2011). They showed that constitutive expression of LRRK2 fails to induce locomotor abnormalities, whereas the conditional expression of LRRK2 in adults causes impaired DA re-uptake leading to enhanced locomotor activity. This suggests an involvement of the DA transporter (DAT). Unfortunately, this behavioral alteration is not associated with pathological dopaminergic features such as α-synuclein or ubiquitin inclusion. This model likely recapitulates early dopaminergic neuronal dysfunction potentially akin to asymptomatic subjects carrying the G2019S mutation (Zhou et al., 2011).
In addition to the above mentioned transgenic animals, different groups generated models using the bacterial artificial chromosome (BAC) construct which typically randomly integrates within the genome at a lower copy number than mini-gene cassettes used for the conventional transgenic models. Using a BAC clone expressing the entire mouse LRRK2 genomic sequence, Li and colleagues showed that expression of WT or G2019S LRRK2 alters striatal dopamine transmission in an opposite manner. Indeed WT BAC LRRK2 mice have enhanced striatal dopamine release and are hyperactive, while G2019S BAC LRRK2 mice show normal motor function, but display an age-dependent decrease of

striatal DA release (Li et al., 2010). Unexpectedly, WT LRRK2 BAC mice exhibit, albeit to a lesser extent than G2019S BAC mice, a number of phospho-tau-positive cells in striatum. G2019S LRRK2 BAC mice generated by Melrose and coworkers (Melrose et al., 2010) showed reduced extracellular DA levels in striatum and an age-dependent increase in tau levels and phosphorylation, suggesting altered tau metabolism. Furthermore G2019S LRRK2 BAC mice also exhibited reduced adult neurogenesis (Winner et al., 2011) and altered neurite outgrowth and spine density of hippocampal neurons. Collectively, studies in BAC mice show a neuropathological phenotype characterized by dysfunction of nigrostriatal dopaminergic neurotransmission, and suggest a probable role for LRRK2 in the regulation of motor function, although they do not exhibit the dopaminergic neurodegeneration shown by the transgenic models (Ramonet et al., 2011). Simultaneously with the generation of transgenic models, different groups adopted other approaches, such as developing knockin (KI) mice or directly delivering genes into the rodent brain by the use of viral vectors. LRRK2 R1441C KI mice have been generated by introducing the R1441C mutation into exon 31, thereby allowing its expression under the control of endogenous regulatory elements. Unfortunately, this model failed to summarize the principal features of the PD phenotype, showing only an impairment in amphetamine-stimulated locomotor activity, altered dopamine D2 receptor-mediated function in the striatum and reduced catecholamine release in cultured chromaffin cells (Tong et al., 2009). On the other hand, acute injection of LRRK2 via viral vectors provided evidence of direct neuronal toxicity. Recently, two rodent models of viral-mediated LRRK2 expression have been reported. In the first study, Lee and coworkers, via a single unilateral striatal injection of herpes simplex virus (HSV) expressing a CMV-driven GFP reporter and untagged human LRRK2, reported a modest toxic effect of WT LRRK2 (∼10–20%) and a significant 50% nigral DA cell loss associated with reduced striatal DA levels following G2019S LRRK2 expression. In the other study, human WT or G2019S LRRK2 has been tagged by using a second-generation human serotype 5adenoviral (rAd) vectors. After striatal injection, G2019S LRRK2 expression in rats induced the progressive loss of ∼20% of dopaminergic neurons in the ipsilateral SN, without a corresponding reduction of striatal dopaminergic fiber density (Dusonchet et al., 2011).

Unfortunately, these models display important limitations such as the poor retrograde transport of adenovirus to the SN and a progressive reduction of transgene expression over time, making them unsuitable for long-term studies on the pathological effects of G2019S LRRK2 expression in vivo.

AIMS OF THE STUDY

The main goal of this thesis work was to evaluate the role played by the kinase function of LRRK2 in the expression of motor phenotype and dopamine transmission in mice.

To directly explore the impact of the kinase-enhancing G2019S mutation on motor activity in vivo, a longitudinal phenotyping approach was developed. To this purpose we enrolled two cohorts of G2019S knock-in (KI) mice and wild-type littermates (WT), and analyzed their motor activity from the age of 3 to 19 months, using a set of complementary behavioral tests, specific for akinesia, bradykinesia and overall gait ability. To confirm that enhanced kinase activity accounts for this phenotype we used both a genetic and a pharmacological approach. We first performed a parallel longitudinal study in mice carrying a LRRK2 mutation (D1994S) that impairs kinase activity (kinase-dead, D1994S KD), in comparison with their own WT. Then we tested the ability of small molecular-weight ATP analogous LRRK2 kinase inhibitors to reverse the hyperkinetic phenotype of G2019S KI mice.

In order to investigate whether the hyperkinetic phenotype of G2019S mice was associated with dysfunction of striatal dopamine neurotransmission, in the second part of this study we carried out a series of behavioral, biochemical, and neurochemical experiments. The motor responses of these mice to DA receptor agonists and antagonists were analyzed. Moreover we focused our attention on the impact of G2019S LRRK2 mutation on DA reuptake and release processes, using in vitro and in vivo (microdialysis) techniques.

METHODS

SUBJECTS

Male homozygous LRRK2 G2019S KI and D1994S KD mice backcrossed on a C57Bl/6J background were used in this study. Mice were obtained from Novartis Institutes for BioMedical Research, Novartis Pharma AG (Basel, Switzerland) at the age of about 2 months, and accommodated in the vivarium of the University of Ferrara. Male non-transgenic wild-type (WT) mice were littermates obtained from the respective heterozygous breeding. The mice used in our study were generated at Novartis laboratories, and were previously characterized from several biochemical and neuropathological standpoints, although motor analysis was limited to the open field in 5-month old animals (Herzig et al., 2011). Mice employed in the study were kept under regular lighting conditions (12 h light/dark cycle) and given food and water ad libitum. Experimental procedures involving the use of animals were approved by the Ethical Committee of the University of Ferrara and the Italian Ministry of Health (licenses 171/2010-B and 318/2013-B). Adequate measures were taken to minimize animal pain and discomfort.

BEHAVIORAL ANALYSIS

Experimental design: longitudinal study (Part 1)

The longitudinal study was conducted on two cohorts of G2019S KI (n = 19) and their WT (n = 12) littermates. Mice were subjected to motor tests at 3, 6, 10, 15 and 19 months (Fig. 4). D1994S KD and their WT mice (n= 10 each) were tested at 3, 6, 10 and 15 months (Fig. 4). Separate, age-matched cohorts of 3, 10, 14 and 18-month-old WT and G2019S KI mice (6–8 mice per group) were enrolled in transversal behavioral studies, to parallel the results of the longitudinal study. Finally, other cohorts of mice (n= 10 each genotype) were used for pharmacological studies with LRRK2 kinase inhibitors at 6, 12 and 15 months (G2019S KI), or 12 months (D1994S KD).

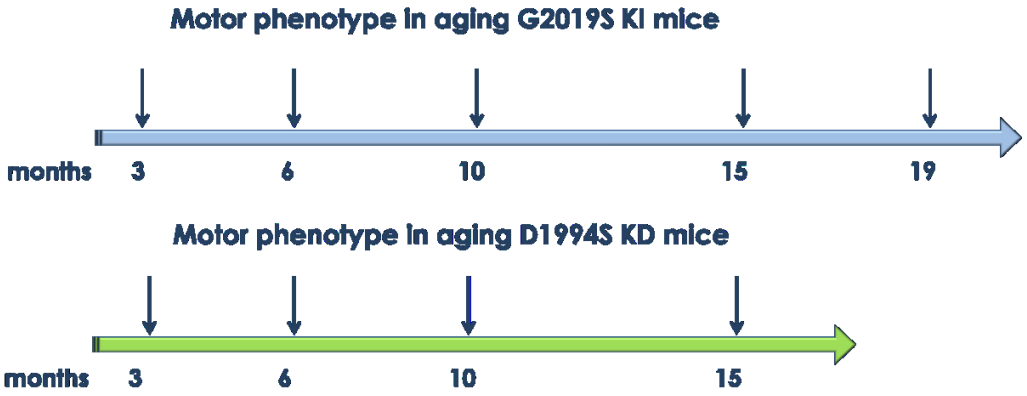

Fig. 4. Experimental design adopted in longitudinal study.

LRRK2 kinase inhibitor administration

Twelve-month-old mice were administrated i.p. with the LRRK2 kinase inhibitor H-1152 (Nichols et al., 2009; Sasaki et al., 2002; Tamura et al., 2005) at two different dose levels (0.1 and 1 mg/kg), or with the LRRK2 kinase inhibitor Nov-LRRK2-11 (Herzig et al., 2011; Troxler et al., 2013), at two different dose levels (1 and 10 mg/kg) for the indicated time. H-1152 was dissolved in 0.9% saline solution whereas Nov-LRRK2-11 in 3% DMSO/3% Tween 80.

Experimental design: study on dopaminergic transmission (Part 2)

Pharmacological studies were performed on two cohorts of 11-16 month-old G2019S KI (n= 8-10) and their WT (n= 7-9) littermates. Prior to pharmacological testing, animals were trained for approximately 6 days to the specific motor tasks until their performance became reproducible. Tests were repeated in a fixed sequence before (control session) and at different time-points (depending on the experiment) after drug administration. Experimenters were unaware of genotype and treatments. Separate cohorts of 19 months old G2019S KI and WT mice were enrolled in neurochemical analysis by using in vivo microdialysis (18-16 mice per group).

Drugs administration

Eleven-month-old mice were acutely administrated i.p. with the D2/D3 receptor antagonist haloperidol at the dose of 0.3 mg/kg, or with the D2/D3 receptor agonist pramipexole at four different dose levels (0.0001-0.001-0.01 and 0.1 mg/kg (Viaro et al., 2013). Sixteen-month-old mice were injected i.p. with D1/D5 receptor antagonist SCH-23390 at the dose of 0.01 mg/kg, or with the DAT inhibitor GBR-12783 at two different dose levels (6 and 20 mg/kg). Seventeen-month-old G2019S KI mice were administrated i.p. with the LRRK2 kinase inhibitor Nov-LRRK2-11 (Herzig et al., 2011; Troxler et al., 2013) at the dose of 10 mg/kg, and 15 min, later with GBR-12783 (20 mg/kg; i.p.). Haloperidol, pramipexole and SCH-23390 were dissolved in 0.9% saline solution; GBR-12783 was dissolved in 0.3 % DMSO /0.9% saline solution whereas Nov-LRRK2-11 in 3% DMSO/3% Tween 80/0.9% saline solution.

Bar test

Originally developed to quantify morphine-induced catalepsy (Kuschinsky and Hornykiewicz, 1972), this test measures the ability of the animal to respond to an externally imposed static posture. Also known as the catalepsy test (for a review see (Sanberg et al., 1988)), it can also be used to quantify akinesia (i.e. time to initiate a movement) also under conditions that are not characterized by increased muscle tone (i.e. rigidity) as in the cataleptic/catatonic state. Mice were gently placed on a table and forepaws were placed alternatively on blocks of increasing heights (1.5, 3 and 6 cm). The time (in seconds) that each paw spent on the block (i.e. the immobility time) was recorded (cut-off time of 20 s). Performance was expressed as total time spent on the different blocks.

Drag test

Modification of the ‘wheelbarrow test’ (Schallert et al., 1979), this test measures the ability of the animal to balance its body posture with the forelimbs in response to an externally imposed dynamic stimulus (backward dragging) (Marti et al., 2005). It gives information regarding the time to initiate and execute (bradykinesia) a movement. Animals were gently lifted from the tail leaving the forepaws on the table, and then dragged backwards at a

constant speed (about 20 cm/s) for a fixed distance (100 cm). The number of steps made by each paw was recorded. Five to seven determinations were collected for each animal.

Rotarod test

The fixed-speed rotarod test (Rozas et al., 1997) measures different motor parameters such as motor coordination, gait ability, balance, muscle tone and motivation to run. Mice were tested over a wide range of increasing speeds (0–55 rpm; 5 rpm steps, increased every 180 s) on a rotating rod (diameter of the cylinder 8 cm) (Marti et al., 2004; Viaro et al., 2008) and the total time spent on the rod was recorded.

Spontaneous motor activity

The open field test was used to measure spontaneous locomotor activity in 15-month-old mice. The ANY-maze video tracking system was used (Ugo Basile, application version 4.52c Beta) as previously described (Rizzi et al., 2008). Briefly, mice were placed in a square plastic cage (40 × 40 cm), one mouse per cage, and ambulatory behavior (horizontal activity) was monitored for 60 min with a camera. Four mice were monitored simultaneously each experiment. Total distance traveled (m) and immobility time (sec) were recorded.

In vivo microdialysis

Two concentric microdialysis probes (1 mm Cuprophane membrane with a 6 kDa cut-off; AgnTho's, Stockolm, Sweden) were stereotaxically implanted in both dorsal striata (coordinates from the bregma: AP +0.6, ML ±2.0, DV −2.0; Paxinos and Franklin, 2001; Fig. 5) of isoflurane-anesthetized mice. Twenty-four hours after implantation, probes were perfused (2.1 µl/min) with a modified Ringer solution (in nM $CaCl_2$ 1.2; KCl 2.7; NaCl 148 and $MgCl_2$ 0.85) and samples were collected every 20 min (Bido et al., 2011; Mabrouk et al., 2010; Volta et al., 2010) after a 6 h wash-out period. Experiments were run at 24, and 48 h after implantation, and treatments were randomized. GBR-12783 and Nov-LRRK2-11 were administrated i.p. at the respective dose of 20 mg/kg and 10 mg/kg. At least three baseline samples were collected before drug treatment. At the end of the

experiments, animals were sacrificed and the correct placement of the probes was verified histologically.

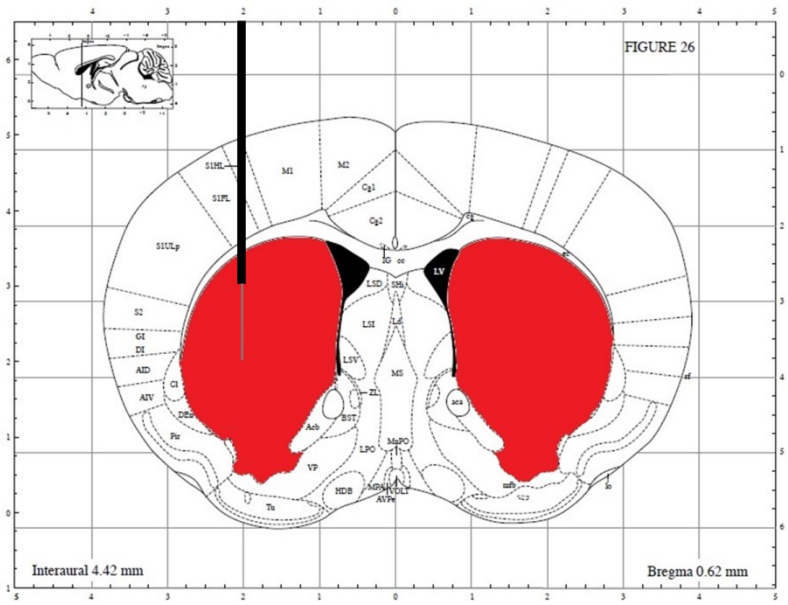

Fig. 5. Probe position during in vivo microdialysis experiments (Paxinos and Franklin, 2001).

Neurochemical analysis using LC-MS

Dopamine (DA), glutamate and GABA concentrations in dialysates were analyzed using a benzyolation derivatization LC-MS method described by (Song et al., 2012). Briefly, 5 µl dialysate samples were derivatized by adding 2.5 µl of 100 mM sodium tetraborate, 2.5µl of 2% benzoyl chloride in acetonitrile, and then 2.5 µl of a stable 13C benzoylated isotope internal standard mixture was then added to improve quantitation. A Thermo Fisher Accela UHPLC (Waltham, MA) system automatically injected 5 µl of the sample onto a Waters (Milford, MA) HSS T3 reverse phase HPLC column (1 mm X 100 mm, 1.8 µm). Mobile phase A consisted of 10 mM ammonium formate and 0.15% formic acid. Mobile phase B was pure acetonitrile. Analytes were detected by an Thermo Fisher TSQ Quantum Ultra triple quadrupole mass spectrometer operating in multiple reaction monitoring (MRM) mode. Run times were approximately 6 min.

EX VIVO STUDIES

Synaptosomes preparation

Mice were anesthetized and decapitated, the brains were quickly removed, and striatal tissue was rapidly dissected. To prepare synaptosomes, striatal tissue from each mouse was homogenized in ice-cold 0.32 M sucrose (pH 7.4) with a Teflon-glass homogenizer and centrifuged at 1000 g for 10 min at 4°C. The supernatant was then centrifuged at 12,000 g for 20 min at 4°C. The resultant pellet was resuspended in binding buffer (50 mM Tris HCl, pH 7.4, 100 mM NaCl) for [3H]-WIN 35,428 saturation binding experiments or ice-cold uptake buffer (125 mM NaCl, 5 mM KCl, 1.5 mM MgSO4, 1.25 mM CaCl2, 1.5 mM KH_2PO_4, 10 mM D-glucose, 25 mM HEPES, 0.1 mM pargyline, and 0.5 mM L-ascorbic acid, pH 7.4) for DA uptake assays.

[^{3}H]-WIN 35,428 saturation binding experiments

Saturation binding experiments were carried out with [^{3}H]-WIN 35,428 (specific activity 84 Ci/mmol; Perkin-Elmer, Boston, MA, USA) as radioligand (Chen et al., 1996). Synaptosomes from WT (n = 3) and G2019S KI (n = 3) mice were incubated in assay buffer (50 mM Tris HCl, pH 7.4, 100 mM NaCl) with different concentrations (0.5 – 50 nM) of radioligand for 120 min at 4°C. Nonspecific binding was determined in the presence of 5 μM GBR-12783. At the end of the incubation time, bound and free radioactivity were separated by filtering the assay mixture through Whatman GF/B glass fiber filters in a Brandel cell harvester (Brandel Instruments, Unterföhring, Germany). Filter bound radioactivity was counted in a Perkin Elmer 2810TR scintillation counter (Perkin-Elmer, Boston, MA, USA).

Dopamine Uptake Assay

Synaptosomal preparations from G2019S KI (n = 3) and WT (n = 3) mice were incubated for 5 min at 37°C with 20 nM [3H]-DA (specific activity 40 Ci/mmol; Perkin-Elmer, Boston, MA, USA) isotopically diluted with varying concentrations of unlabeled DA to obtain final DA concentrations in the range 20 nM – 2.0 μM. Non-specific dopamine uptake was evaluated in the presence of 5 μM GBR-12783. The reaction was terminated by filtering the assay mixture through Whatman GF/B glass fiber filters using a Brandel cell

harvester (Brandel Instruments, Unterföhring, Germany). The filter-bound radioactivity was counted using a Perkin Elmer Tri Carb 2810 TR scintillation counter. Specific DA uptake, defined as the difference between DA accumulated in the absence and in the presence of GBR-12783, was expressed as picomoles per milligram of protein per minute (Zhu et al., 2009).

The protein concentration was determined according to a Bio-Rad method with bovine albumin as standard reference. Kinetic parameters (Vmax and Km) were determined using Prism 5.0 (GraphPad Software Inc., San Diego, CA).

In vivo PK study

In order to gain insights on the brain penetration of Nov-LRRK2-11, a screening cassette approach was used, as previously described (Troxler et al., 2013). Adult male C57Bl/6 mice (20–30 g, Iffa-Credo, France) were orally administered (by gavage) with Nov-LRRK2-11 (suspended in carboxymethylcellulose 0.5 % w/v in water with Tween 80 at 0.5% v/v) at a dose of 3 mg/kg p.o.. Volume of oral administration was 10 mL/kg body weight. After drug cassette administration, blood (~50 µL in EDTA) was collected at different time points (15 min, 30 min, 1, 2, 4, 8 and 24 h postdose, n = 3 mice per time-point,) either by puncture of the sublingual vein (~70 µL/mouse, under light anesthesia) or by puncture from the vena cava at sacrifice (~300 µL/mouse). Moreover, at sacrifice (at 15 min, 1, 4, and 24 h post-dose), brains were removed, weighted and immediately frozen on dry ice. Blood and brain samples were stored at −20 °C until analysis. Samples were analyzed for Nov-LRRK2-11 content with LC–MS/MS methodologies.

Cell cultures and treatments

NIH3T3 cells were cultured in Dulbecco's Modified Eagle's medium (Life technologies) supplemented with 10% fetal bovine serum (Life technologies), penicillin and streptomycin (Life technologies) and maintained at 37 °C in a 5% CO2 controlled atmosphere. H-1152 and Nov-LRRK2-11 were dissolved in 0.9% saline solution and in 3% DMSO/3% Tween 80/0.9% saline, respectively. Inhibitors were used at the indicated concentrations, and equivalent volumes of saline solution were used as control. Inhibitors were added to the culture medium for 90 min before cell lysis.

Cells and tissue lysis

NIH3T3 cells, as well as striatum and cortex obtained from brain dissection were homogenized and solubilized in lysis buffer (20 mM Tris– HCl pH 7.5, 150 mM NaCl, 1mM EDTA, 2.5 mM sodium pyrophosphate, 1 mM β-glycerophosphate, 1 mM Na_3VO_4) supplemented with 1% Triton X-100 (Sigma Aldrich) and protease inhibitor cocktail (Roche), then cleared at 14,000 g at 4 °C for 30 min. Protein concentrations were determined using the bicinchoninic acid assay (BCA) as manufacturer's instructions (Thermo Scientific).

Western blotting

Proteins were separated by electrophoresis into pre-casted 4-20% SDS-PAGE gels (Biorad) and subsequently transferred onto Immobilon-P membrane (Millipore). Membranes were first incubated 1 h at RT with rabbit anti-LRRK2 phospho Ser935 (1:300, Abcam, RabMAbs cat#ab133450), rabbit anti-LRRK2 UDD3 (1:1000, Abcam, RabMAbs cat# ab133518), rabbit anti-DAT (1:1000, Sigma Aldrich), anti-VMAT2 (1:300, Sigma Aldrich), mouse anti-GADPH (1:4000, Millipore) and mouse anti-tubulin (1:3000, Millipore) then with HRP-conjugated secondary antibodies (Sigma) for 1 h at room temperature and then incubated with enhanced chemiluminescent (ECL) western blot substrate (Thermo Scientific).

Immunohistochemistry

Mice were deeply anesthetized (ketamine 85 mg/kg; i.p.) and transcardially perfused with 4% paraformaldheyde in Phosphate Buffer Solution (PBS; 0.1 M, pH 7.4). Brains were removed, transferred to a 20% sucrose solution in PBS for cryoprotection and then stored at -80°C. They were then cut with a cryostat (Leica, Nussloch, Germany) to obtain 35 µm coronal sections of Striatum (STr; AP from +1,42 to +0,14 from bregma) and Substantia Nigra Pars Compacta (SNc; AP from -3,16 to -3,52 from bregma; Paxinos and Franklin, 2001).

Sections were rinsed in TBS (Tris Buffered Saline), incubated for 1 hr with blocking solution (Bovin Serum Albumin; 3% in TBS) and then incubated overnight with TH primary antibody (Purified rabbit polyclonal antibody; 1:500 in BSA 1% TBS; Merck

Millipore, Darmstadt, Germany) and with a fluorescent marker of Nissl Bodies (Neurotrace; 1:150; Life Technologies, Grand Island, NY, USA). After being rinsed in TBS, sections were incubated with a secondary antibody (AlexaFluor 488, Goat anti-rabbit IgG; 1:500 in TBS; Life Technologies). Sections were then mounted on slides with Shur/Mount Water Based (Hatfield, USA)

Stereology and neuron counting

Stereological analysis was performed with a fluorescence microscope (Leica, Nussloch, Germany) equipped with a motorized Z and X-Y stage; for each animal 5 slices were used in order to analyze the entire volume of the SNc and the area was identified with 10x magnification according to the mouse brain atlas (Paxinos and Franklin, 2001); the area was then divided into 3 rectangles (350 x 260 μm) and each rectangle was then amplified with 40x magnification. To count TH-immunoreactive neurons (phenotypic marker) and Neurotrace stained cells (structural marker) in SNc 8 images of the same rectangle were taken at different levels of the Z axis. The images were then mounted and analyzed off-line using ImageJ (NIH, USA). Every neuron appearing on focus was counted. Average number of neurons ± SEM was calculated for each group.

To analyze dopaminergic striatal innervation, striatal sections were incubated for 1 hr with a blocking solution (Goat Serum 5% in TBS) and overnight with the same TH antibody described above. After rinsing, sections were incubated for 40 min with the same secondary antibody described above and then mounted on slides. Images were taken at 10x magnification with a fluorescence microscope and later analyzed off-line for optical intensity with ImageJ, using Corpus Callosum (ACC) as background.

Data presentation and statistical analysis

Data are expressed as absolute values and are mean ± SEM (standard error of the mean) of n mice. To assess the significance of behavioral changes over the 19-month longitudinal study (Figs. 1-2) a linear mixed-model repeated measures analysis using the REPEATED statement was used, followed by the Bonferroni test (PROCMIXED, SAS, version 9.2, SAS Institute Inc, Cary, NC, USA). Genotype was set as discrete variable, weight as continuous variable. This allowed to verify whether changes in weight could account for changes in behavioral performances. Statistical analysis of drug effect was performed by one-way repeated measure (RM) analysis of variance (ANOVA) followed by the

Newman–Keuls test for multiple comparisons, or by two-way ANOVA followed by Bonferroni test for multiple comparisons (Table 2). The Student's t-test, two tailed for unpaired data was used to compare two groups of data. P-values < 0.05 were considered to be statistically significant.

Drugs

Haloperidol hydrochloride, SCH23390 hydrochloride, pramipexole dihydrochloride, GBR-12783 dihydrochloride and quinpirole hydrochloride were purchased from Tocris Bioscience (Bristol, UK). H-1152 was purchased from SiChem GmbH -BITZ (Bremen, Germany) and Nov-LRRK2-11 was obtained from Novartis Institutes for BioMedical Research, Novartis Pharma AG (Basel, Switzerland).

RESULTS

Part 1

Behavioral analysis of mice carrying mutations within the LRRK2 kinase domain

Characterization of motor phenotype in aging G2019S KI and WT mice

In order to investigate whether the kinase-enhancing G2019S point mutation in murine LRRK2 affects motor performance, two cohorts of G2019S KI mice and age-matched WT littermates (WT) were enrolled in a longitudinal study in which motor activity was measured using the fixed sequence of bar, drag and rotarod tests from 3 through 19 months of age.

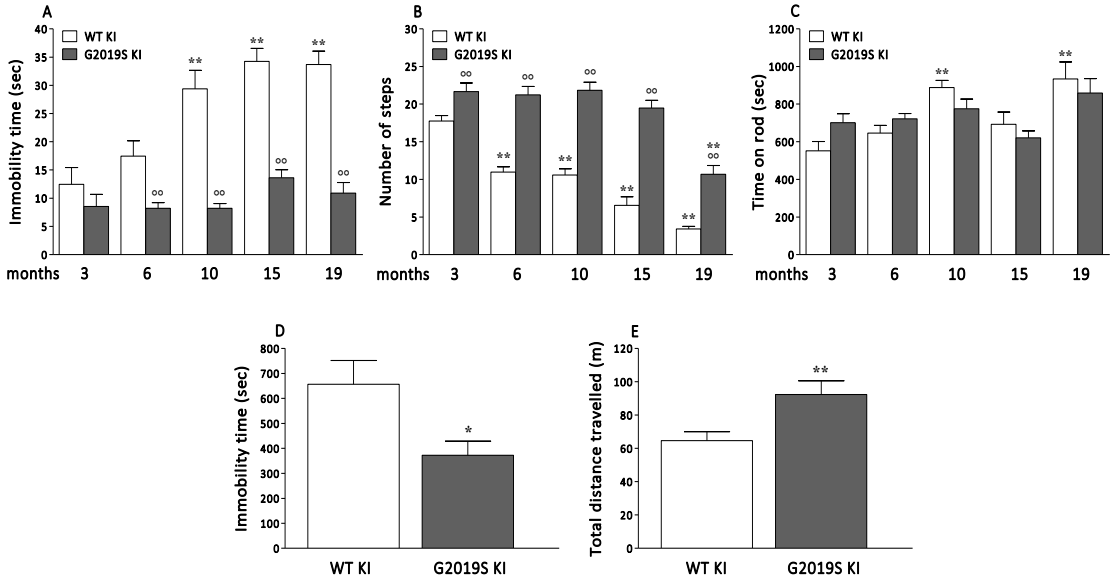

Fig. 6. Motor phenotype in mice during aging. Mice were subjected to a set of tests, namely the bar (A), drag (B) and rotarod (C) tests, from 3 up to 19 months of age. In addition, an open field test was performed in 15-month old animals (D–E). Motor activity was expressed as immobility time (sec; A, D), number of steps (B), time on rod (sec; C), and total distance traveled (m; E). Data are means ± SEM of 9–10 (3–15 months) or 6 (19 months) mice per group, and were analyzed using one-way RM ANOVA followed by the Newman–Keuls test for multiple comparisons. Differences between genotypes at the single time-point levels were evaluated using the Student t-test, two tailed for unpaired data. *P<0.05, **P<0.01 different from3-month-old mice of the same genotype. °P < 0.05,°°P < 0.01 different from age-matched littermates.

Immobility time of G2019S KI mice in the bar test (8.5 ± 2.1 s) was not different from that of WT (12.4 ± 2.9 s) at 3 months (Fig. 6A). Immobility time increased along with aging in WT mice reaching a maximum of 33.7 ± 2.3 s at 19 months. Conversely, G2019S KI mice did not become akinetic with aging, showing similar performances across the study. The difference between genotypes was evident starting at 6 months (~2-fold), and attained

stable values (~3-fold) from 10 months onward. In the drag test (Fig. 6B), a significant effect of genotype ($F_{1,75}$ = 91.11, p < 0.0001), time ($F_{4,75}$ = 26.78, p = 0.0027) and their interaction ($F_{4,75}$ = 6.11, p = 0.0003) was found. As in the bar test, no significant influence of weight was observed ($F_{1,75}$ = 1.54, p = 0.22). G20 19S KI mice showed a significant 23% greater stepping activity than WT at 3 months (21.7 ± 1.1 vs 17.7 ± 0.7 steps, respectively). This difference became 2–3-fold larger in older animals, since stepping activity of WT mice progressively worsened over time, reaching 3.4 ± 0.3 steps at 19 months, whereas that of G2019S KI mice remained stable up to 15 months, showing a significant decline only at 19 months (10.7 ± 1.1 steps). Different from the bar and drag test, no significant effect of genotype was found in the rotarod test ($F_{1,75}$ = 0.01, p = 0.92), but a significant effect of time ($F_{4,75}$ = 8.24, p < 0.0001) and genotype × time interaction ($F_{4,75}$ = 3.81, p = 0.0071). Also in this test, the influence of weight was not significant ($F_{1,75}$ = 0.03, p = 0.86). Mild improvement of rotarod performance in WT mice was observed along with aging (10 and 19 months), whereas that of G2019S KI mice remained stable throughout the study (Fig. 6C). The open field test was performed in 15-month-old animals. G2019S KI mice showed 42% shorter immobility time (t= 2.53, df=8, p= 0.036; Fig. 6D) and 43% longer distance traveled (t = 4.15, df = 8, p = 0.003; Fig. 6E) compared to WT. To confirm the hyperkinetic phenotype of G2019S KI mice, the bar, drag, rotarod and open field tests were repeated in age-matched separate cohorts of 3, 10, 14 and 18-month-old-mice, not involved in the longitudinal study (Fig. 7). These experiments substantially confirmed that G2019S KI mice were hyperactive, with significant differences with WT emerging already at 3 months in the bar and drag tests, and at 10 months in the open field. As in the longitudinal study, no differences in rotarod performance were observed between age matched cohorts of WT and G2019S KI mice.

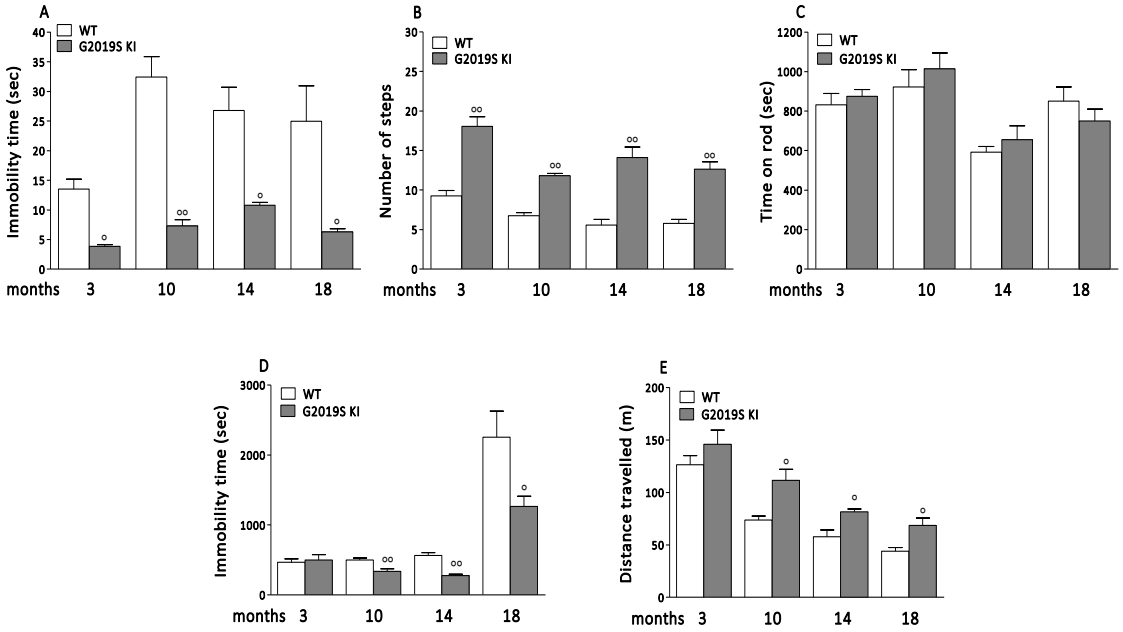

Fig. 7. Motor performance was evaluated in age-matched cohorts of 3, 10, 14 and 18-month-old G2019S KI and WT mice, using the bar (A), drag (B), rotarod (C) and open field (D-E) tests. Motor activity was expressed as immobility time (sec; A, D), number of steps (B), time on rod (sec; C), and total distance travelled (m; E). Data are means ± SEM of 6-8 mice per group, and were analyzed using the Student t-test two-tailed for unpaired data. °P<0.05,°°P<0.01 different from age-matched WT.

G2019S KI mice had throughout the study a lower body weight than WT (Table 2). The difference was 14% on average. In the bar test (Fig. 6A), a significant effect of genotype ($F_{1,75}$ = 45.52, p < 0.0001), time ($F_{4,75}$ = 4.47, p = 0.0027) and their interaction ($F_{4,75}$ = 6.40, p = 0.0002) was found. The influence of weight was found not to be significant ($F_{1,75}$ = 3.50, p = 0.07).

	Age (months)				
Genotype	**3**	**6**	**9**	**15**	**19**
G2019S KI (g)	23.8 ± 0.9** (11)	27.5 ± 0.4** (11)	30.4 ± 0.4** (11)	30.9 ± 0.4** (11)	31.8 ± 0.4* (6)
WT (g)	28.8 ± 0.8 (9)	31.5 ± 0.8 (9)	34.7 ± 0.8 (9)	35.3 ± 1.2 (9)	36.2 ± 1.4 (6)
D1994S KD (g)	25.6 ± 0.4 (10)	nt	32.0 ± 0.6 (10)	33.1 ± 0.7 (10)	Nt
WT(g)	26.0 ± 0.4 (9)	nt	33.4 ± 0.7 (9)	34.6 ± 0.7 (9)	Nt

Table 2. G2019S KI mice weighed less than WT littermates throughout the study. No difference was observed between D1994S KD and respective WT littermates. Data are expressed in grams and are means ± SEM of the number of mice indicated in parentheses. *P < 0.05, **P < 0.01 different from WT (2-way ANOVA followed by the Bonferroni post hoc test). nt= not tested

Characterization of motor phenotype in aging D1994S KD and WT mice

Since experiments in G2019S KI mice suggested that enhancement of kinase activity is associated with greater motor performance, we investigated if kinase activity silencing mutation might cause a differential effect. To this purpose, we used mice bearing the kinase-inactivating point mutation D1994S (D1994S KD) and age-matched WT littermates. No difference in weight was observed between D1994S KD and WT mice throughout the study (Table 2). Statistical analysis of bar test values revealed no significant effect of genotype ($F_{1,67} = 0.1$, $p = 0.74$), a significant effect of time ($F_{3,67} = 31.23$, $p < 0.001$) but not a genotype × time interaction ($F_{3,67} = 1.17$, $p = 0.31$). Likewise, in the drag test, a significant effect of time ($F_{3,67}= 42.21$, $p < 0.001$), but not of genotype ($F_{1,67} = 0.48$, $p = 0.49$) or genotype × time interaction ($F_{3,67}= 0.56$, $p= 0.64$) was found. Only in the rotarod test, a significant effect of genotype ($F_{1,67}= 16.11$, $p= 0.0002$) and time ($F_{3,67}= 10.79$, $p < 0.0001$) but not their interaction ($F_{3,67}= 0.63$, $p= 0.62$) was found. Overall, basal activity in the bar (Fig. 8A), drag (Fig. 8B) and rotarod (Fig. 8C) test was similar between D1994S KD mice and their WT at any age analyzed. As expected, WT but as well D1994S KD mice showed a significant worsening of motor activity in the bar (increase of immobility time) and drag (reduction of stepping activity) tests at 10 and 15 months. Transient improvement of rotarod performance was observed in WT and D1994S KD mice at 10 months. Consistently, no difference in exploratory behavior was observed between genotypes in the open field at 15 months (immobility time $t=0.21$, $df=7$, $p=0.84$; distance traveled $t=0.03$, $df=7$, $p=0.97$; Figs. 8 D–E).

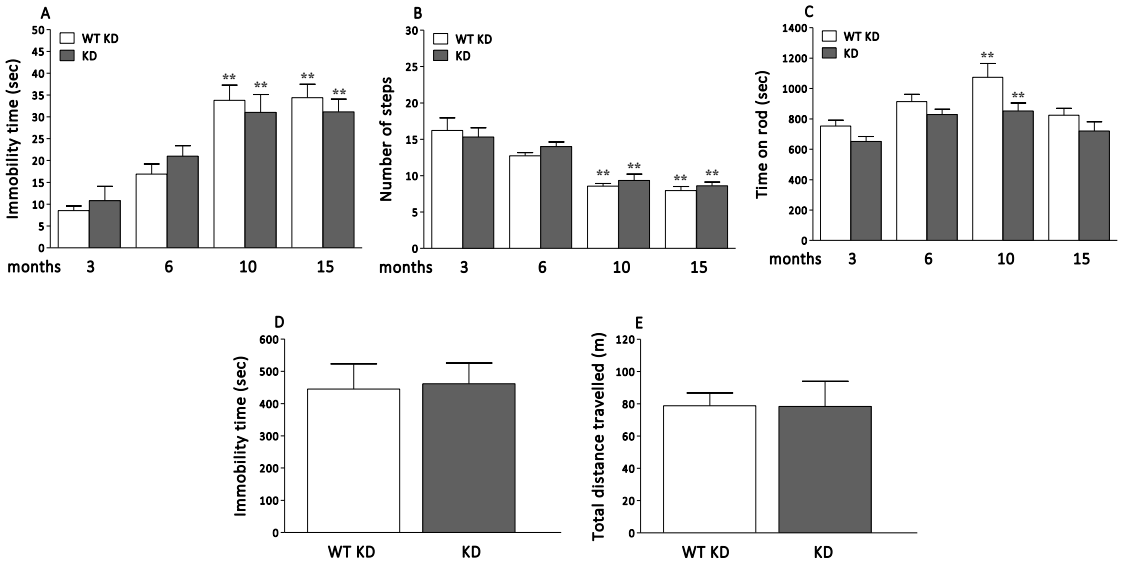

Fig. 8. Mice were subjected to a set of tests, namely the bar (A), drag (B) and rotarod (C) tests, starting at 3 months up to 19 months of age. In addition, an open field test was performed in 15-month-old animals (D–E). Motor activity was expressed as immobility time (sec; A, D), number of steps (B), time on rod (sec; C), and total distance traveled (m; E). Data are means ± SEM of 10 mice per group, and were analyzed using one-way RM ANOVA followed by the Newman–Keuls test for multiple comparisons. Differences between genotypes at the single time-point levels were evaluated using the Student t-test, two-tailed for unpaired data. **P < 0.01 different from 3-month-old mice of the same genotype.

WT mice obtained from both colonies (G2019S KI and D1994S KD) showed substantially similar performances throughout the study (Tab. 3), with the exception of rotarod performance which was significantly lower at 3 and 6 months in WT littermates of G2019S KI mice.

	Age (months)	3	6	9	15	19
WT KI	Bar (sec)	12.5 ± 2.9	17.4 ± 2.7	29.3 ± 3.2	34.2 ± 2.2	33.7 ± 2.3
	Drag (steps)	17.7 ± 0.7	10.9 ± 0.7	10.5 ± 0.8	6.5 ± 1.1	3.4 ± 0.3
	Rotarod (sec)	551.8 ± 49.5*	646.0 ± 40.3*	888.1 ± 37.7	691.9 ± 65.6	934.1 ± 40.2
	Distance (m)	nt	Nt	nt	64.6 ± 5.4	Nt
	Immobility (sec)	nt	Nt	nt	656.3 ± 95.1	Nt
WT KD	Bar (sec)	8.5 ± 1.0	16.9 ± 2.2	33.8 ± 3.4	34.3 ± 3.0	Nt
	Drag (steps)	16.2 ± 1.7	12.7 ± 0.4	8.5 ± 0.3	7.9 ± 0.6	
	Rotarod (sec)	752.3 ± 39.1	913.9 ± 47.4	1075.1 ± 90.1	824.4 ± 44.2	
	Distance (m)	nt	Nt	nt	78.8 ± 7.9	Nt
	Immobility (sec)	nt	Nt	nt	445.0 ± 77.8	Nt

Table 3. A comparison between motor performances of wild-type mice used in the study, i.e. G2019S LRRK2 knock-in (KI) littermates (WT KI) and D1994S LRRK2 kinase-dead (KD) littermates (WT KD). Data are expressed as absolute values and are means ± SEM. *P<0.05, different from WT KD (Student t-test, two-tailed for unpaired data). nt = not tested

Pharmacological inhibition of the LRRK2 kinase activity

Effect of the LRRK2 kinase inhibitor H-1152 on motor phenotype

Since results obtained with G2019S KI and D1994S KD mice suggest that the greater motor performance associated with the G2019S mutation is dependent on kinase activity, we next asked whether LRRK2 kinase inhibitors acutely administered to G2019S KI mice were effective at returning the hyperkinetic phenotypes to WT levels. We first used H-1152, a ROCK (Rho kinase) inhibitor (Nichols et al., 2009; Sasaki et al., 2002; Tamura et al., 2005) which has been previously shown to display high potency against LRRK2 (Gilsbach et al., 2012; Nichols et al., 2009). We initially confirmed that H-1152 was effective at inhibiting endogenous LRRK2 in NIH3T3 mouse fibroblasts, using dephosphorylation of Ser935 as readout of LRRK2 kinase activity, as previously described (Dzamko et al., 2010). As shown in Fig. 9, H-1152 induced Ser935 de-phosphorylation in a concentration-dependent manner, with apparent IC_{50} of 170 nM.

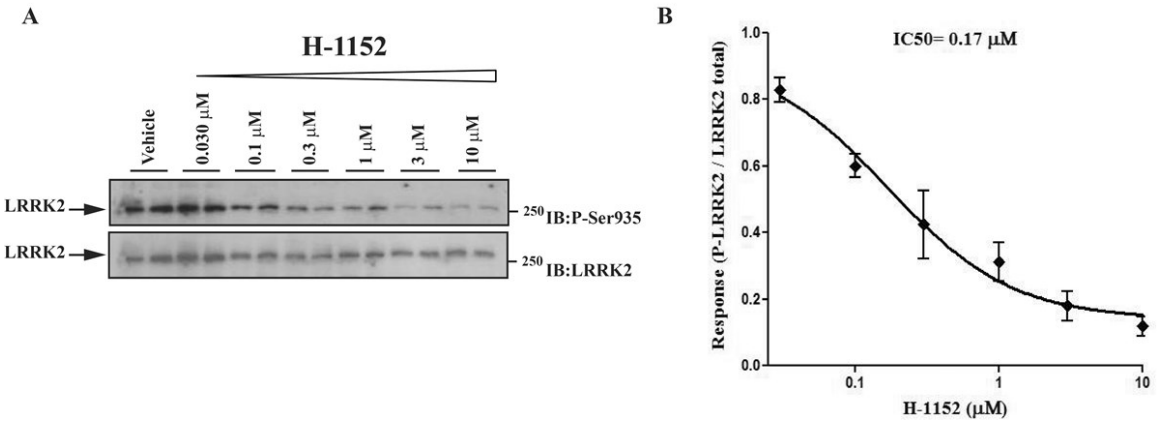

Fig. 9. Blots from lysates of NIH3T3 cells (A) exposed to vehicle or increasing concentrations of H-1152 (0.03–10 µM) for 90 min (B). Data are means ± SEM of 2 experiments performed in duplicate.

We next assessed H-1152 in vivo. In 6-month-old mice, H-1152 was ineffective at 0.1 mg/kg, but increased immobility time (treatment $F_{2,21}$=5.37, p=0.013; time $F_{1,21}$=0.72, p=0.41; time × treatment interaction $F_{2,21}$=10.87, p<0.0001; Fig. 10A) and reduced stepping activity (treatment $F_{2,21}$=4.69, p=0.021; time $F_{1,21}$=22.58, p<0.0001; time × treatment interaction $F_{2,21}$=5.93, p<0.009; Fig. 10B) of G2019S KI mice to the levels of WT mice at 1 mg/kg. The same dose of H-1152 did not affect rotarod performance (treatment $F_{2,21}$=0.06, p=0.94; time $F_{1,21}$=1.79, p=0.19; time × treatment interaction $F_{2,21}$=0.02, p=0.98; Fig. 10C).

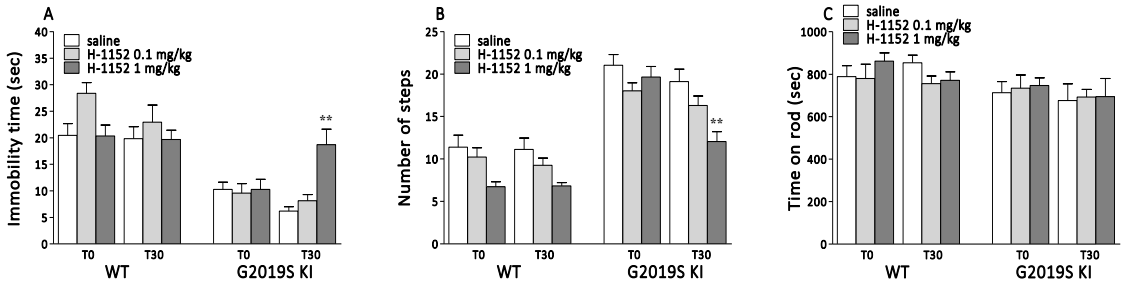

Fig. 10. H-1152 was administered at 0.1 and 1 mg/kg (i.p.) in 6 month-old mice, and motor activity assessed using the bar (A), drag (B) and rotarod (C) tests, before (time 0; basal values) and 30 min after drug administration. Data are means ± SEM of 8 mice per group, and were analyzed using one-way RM ANOVA followed by the Newman-Keuls test for multiple comparisons. *P<0.05 ,**P<0.01 different from basal values.

The time-course of the response to H-1152 (1 mg/kg) was next studied in 12-month-old mice (Fig. 11). Saline-treated WT and G2019S KI mice showed stable responses in the bar

(Fig. 11A) and drag (Fig. 11B) tests across the 24-h observation period. Administration of H-1152 induced a rapid (maximal within 30 min) and prolonged (up to 6 h) increase of immobility time (treatment $F_{1,8}$=59.32, p<0.0001; time $F_{5,8}$=14.25, p<0.0001; time × treatment interaction $F_{5,40}$=14.17, p<0.0001; Fig. 11A) and reduction of stepping activity (treatment $F_{1,8}$=14.64; p=0.005; time $F_{5,8}$=14.12, p<0.0001; time × treatment interaction $F_{5,40}$=13.61, p<0.0001; Fig. 11B) in G2019S KI mice, being ineffective in WT mice (bar test: treatment $F_{1,8}$=0.39, p=0.84; time $F_{5,40}$=2.77, p=0.03; time × treatment interaction $F_{5,40}$=0.92, p=0.47; drag test: treatment $F_{1,8}$=0.76, p=0.41; time $F_{5,40}$=1.57, p=0.19; time × treatment interaction $F_{5,40}$=1.94, p=0.11 Fig. 11A). No residual effect of H-1152 was detected 24 h after administration.

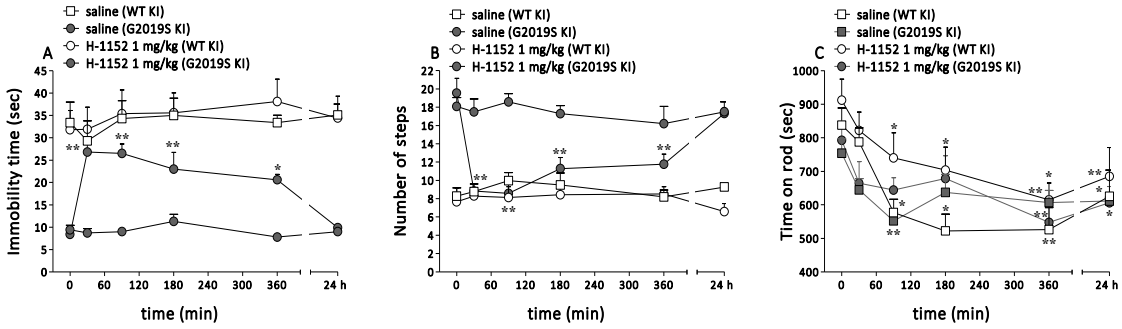

Fig. 11. Time-course of the motor effects of the LRRK2 kinase inhibitor H-1152 in 12-month-old G2019S KI mice and wild-type littermates (WT). H-1152 (1 mg/kg; i.p.) or saline were administered to 12-month-old mice, and motor activity assessed using the bar (A), drag (B) and rotarod (C) tests, before (time 0; basal values) and after (30, 90, 180, 360 min, 24 h) drug administration. Data are means ± SEM of 6 mice per group, and were analyzed using one-way RM ANOVA followed by the Newman–Keuls test for multiple comparisons. *P<0.05, **P< 0.01 different from basal values.

Rotarod performance was not significantly affected by H-1152 (G2019S KI: treatment $F_{1,8}$=0.21, p=0.65; time $F_{5,40}$=6.27, p<0.0001; time × treatment interaction $F_{5,40}$=0.81, p=0.54; WT: treatment $F_{1,8}$=2.94, p=0.12; time $F_{5,40}$=10.85, p<0.0001; time × treatment interaction $F_{5,40}$=0.65, p=0.64; Fig.11C). Indeed, performances worsened within 75 min after administration and remained stable afterwards in mice of both genotypes treated with saline or H-1152. Motor tests were repeated in 15-month-old mice with substantially similar results (Fig. 11C), although H-1152 (1 mg/kg) also mildly and transiently impaired rotarod performance in G2019S KI mice.

To account for a certain compound specificity of LRRK2 activity inhibition we also treated D1994S KD mice and their wild-type controls (Figs. 12A-C). H-1152 (1 mg/kg) treatment did not affect motor activity in any genotypes (bar test: genotype $F_{1,8}$=1.03, p=0.34; time

$F_{4,32}$=0.34, p=0.84; time× treatment interaction $F_{4,32}$=0.53, p=0.71; drag test: genotype $F_{1,8}$=0.25, p=0.63; time $F_{4,32}$=2.28, p=0.08; time × treatment interaction $F_{4,32}$=0.34, p=0.85; rotarod test: genotype $F_{1,8}$=2.64, p=0.14; time $F_{4,32}$=3.98, p=0.01; time × treatment interaction $F_{4,32}$=0.79, p=0.53), consistent with the lack of motor abnormalities in these animals.

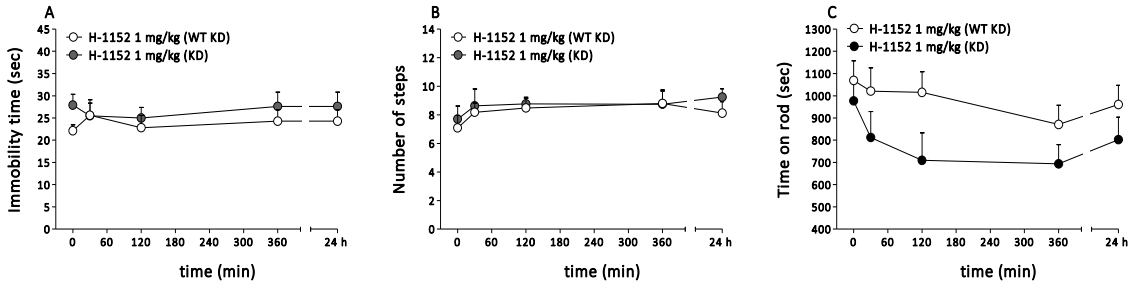

Fig. 12. Time-course of the motor effects of H-1152 (1 mg/kg, i.p.) in 12-month-old D1994S KD mice and wild-type littermates (WT), assessed using the bar (A), drag (B) and rotarod (C) tests, before (time 0; basal values) and after (30, 120, 360min, 24 h) drug administration. Data are means ± SEM of 6mice per group, and were analyzed using one-way RM ANOVA followed by the Newman– Keuls test for multiple comparisons.

Effect of the LRRK2 kinase inhibitor H-1152 on LRRK2 phosphorylation at Ser935

Finally, we evaluated in vivo on-target engagement of H-1152 by measuring LRRK2 phosphorylation at Ser935 in ex-vivo samples of the striatum and cerebral cortex obtained from 12-month-old G2019S KI (Figs. 13A-B) and WT (Figs. 13C-D) mice.

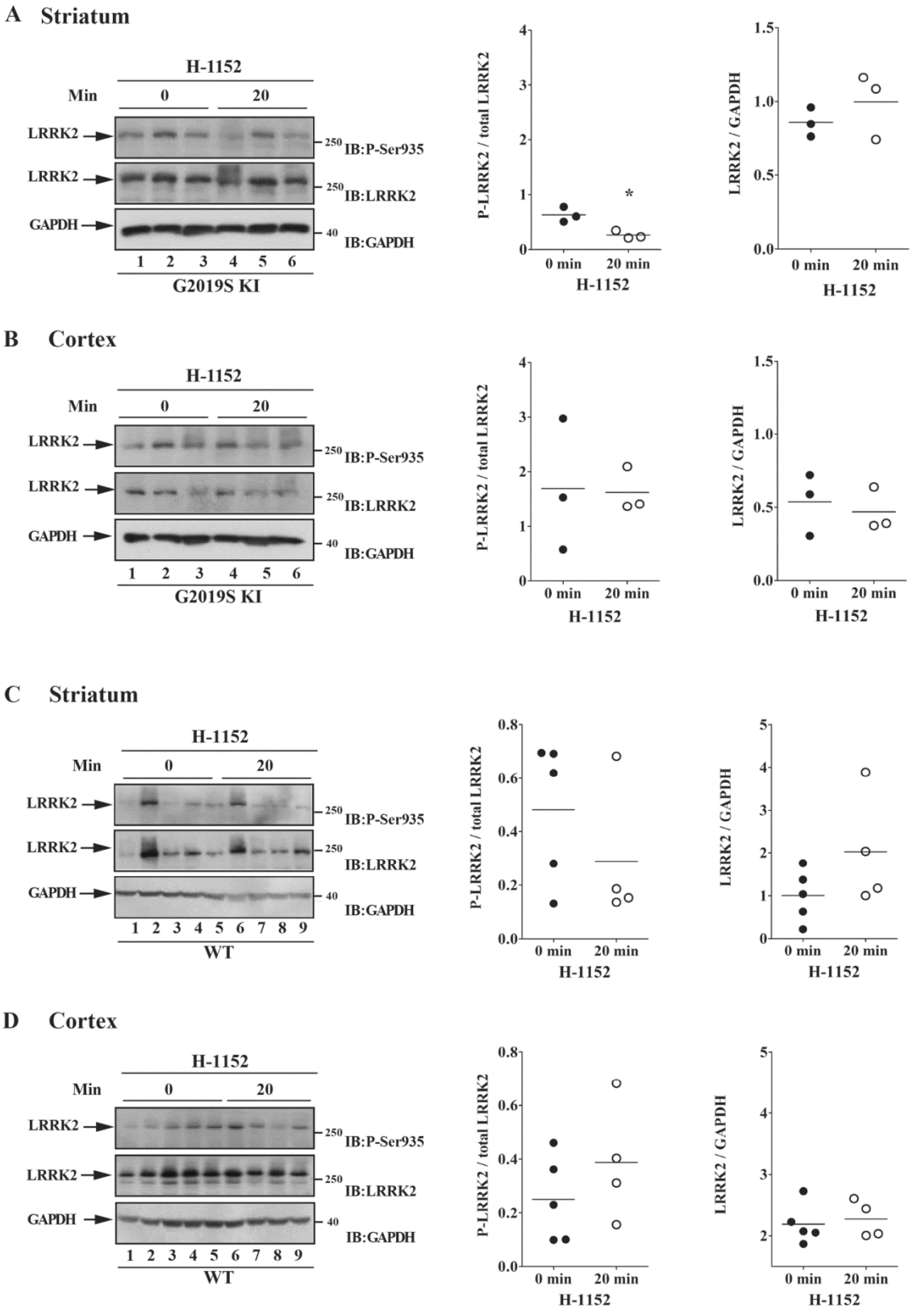

Fig. 13. The LRRK2 kinase inhibitor H-1152 attenuated endogenous LRRK2 phosphorylation at Ser935 in striatum but not cerebral cortex of G2019S knock-in (G2019S KI) mice, being ineffective in wild-type littermates (WT). Three 12-month-old LRRK2 G2019S KI mice (A–B) were used as untreated controls, and three G2019S KI mice were administered with H-1152 (1 mg/kg, i.p.). In parallel, five WT KI mice (C–D) were used as controls, and four WT KI mice were treated with the same dose of H-1152 (1 mg/kg, i.p.). LRRK2 phosphorylation was measured ex-vivo in the striatum (A, C) and cerebral cortex (B, D), before (time 0; T0) and 20 min after H-1152 administration. Results are mean ± SEM of 3–5 mice per group, and were analyzed using the Student t-test, two tailed for unpaired data. To minimize

experimental variability, each sample was loaded in duplicate and the numbers plotted represent the mean of the two technical replicates. *P<0.05 different from basal values (T0).

A decrease of LRRK2 phosphorylation was observed in striatum (p=0.015, t=4.05, df=4), but not cerebral cortex (p=0.095, t=0.98, df=4), at 20 min after administration of 1 mg/kg H-1152 but not later time-points (i.e. 90 and 360 min; Figs. 14A-B). Contrary to G2019S KI mice, no effect of H-1152 on LRRK2 phosphorylation was detected in striatum (p=0.30, t=1.11, df=7) or cerebral cortex (p=0.31, t=1.08, df=7) at 20 min after administration in WT mice (Fig. 13B-D)

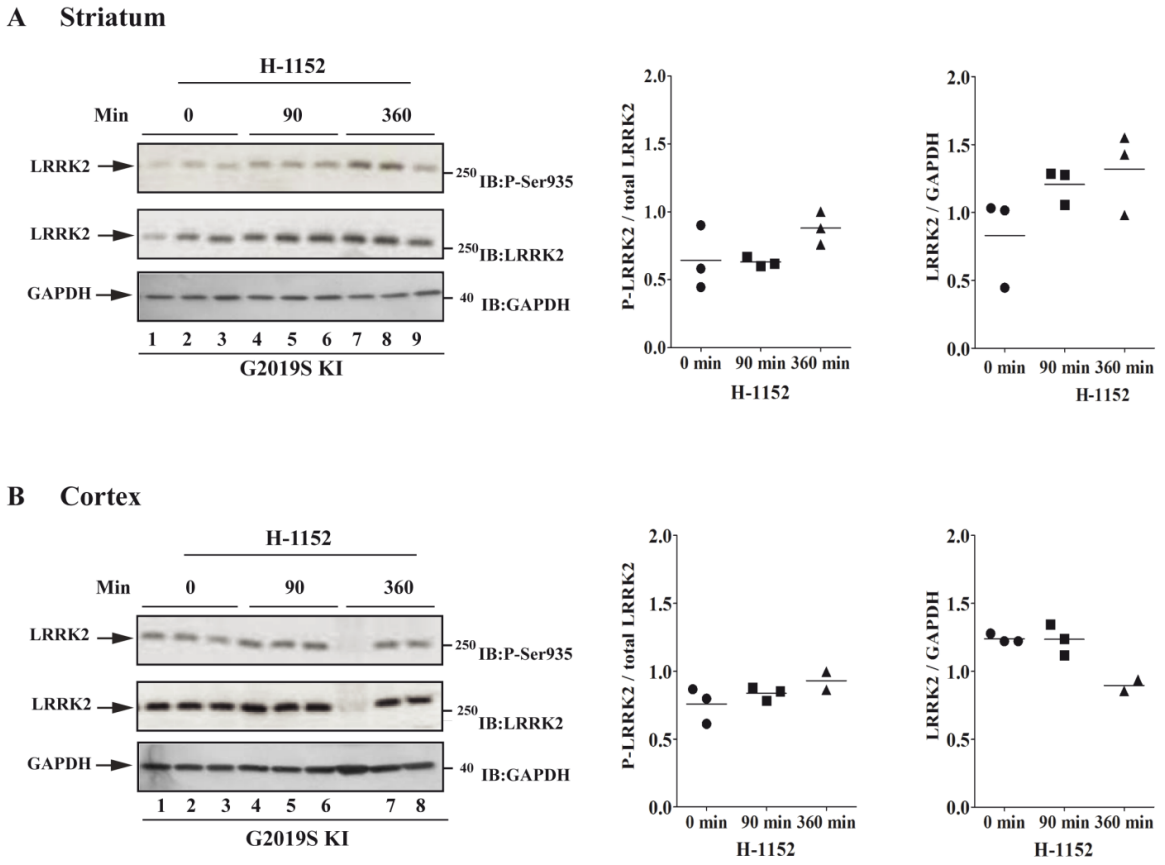

Fig. 14. The LRRK2 kinase inhibitor H-1152 did not affect phosphorylation of LRRK2 at Ser935 ex-vivo at 90 and 360 min after administration. Twelve-month-old LRRK2 G2019S knock-in (G2019S KI) mice were treated with H-1152 (1 mg/Kg, i.p.), and sacrificed 90 or 360 min later. LRRK2 phosphorylation was measured ex-vivo in the striatum (A) and cerebral cortex (B), before (time 0; T0), 90 min or 360 min after H-1152 administration. Results are the mean ± SEM of 3 mice per group, and were analysed using one-way ANOVA followed by the Newman Keuls test.

Effect of the LRRK2 kinase inhibitor Nov-LRRK2-11 on motor phenotype in LRRK2 G2019S KI and WT mice

To confirm that the results obtained with H-1152 are due to LRRK2 inhibition and not other off-target kinases, we employed a second small molecule ATP analog inhibitor, Nov-LRRK2-11,which has been recently shown to be brain penetrant and reasonably selective (Troxler et al., 2013). We first tested Nov-LRRK2-11 in vitro for its ability to inhibit LRRK2 Ser935 phosphorylation. Nov-LRRK2-11 resulted in being very potent at reducing LRRK2 phosphorylation in NIH3T3 cells, with IC_{50} of 0.38 nM (Fig. 15).

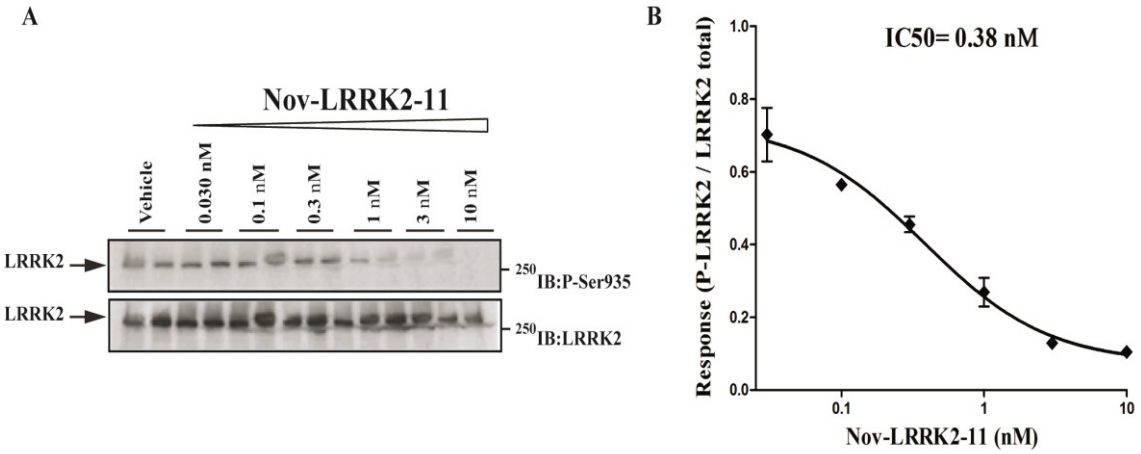

Fig. 15. The LRRK2 kinase inhibitor Nov-LRRK2-11 attenuated endogenous LRRK2 phosphorylation at Ser935 in cells. Blots from lysates of NIH3T3 cells (A) exposed to vehicle or increasing concentrations of Nov-LRRK2-11 (0.03–10 nM) for 90 min (B). Data are means ± SEM of 2 experiments performed in duplicate.

Next, we assessed the compound in vivo (Fig. 16). Nov-LRRK2-11 (1 and 10 mg/kg, i.p.) did not induce any obvious behavioral change on immobility time and step number in WT mice (bar test: treatment $F_{2,13}$=39.83, p<0.001; time $F_{4,52}$=2.33, p=0.07; time × treatment interaction $F_{8,52}$=0.75, p=0.65; drag test: treatment $F_{2,13}$=1.05, p=0.37; time $F_{4,52}$=2.34, p=0.07; time × treatment interaction $F_{8,52}$=0.95, p=0.48; Fig. 16A-B). However, Nov-LRRK2-11 acute treatment phenocopied the motor inhibiting effects of H-1152 in G2019S KI mice (bar test: treatment $F_{2,13}$=60.05, p<0.0001; time $F_{4,60}$=29.15, p<0.0001; time × treatment interaction $F_{8,60}$=29.15, p<0.0001; drag test: treatment $F_{2,15}$=12.65, p=0.001; time $F_{4,60}$=18.51, p<0.0001; time × treatment interaction $F_{8,60}$= 15.55, p<0.0001; Figs. 16A-B). Nov-LRRK2-11 was ineffective at 1 mg/kg, and induced a rapid (significant at 20 min, maximal at 75 min) increase in immobility time (Fig. 16A) and reduction of stepping activity (Fig. 16B) at 10 mg/kg. These effects were shorter lasting than those of H-1152,

since stepping activity was normalized and immobility time only mildly elevated at 360 min after administration.

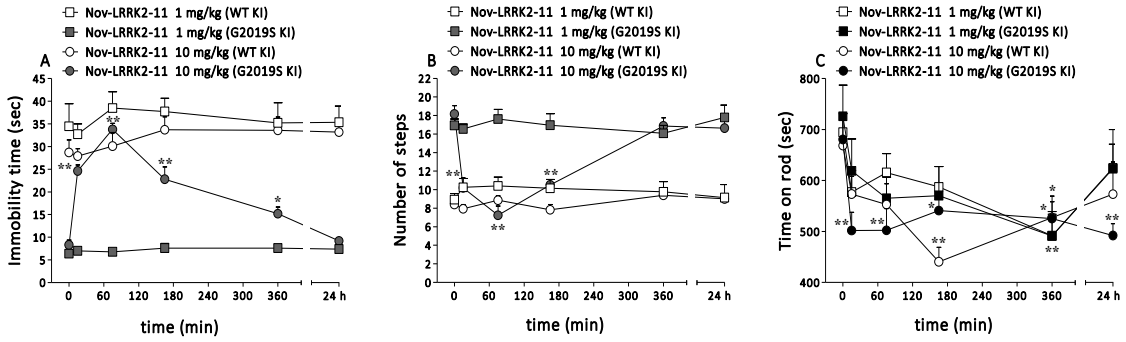

Fig. 16. The LRRK2 kinase inhibitor Nov-LRRK2-11 reversed motor phenotype in G2019S knock-in (G2019S KI) mice being ineffective in wild-type littermates (WT). Time-course of the motor effects of Nov-LRRK2-11 (1 and 10 mg/kg, i.p.), in 12-month-old G2019S KI and WT mice. Motor activity was assessed using the bar (A), drag (B) and rotarod (C) tests, before (time 0; basal values) and after (15, 75, 165, 360 min, 24h) drug administration. Data are means ± SEM of 6–8 mice per group, and were analyzed using one-way RM ANOVA followed by the Newman–Keuls test for multiple comparisons. *P<0.05, **P<0.01 different from basal values.

Nov-LRRK2-11 caused a delayed reduction of rotarod performance in WT mice at 1 and 10 mg/kg, the latter dose inducing a more rapid effect (rotarod test: treatment $F_{2,13}$=0.78, p=0.47; time $F_{4,52}$=12.96, p<0.0001; time × treatment interaction $F_{8,52}$=3.52, p=0.002; 175 min; Fig. 16C). In G2019S KI mice, the lower dose induced a response that was superimposable to that observed in WT, albeit more rapid in onset (within 15 min) (rotarod test: treatment $F_{2,20}$=0.94, p=0.40; time $F_{4,80}$=18.37, p<0.0001; time × treatment interaction $F_{8,80}$=3.29, p=0.003). Behavioral data were in line with pharmacokinetic data. In fact, following an oral dose of 3 mg/kg Nov-LRRK2-11, brain and blood concentrations were maximal at 1 h, and only minimally detected at 4 h; at 24 h, compound levels were below detection (Fig. 17).

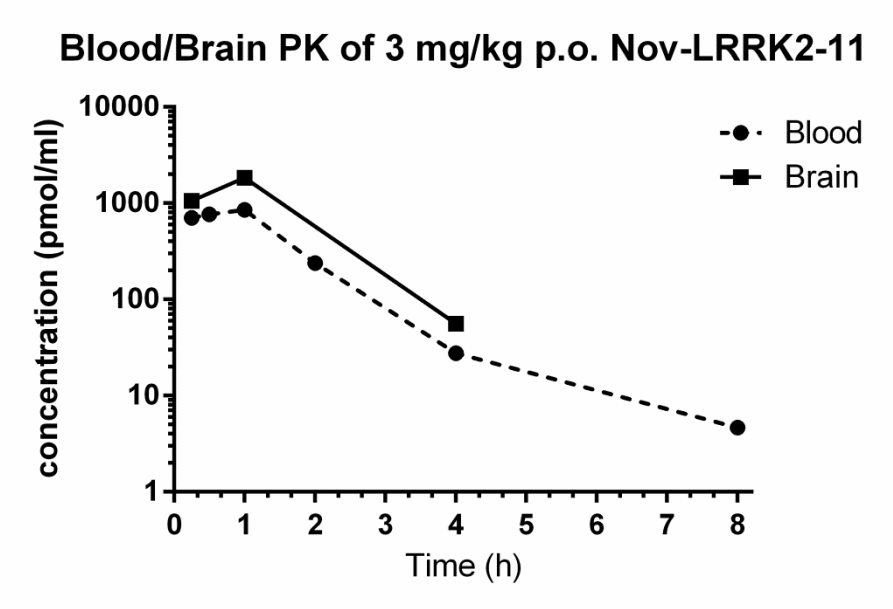

Fig. 17. Pharmacokinetic study showing blood and brain concentrations of Nov-LRRK2-11 after oral administration (by gavage) of the 3 mg/Kg dose. Each time-point represents the mean of 3 ± SEM of 3 mice.

Effect of the LRRK2 kinase inhibitor Nov-LRRK2-11 on LRRK2 phosphorylation at Ser935

To confirm in vivo LRRK2 targeting, we measured LRRK2 phosphorylation at Ser935 30 min after Nov-LRRK2-11 (10 mg/kg) administration in 12-month old G2019S KI and WT animals (Fig. 18). Nov-LRRK2- 11 markedly reduced LRRK2 phosphorylation in the striatum and cerebral cortex of G2019S KI mice (by 75% and 50%, respectively, n=3 animals each; striatum p=0.008, t=4.78, df=4; cortex p=0.011, t=4.41, df=4; Figs. 18A-B) as well as WT mice (by 60% and 80%, respectively, n=5 animals each, striatum p=0.004, t=3.95, df=8; cortex p=0.044, t=2.37, df=8; Figs. 18C-D). Interestingly, in the cerebral cortex but not striatum, pharmacological blockade of LRRK2 kinase activity reduced protein LRRK2 levels (Figs. 18B and D).

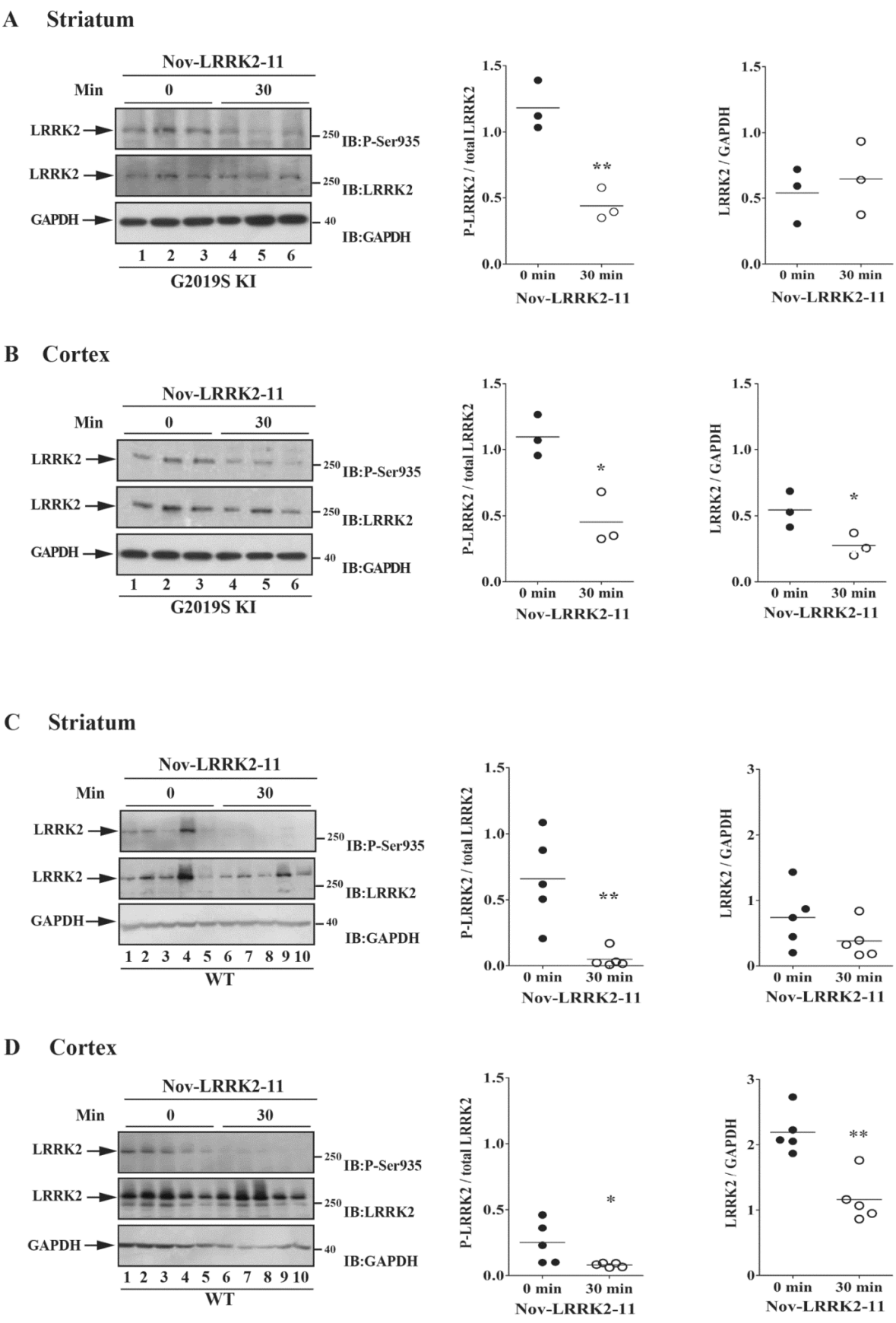

Fig. 18. The LRRK2 kinase inhibitor Nov-LRRK2-11 attenuated endogenous LRRK2 phosphorylation at Ser935 in the striatum and cortex of both G2019S knock-in (G2019S KI) mice and wild-type littermates (WT). Three 12-month-old G2019S KI mice (A–B) were used as untreated controls, and three G2019S KI mice were administered with Nov-LRRK2-11 (10 mg/kg, i.p.). In parallel, five WT KI mice (C–D) were used as controls, and five WT KI mice were treated

with the same dose of Nov-LRRK2-11 (10 mg/kg, i.p.). LRRK2 phosphorylation was measured ex vivo in the striatum(A, C) and cerebral cortex (B, D), before (time 0; T0) and 30min afterNov-LRRK2-11 administration. Results are mean ± SEM of 3–5mice per group, and were analyzed using the Student t-test, two tailed for unpaired data. *P<0.05, **P<0.01 different from basal values (T0).

Finally, pSer935 LRRK2 and endogenous LRRK2 protein levels were monitored in 12-month-old G2019S KI and KD mice in comparison with their WT controls (Fig. 19). pSer935 LRRK2 levels in striatum and cortex, as well as LRRK2 protein levels in striatum were similar across genotypes. Likewise, similar levels of LRRK2 were found in the cortex of G2019S KI and WT mice. D19994S KD levels were also in the same range of G2019S KI mice, although lower than those found in their littermates.

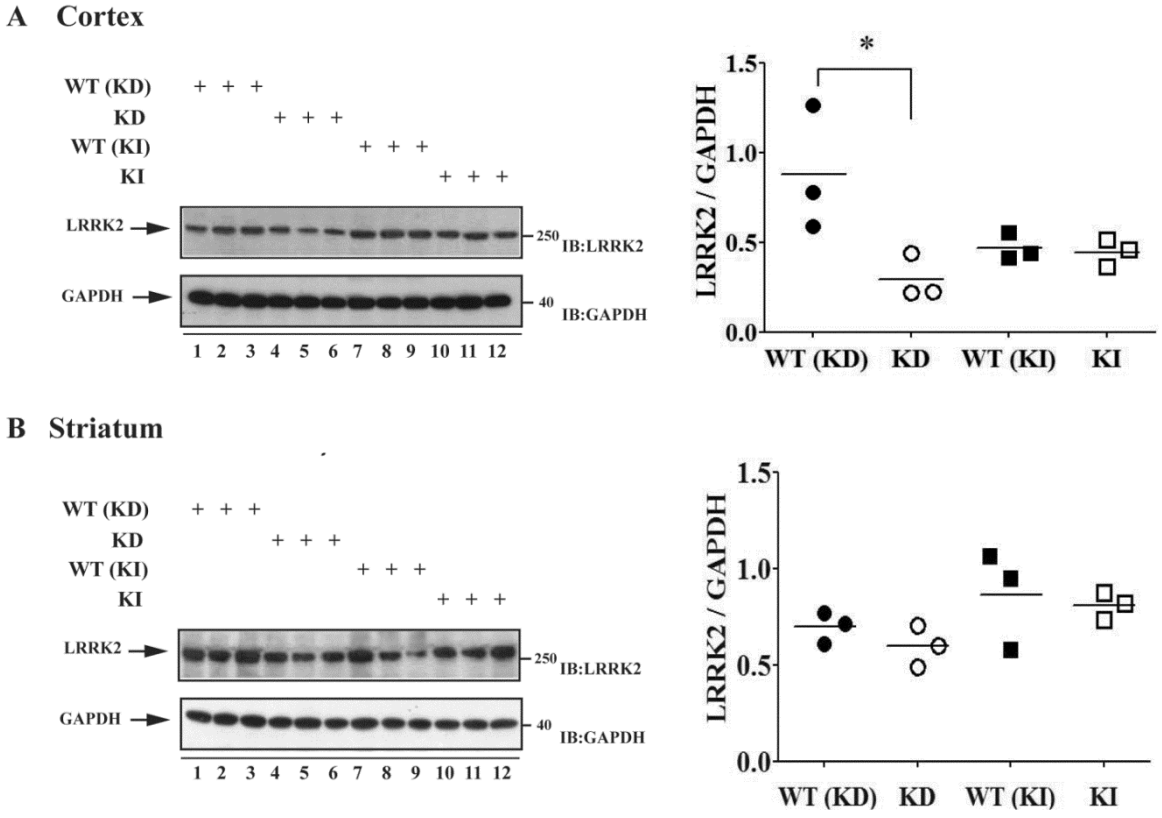

Fig. 19. LRRK2 expression in the cortex (A) and striatum (B) of 12-month-old G2019S KI mice, D1994S KD mice, and respective WT littermates. Data are means ± SEM of 3 mice per genotype, and were analyzed using the Student t-test two-tailed for unpaired data. *P<0.05 different from WT

Part 2

The identification of a LRRK2 kinase activity-dependent hyperkinetic phenotype resistant to age-related motor decline in G2019S KI mice, prompted us to investigate the underlying biochemical and neurochemical mechanisms. In particular, we investigated whether such a hyperkinetic phenotype was associated with dysregulation of dopaminergic transmission.

Pharmacological manipulation of dopaminergic transmission in G2019S KI mice

In the first series of behavioral pharmacology experiments, the responsiveness to dopaminergic drugs was evaluated. The fixed sequence of bar, drag and rotarod tests was performed in 11-month-old mice before (control session) and after systemic administration of the D2/D3 receptor selective antagonist haloperidol, the D1/D5 receptor selective antagonist SCH23390, and the D2/D3 selective agonist pramipexole.

Haloperidol

Haloperidol was injected systemically (i.p.) at the dose of 0.3 mg/kg, which was previously found effective in causing motor impairment in naïve mice (Mabrouk et al., 2010; Marti et al., 2005; Viaro et al., 2013). In the bar test (Fig. 20A), haloperidol induced severe akinesia in G2019S KI mice, resulting in a 4-fold increase of immobility time ($t=9.58$, $df=7$, $p<0.001$) at 60 min after drug administration. Conversely, haloperidol was ineffective in WT mice ($t=1.93$, $df=6$, $p=0.10$; Fig. 14A). In parallel, haloperidol-treated G2019S KI mice showed ~75% reduction in the number of steps ($t=14.68$, $df=7$, $p<0.001$; Fig. 20B), whereas stepping activity of WT mice was unchanged ($t=0.66$, $df=6$, $p=0.53$; Fig 20B). Finally, haloperidol markedly reduced by ~50% rotarod performance (Fig. 20C) in both G2019S KI mice ($t=7.6$, $df=7$, $p<0.001$) and WT mice ($t=4.42$, $df=6$; $p<0.01$).

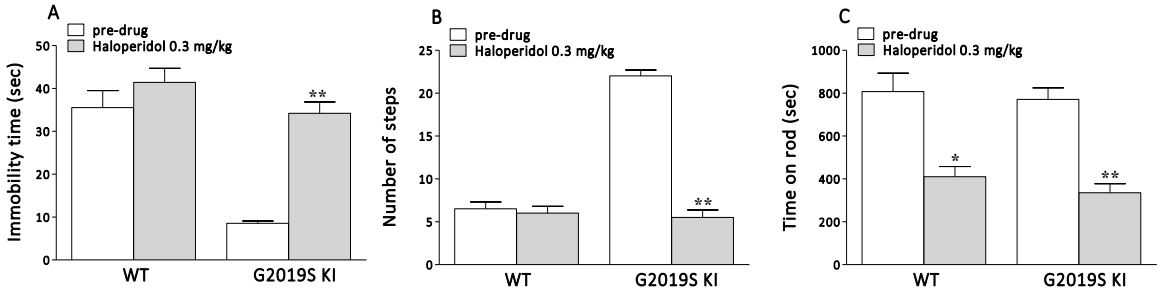

Fig. 20. Effect of systemic injection of haloperidol on motor activity in 11-month-old G2019S KI and WT mice. Motor activity was evaluated in the bar (A), drag (B) and rotarod (C) tests at 60 min after haloperidol (0.3 mg/kg, i.p.) administration, and expressed as immobility time (sec; A), number of steps (B), and time on rod (sec; C). Data are means ± SEM of 7 (WT) or 8 (G2019S KI) mice per group and were analyzed using the Student t-test, two tailed for paired data. *p<0.05, **p<0.01 significantly different from pre-drug.

SCH23390

SCH23390 was systemically (i.p.) injected in 12-month-old mice (Fig. 21), at the dose of 0.01 mg/kg, which was previously found to cause motor impairment in naive mice (Viaro et al., 2013). SCH23390 increased by ~60% the immobility time in the bar test (Fig. 21A), simultaneously reducing by ~35% the number of step in drag test (Fig. 21B) and by ~20% the rotarod performance (Fig. 21C) in G2019S KI mice (bar test: genotype $F_{1,13}$=20.32 p=0.001, time $F_{2,26}$=6.40 p=0.005, time x genotype $F_{2,26}$=11.84 p<0.001; drag test: genotype $F_{1,13}$=12.61 p=0.004, time $F_{2,26}$ =16.04 p<0.001, time x genotype $F_{2,26}$=12.60 p<0.001; rotarod test: genotype $F_{1,13}$=2.10 p=0.17, time $F_{2,26}$=2.24 p=0.12, time x genotype $F_{2,26}$=3.34 p=0.051). Conversely, SCH23390 did not cause any significant change of immobility time (Fig. 21A), number of steps (Fig. 21B) or rotarod performance (Fig. 21C) in WT mice.

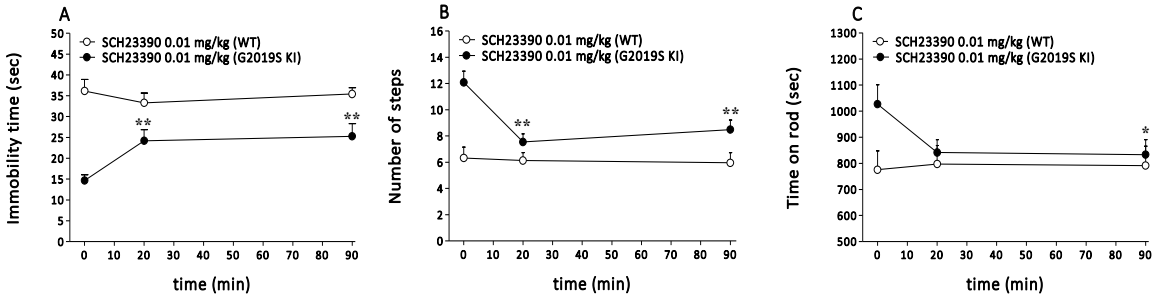

Fig. 21. Time-course of the motor effects of systemic injection of SCH23390 (0.01 mg/kg, i.p.) in 11-month-old G2019S KI mice and wild-type littermates (WT). Motor activity was assessed using the bar (A), the drag (B) and the rotarod tests,

before (time 0; basal values) and after (20 and 90 min) drug administration and was expressed as immobility time (sec; A), number of steps (B), time on rod (sec; C). Data are means ± SEM of 7 (WT) or 8 (G2019S KI) determinations per group and were analyzed using one-way RM ANOVA followed by the Newman–Keuls test for multiple comparisons. *p<0.05, **p<0.01 significantly different from pre-drug (T0).

Pramipexole

The data collected with DA antagonists would suggest a greater tonic activation of DA receptors in G2019S KI mice. To confirm this view, the D2/D3 receptor agonist pramipexole (PPX) was tested in 11-month-old mice. In WT mice, PPX reduced the immobility time in the bar test (treatment $F_{4,27}$=15.76 p<0.001; Fig. 22A) at 0.0001 (~70%) and 0.001 mg/Kg (~60%) but was ineffective at higher does (0.01 and 0.1 mg/Kg), thus showing a bell-shaped curve. In parallel, PPX increased stepping activity in the drag test (treatment $F_{4,27}$=37.83 p<0.001; Fig. 22B) at low doses (0.0001 and 0.001 mg/kg), being ineffective at higher doses (0.01 and 0.1 mg/Kg). Conversely, in G2019S KI mice, PPX was ineffective at low doses (0.0001and 0.001 mg/kg), causing motor inhibition at the higher ones (0.01 and 0.1 mg/Kg; bar test: treatment $F_{4,31}$=24.35 p<0.001, drag test: treatment $F_{4,31}$=51.12 p<0.001; Fig. 22A-B). Finally, PPX reduced rotarod performance at 0.1 mg/Kg in both genotypes (WT: treatment $F_{4,27}$=6.37 p=0.001; G2019S KI: treatment $F_{4,31}$=4.55 p=0.005; Fig. 22C).

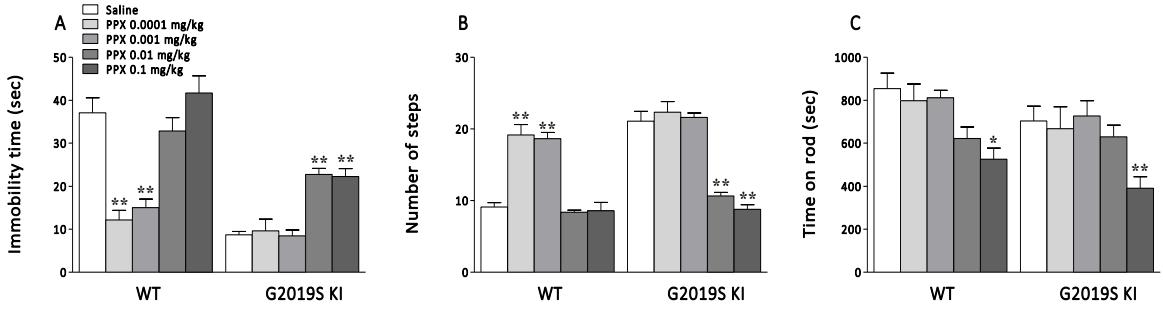

Fig. 22. Effect of systemic injection of pramipexole on motor activity in 11-month-old G2019S KI and WT mice. Motor activity was evaluated in the bar (A), drag (B) and rotarod (C) tests at 60 min after pramipexole (0.0001- 0.1 mg/kg, i.p.) or saline administration, and expressed as immobility time (sec; A), number of steps (B), and time on rod (sec; C). Data are means ± SEM of 7 (WT) or 8 (G2019S KI) mice per group and were analyzed using 1way ANOVA followed by the Newman–Keuls test for multiple comparisons. *p<0.05, **p<0.01 significantly different from saline.

Relationship between G2019S mutation and DA reuptake in phenotypic mice

Since experiments in G2019S KI mice suggested that hyperkinetic phenotype is associated with a greater saturation of postsynaptic DA receptors, we investigated if DA transporter (DAT) function might be dysregulated, thus leading to higher endogenous DA levels.

GBR-12783

We first investigated DAT function *in vivo,* using the DAT inhibitor GBR-12783. Motor tests were performed in 16-month-old mice at 20 and 60 min after drug administration, at two different doses of GBR-12783 (6 and 20 mg/Kg).

In WT mice, GBR-12783 caused a dose-dependent inhibition of immobility time in the bar test at 20 min after administration (Fig. 23A). At later time-point only the higher dose (20 mg/kg) was effective (time $F_{2,24}$=27.94 p<0.001, treatment $F_{1,12}$=4.09 p=0.06, time x treatment $F_{2,24}$=4.05 p=0.031). In the drag test (Fig. 23B), both doses equally improved (~50%) stepping activity, although in this case only the lower one (6 mg/kg; time $F_{2,24}$=33.38 p<0.001, treatment $F_{1,12}$=1.35 p=0.27, time x treatment $F_{2,24}$=4.19 p=0.03) exerted a long-lasting effect. Finally, GBR-12783 did not alter rotarod performance in WT mice (time $F_{2,24}$=0.79 p=0.47, treatment $F_{1,12}$=12.18 p=0.004, time x treatment $F_{2,24}$=2.40 p=0.11). Different from WT mice, GBR-12783 did not affect motor performance in G2019S KI mice at any doses (bar test: time $F_{2,26}$=0.14 p=0.87, treatment $F_{1,13}$=0.003 p=0.96, time x treatment $F_{2,26}$=1.16 p=0.33; drag test: time $F_{2,26}$=0.73 p=0.49, treatment $F_{1,13}$=1.57 p=0.23, time x treatment $F_{2,26}$=0.58 p=0.57; rotarod test: time $F_{2,26}$=0.44 p=0.65, treatment $F_{1,13}$=8.2 p=0.013, time x treatment $F_{2,26}$=2.82 p=0.08).

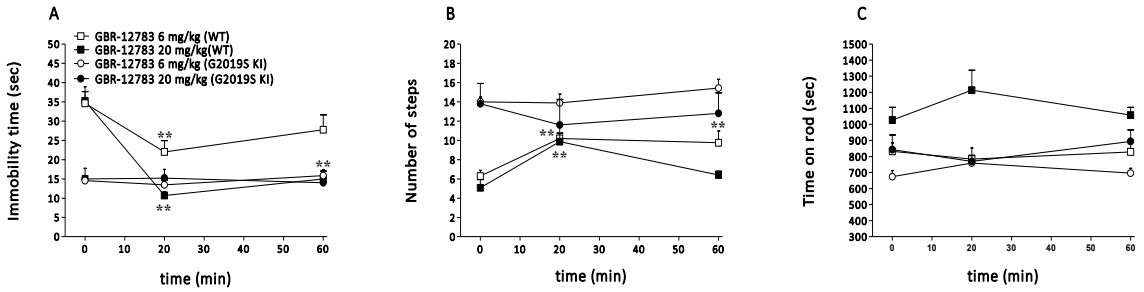

Fig. 23. Time-course of the motor effects of systemic injection of GBR-122783 (6 and 20 mg/kg, i.p.) in 16-month-old G2019S KI mice and wild-type littermates (WT). Motor activity was assessed using the bar (A), drag (B) and rotarod tests, before (time 0; basal values) and after (20 and 90 min) drug administration, and was expressed as immobility time (sec; A), number of steps (B), and time on rod (sec; C). Data are means ± SEM of 9-10 (6 mg/kg) or 5 (20 mg/kg) mice per group and were analyzed using one-way RM ANOVA followed by the Newman–Keuls test for multiple comparisons. *p<0.05, ** p<0.01 significantly different from pre-drug (T0).

GBR-12783 and Nov-LRRK2-11

The insensitivity of G2019S KI mice to GBR-12783, led us to suppose that DAT was dysfunctional in these mice. As we previously observed that blocking LRRK2 kinase activity with Nov-LRRK2-11 worsened motor activity in G2019S mice, we investigated the cross-talk between the G2019S LRRK2 mutation and DAT-mediated motor behavior.

To this purpose, 16-month-old mice were divided into three different experimental groups. One group was systemically injected with vehicle, while the other two with Nov-LRRK2-11 (i.p. 10 mg/kg). Mice treated with Nov-LRRK2-11 were further allotted into two groups and injected (15 min later) either with GBR-12783 (i.p. 20 mg/kg) or vehicle (i.p.).

As expected, Nov-LRRK2-11 increased the immobility time (~2-fold; time $F_{3,51}$=23.73 $p<0.001$, treatment $F_{2,17}$=30.30 $p<0.001$, time x treatment $F_{6,51}$=27.89 $p<0.001$; Fig. 24A) and reduced the number of step (~2-fold; time $F_{3,51}$=30.75 $p<0.001$, treatment $F_{2,17}$=23.80 $p<0.001$, time x treatment $F_{6,51}$=14.99 $p<0.001$; Fig.24B) in G2019S KI mice. Interestingly, these effects were reversed by GBR-12783 in both tests (Fig. 24).

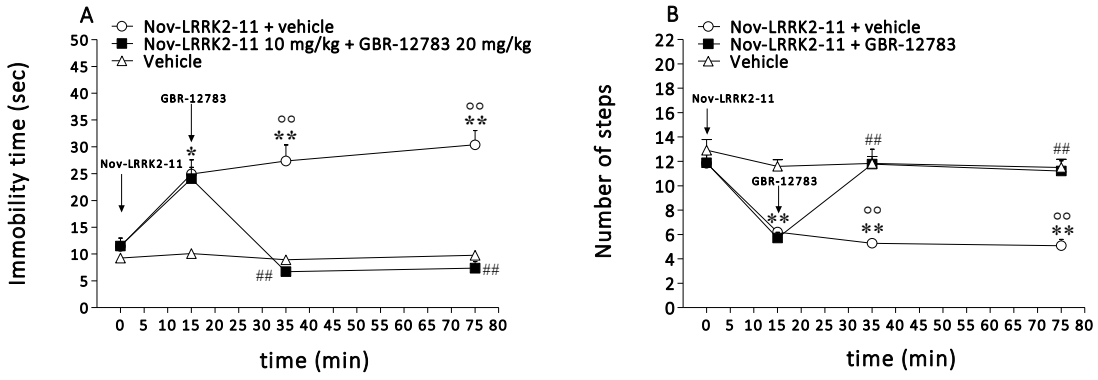

Fig. 24. Time-course of the motor effects of systemic injection of Nov-LRRK2-11 (10 mg/Kg i.p.) and GBR-12783 (20 mg/Kg i.p.) in 16-month-old G2019S KI mice. Motor activity was assessed using the bar (A) and drag (B) tests, before (time 0; basal values) and after (15, 35, 75 min) drug administration, and was expressed as immobility time (sec; A) and number of steps (B). Data are means ± SEM of 6 (vehicle) or 7 (Nov-LRRK2-11; Nov-LRRK2-11 + GBR-12783) mice per group and were analyzed using one-way RM ANOVA followed by the Newman–Keuls test for multiple comparisons. *p<0.05, **p<0.01 significantly different from pre-drug (T0). ##p<0.01 significantly different from the 15 min time-point; °°p<0.01 significantly different from Nov-LRRK2-11 + GBR-12783 at the same time-point.

Analysis on DAT and VMAT2 protein levels

Overall, these data suggest that the G2019S mutation affects DA reuptake in G2019S KI mice, possibly through changes of DAT activity and/or expression.

To investigate whether the G2019S mutation alters DAT (and VMAT2) protein expression we assessed DAT protein levels with western blot in *ex-vivo* striatal samples from 12-month-old G2019S KI and WT mice. G2019S KI mice showed lower protein DAT levels (~50%; Fig. 25) compared to WT mice. Similarly, lower levels of total endogenous VMAT2 were detected in G2019S KI mice (~60%; Fig. 25).

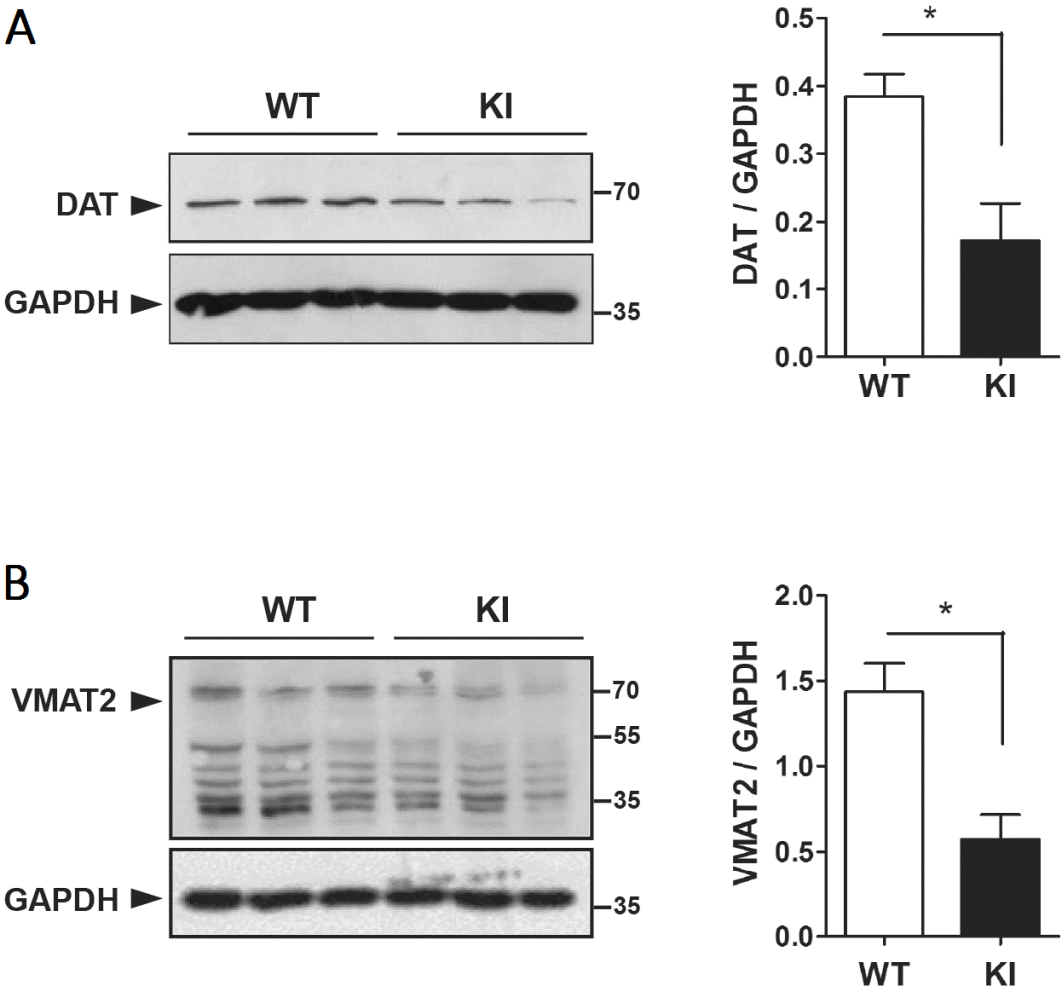

Fig. 25. Expression of DAT (A) and VMAT2 (B) in striatum of 12-month-old G2019S KI mice and WT littermates. Data are means ± SEM of 3 mice per genotype, and were analyzed using the Student t-test two-tailed for unpaired data. *P<0.05 different from WT.

Membrane DAT expression and function

The reduction in DAT protein levels led us to investigated if any change of DAT expression at the presynaptic membrane occurred in G2019S mice. To this purpose, saturation binding experiments in striatal synaptosomes of 7-month-old G2019S KI and WT mice were performed using [^{3}H]-WIN 35,428 as DAT ligand. Data revealed no significant difference in DAT density between G2019S KI and WT mice, according to the similar B_{max} values measured in G2019S KI mice (5.77 ± 0.10 pmol/mg protein) and WT mice (5.46 ± 0.25 pmol/mg protein; Fig. 26A). The affinity of [3H]-WIN 35,428 for DAT was also similar in striatal synaptosomes from G2019S KI and WT mice, with K_D values of 9.08 ± 0.23 nM and 8.93 ± 0.70 nM, respectively.

Since no differences in DAT density were found between genotypes, kinetic analysis of DA uptake was performed. A significant 60% increase of maximal transport rate (V_{max}) in striatal synaptosomes from G2019S KI with respect to WT mice was found (P<0.01, Fig. 26B). No significant differences were observed in K_m values, a measure of DA affinity for the transporter.

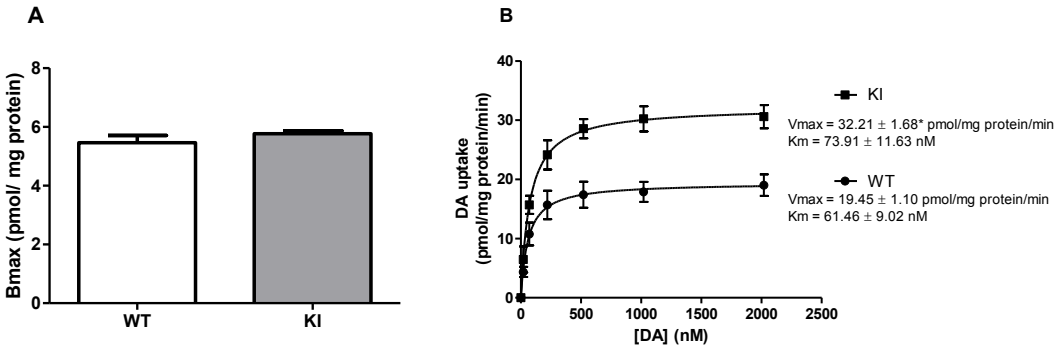

Fig. 26. Expression and function of DAT in striatal synaptosomes of LRRK2 G2019S KI (KI) and WT mice. Dopamine transporter density expressed as B_{max} values obtained from [3H]-WIN 35,428 saturation binding experiments in synaptosomes from KI and WT mice (A). Kinetic analysis of [3H] Dopamine (DA) uptake in synaptosomes from KI and WT mice (B). Values are expressed as mean ± SEM of 3 independent experiments performed in duplicate. *P<0.01 vs WT.

In vivo microdialysis

Since data from behavioral pharmacology studies together with ex-vivo/in vitro experiments are consistent with the view that G2019S KI mice exhibit an altered dopaminergic tone likely associated with dysregulation of DA reuptake, we used microdialysis to measure extracellular levels of DA and DA metabolites in dorsal striatum of 19-month-old mice G2019S KI and WT mice (Figs. 27-28).

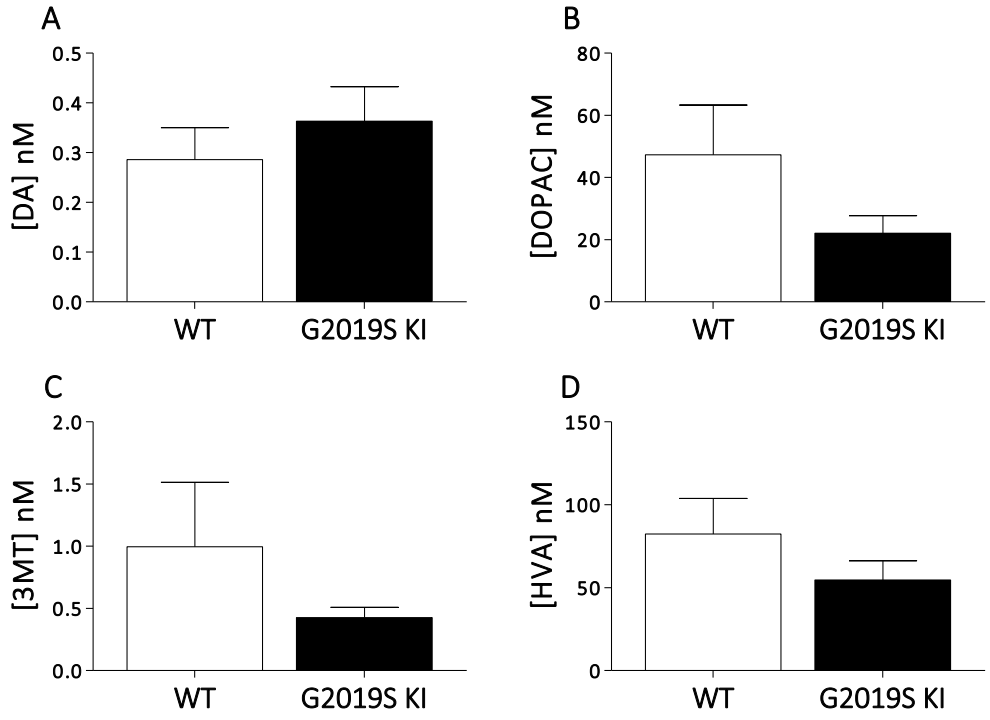

Fig. 27. Basal levels (nM) of DA (A), DOPAC (B), 3MT (C) and HVA (D) from dorsal striatum of 19-month-old G2019S knock-in (G2019S KI) and wild-type littermates (WT) mice. In vivo microdialysis shows similar striatal levels of DA and its metabolites (DOPAC, 3MT and HVA) in both G2019S KI and WT mice. Data are means ± SEM of 11-15 determinations per group and were analyzed using the Student t test, two-tailed for paired data.

No significant difference was detected between levels of DA and DA metabolites in G2019S KI ($t=0.78$, $df=24$, $p=0.43$) and WT mice (Fig. 27). Interestingly, however, G2019S KI mice showed significant lower metabolite/DA ratio (DOPAC/DA: $t=2.17$, $df=17$, $p=0.043$; 3MT/DA: $t=2.26$, $df=11$, $p=0.04$; HVA/DA: $t=2.43$, $df=21$, $p=0.023$; Fig. 28) with respect to WT mice.

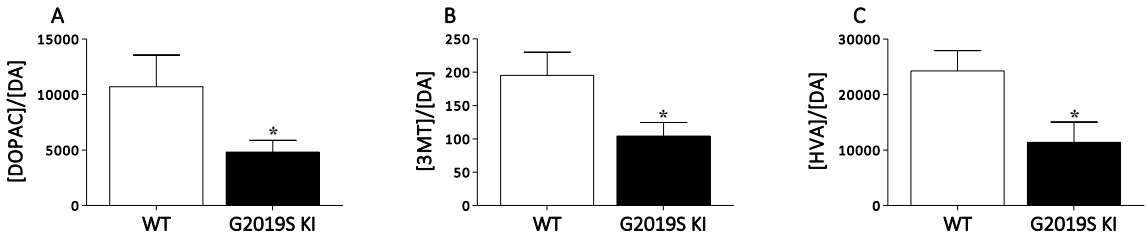

Fig 28. Ratios between basal levels of DOPAC and DA (A), 3MT and DA (B), HVAand DA (C)as obtained from microdialysis in the dorsolateral striatum of G2019S knock-in (G2019S KI) and wild-type littermates (WT) mice. Data are means ± SEM of 10 (WT) or 13 (G2019S KI) determinations per group and were analyzed using the Student t test, two-tailed for paired data. *P<0.05 different from WT.

To test the responsiveness of striatal DA levels to DAT blockade, GBR-12783 was given. In the striatum of WT mice DA levels transiently rose after GBR-12783 challenge, peaking (~ 4-fold over basal) at 40 min (Fig. 29) after administration (time $F_{6,78}$=13,62 p<0.001, time x genotype $F_{6,78}$=3.45 p=0.005, genotype $F_{1,13}$=0.15 p=0.707). G2019S KI mice showed a shallow and slow in onset increase in DA levels after GBR-12783 administration, with maximal levels (0.57 ± 0.084 nM) reached at 60 min (Fig. 29).

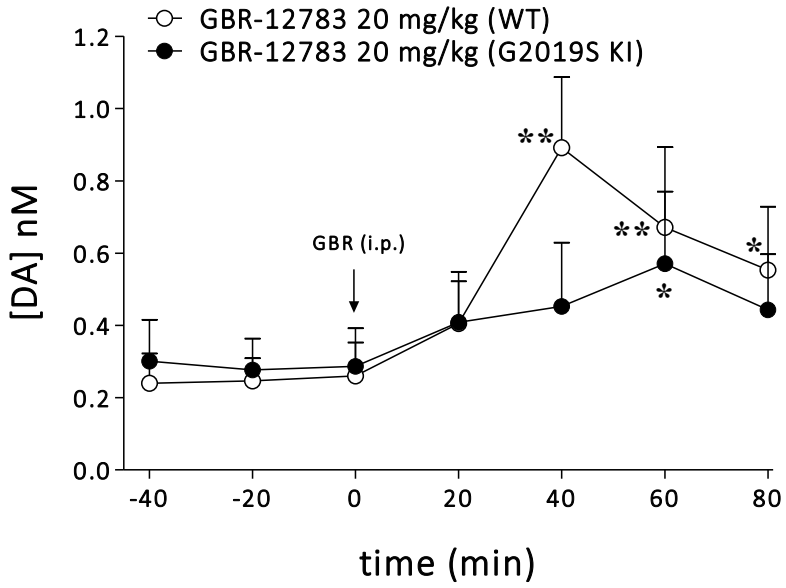

Fig. 29. Neurochemical effects on dorsolateral striatal basal level of DA after systemic injection of GBR-12783 (20 mg/kg, i.p.) in 19-month-old G2019S knock-in (G2019S KI) and wild-type littermates (WT) mice undergoing microdialysis. Basal dialysate levels of DA are expressed as absolute levels (nM) and are mean ± SEM of 6 (WT) or 9 (G2019S KI) animals. Statistical analysis was performed using one-way RM ANOVA followed by the Newman–Keuls's test for multiple comparisons. * p<0.05; ** p<0.01 significantly different from T0 per each genotype

Finally, Nov-LRRK2-11 (i.p.; 10 mg/kg) was injected 48 h after surgery and no differences in DA levels were detected between genotypes (time $F_{7,49}$=0,85 p=0.55, time x genotype $F_{7,49}$=0.86 p=0.54, genotype $F_{1,7}$=1.33 p=0.29; Fig. 30).

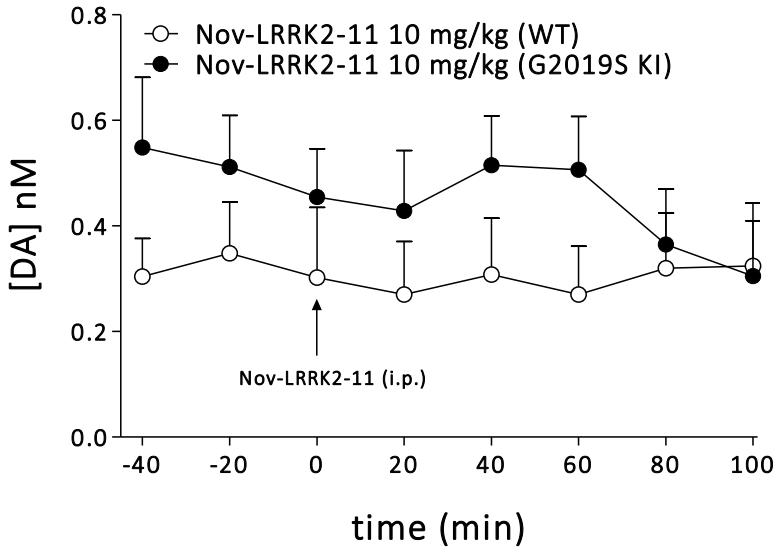

Fig. 30. Neurochemical effects on dorsolateral striatal basal level of DA after systemic injection of Nov-LRRK2-11 (10 mg/kg, i.p.) in 19-month-old G2019S knock-in (G2019S KI) and wild-type (WT) mice undergoing microdialysis. Basal dialysate levels of DA are expressed as absolute values (nM), and are mean ± SEM of 5 (WT) or 6 (G2019S KI) animals.

Nigrostriatal DA system

Stereological techniques and TH-immunostaining were used to analyze the number of DA cells in SNpc as well as the dopaminergic innervation in the striatum of 19-month-old G2019S KI and WT littermates. No differences were found in striatal dopaminergic density (Fig. 30 and Fig. 31A) or in the total number of nigral dopaminergic neurons (Fig. 31B) between genotypes.

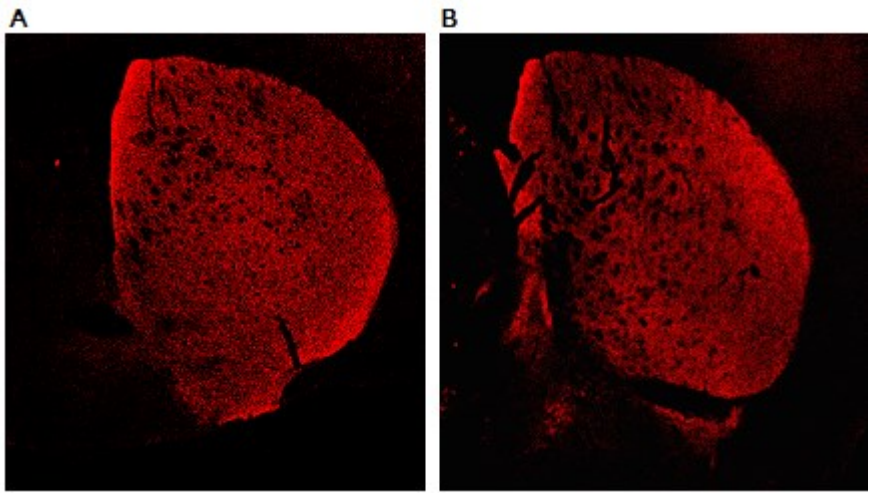

Fig. 30. Immunofluorescence images showing TH positive terminals in the striatum of WT (A) and G2019S KI (B) mice.

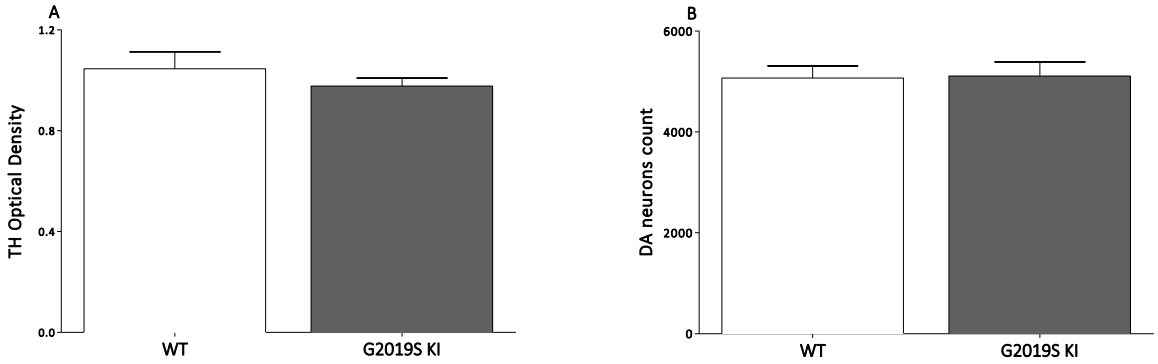

Fig. 31. TH immunoreactivity quantification (A) and sterological count of nigral DA neurons (B) in G2019S KI and WT mice (**B**). Data are expressed as absolute values and represent optical density (A) and number of positive neurons (B) and are means ± SEM of 6 determination per group. Statistical analysis was performed with the Student's t test, two tailed for unpaired data.

DISCUSSION

Previous studies have attempted to replicate a parkinsonian-like phenotype in rodents by overexpressing pathogenic G2019S LRRK2 mutation. These studies differ in many ways, such as the technology used (BAC or cDNA trangenesis, viral vectors), the levels of transgene expression and its neuronal localization, the mouse strain and, not last, the motor tests used. Nonetheless, these studies failed in showing a detrimental effect of G2019S on motor functions, unless high levels of transgene expression are artificially attained in substantia nigra neurons via the CMV/PDGF promoter, leading to 30–50% neuronal loss (Chen et al., 2012). Consistent with this view, no motor change was observed in another study on these mice (although bred on a different background), where a lower level of transgene expression in DA neurons and, consequently, a lower degree of substantia nigra neurodegeneration was achieved (18%) (Ramonet et al., 2011). To extend previous studies, here we provide the results of the first longitudinal phenotyping study in G2019S KI mice, showing that expression of mouse LRRK2 gene carrying the G2019S mutation confers a hyperkinetic phenotype, that is resistant to age-related motor decline. The robust and long lasting hyperkinetic phenotype described was substantially confirmed by a transversal motor analysis of different age-matched cohorts of G2019S KI and WT mice. Two lines of evidence seem to confirm that enhancement of kinase activity, which is a consequence of the G2019S mutation (Greggio et al., 2006; Jaleel et al., 2007; West et al., 2005), is somehow responsible for the increase in motor performance: i) the motor function of mice carrying a kinase-silencing mutation (D1994S) showed normal age-related motor worsening superimposable to that of WT littermates and ii) ATP-competitive kinase inhibitors reversed the hyperkinetic phenotype selectively in G2019S KI mice. Further evidence that enhancement of LRRK2 kinase activity might be responsible for the observed motor phenotype in G2019S KI mice comes from KI mice carrying the R1441C mutation in the ROC domain (Xiong et al., 2012). In fact, the R1441C mutation induces a milder increase of kinase activity with respect to the G2019S mutation (West et al., 2005), or no increase at all (Jaleel et al., 2007), and motor activity of R1441C KI mice in the open field and rotarod appears to be unchanged up to 24 months of age (Tong et al., 2009). The motor phenotype described in the present study clearly differs from that reported in G2019S overexpressing mice, although transient and test-related motor facilitation has been observed in those mice. For instance, BAC mice overexpressing human G2019S LRRK2 showed faster walking speed (and anxiety-like behavior) in the open field (Melrose et al., 2010) whereas human G2019S overexpressors under the Thy1 (Herzig et al., 2011) or the TetO CaMKII (Lin et al., 2009) promoters showed transient improvement in rotarod performance (Herzig et al., 2011) or increased exploratory behavior (Lin et al.,

2009). In addition, rats temporarily, but not constitutively, overexpressing human G2019S LRRK2 showed increased exploratory behavior in the open field at 18 months (Zhou et al., 2011). The influence of G2019S LRRK2 on motor function was evident in tests specific for akinesia/bradykinesia (bar and drag tests), and spontaneous exploratory behavior (open field), but not in a test for exercise driven motor activity (rotarod). This might suggest an influence of G2019S LRRK2 on specific motor parameters. Indeed, stepping activity involves striatal sensory–motor function (Kirik et al., 1998) whereas the rotarod test integrates both motor and non-motor (e.g. motivation to run) functions, and likely involves multiple brain areas (e.g. basal ganglia and cerebellum),where LRRK2 is expressed to a different degree (Higashi et al., 2007; Melrose et al., 2007). However, both in the bar and drag test, the main effect of G2019S was to preserve motor function from aging, suggesting that, more in general, G2019S mutation might confer a phenotype which is more resistant (or less sensitive) to the age-related motor decline. The possibility that this hyperkinetic phenotype is associated with changes of neurotransmitter release should be considered. Indeed, both LRRK2 silencing (Piccoli et al., 2011) or expression of the G2019S mutation (Migheli et al., 2013) has been reported to facilitate exocytosis, consistent with the finding that too much or too little kinase activity has a negative impact on vesicle trafficking (Matta et al., 2012). Consistently, pharmacological inhibition of LRRK2 activity impairs vesicle endocytosis and neurotransmitter release (Cirnaru et al., 2014). Moreover, enhancement of the stimulus-induced DA release has been detected in PC12 cells expressing the G2019S mutation (Migheli et al., 2013). Therefore, we might hypothesize that the hyperkinetic phenotype of G2019S KI mice is due to increased DA concentration at the synaptic cleft. Alternatively, an increased motor activity could result, even in the absence of an elevation of DA levels, from an increased expression of postsynaptic D1 receptors, as suggested by study in G2019S expressing cells (Migheli et al., 2013). The motor phenotype of G2019S KI mice seems to be achieved through a gain-of-function process. Indeed, silencing kinase activity does not affect motor function. The lack of endogenous control over motor activity by endogenous LRRK2 is further supported by the absence of a clear motor phenotype in LRRK2 knockout mice (Herzig et al., 2011; Lin et al., 2009), although exploratory changes consistent with anxiety-like behavior, and (transient) facilitation of rotarod performance have also been reported in these mice (Hinkle et al., 2012).While our results disclose robust motor alterations in G2019S KI mice, KI mice expressing other pathological LRRK2 mutations as well as G2019S KI mice from other laboratories need to be assessed in these motor tests to strengthen the involvement of LRRK2 kinase activity in this paradigm. Interestingly, mice carrying PD-

linked mutations, such as α-synuclein overexpressed under the Thy1 promoter (Lam et al., 2011), or parkin and DJ-1 double knock-out mice (Hennis et al., 2014) were found to be hyperactive and have increased striatal DA levels in their pre-symptomatic phase, possibly indicating compensatory mechanisms preceding nigro-striatal DA system demise. Whether the hyperactive motor phenotype of G2019S KI mice might be considered as the result of pre-symptomatic compensatory changes is presently under investigation. To possibly support this view, asymptomatic human G2019S carriers have higher putaminal DA turnover rate (Sossi et al., 2010). The fact that we did not observe a reversal of motor hyperactivity into frank hypokinesia, as in α-synuclein overexpressors (Lam et al., 2011), up to 19 months, might indicate a longer and slower pre-symptomatic phase in G2019S KI mice, in line with the different ages at onset of the disease, i.e. juvenile for α-synuclein related PD, and late for G2019S related PD (Hardy et al., 2009). To date, the requirement of kinase activity in LRRK2 pathogenic effects is still unclear. For instance, there is also growing evidence that the LRRK2 levels are driving the neuropathology rather than the kinase activity (Herzig et al., 2011; Skibinski et al., 2014). Nevertheless, the influence of LRRK2 on motor function and on neurotoxicity can procede through two independent mechanisms. Another important finding of the present study is the demonstration that ATP-competitive LRRK2 kinase inhibitors reversed the motor phenotype in G2019S KI mice. Both H-1152 and Nov-LRRK2-11 were able to inhibit LRRK2 kinase activity and reduce LRRK2 phosphorylation at Ser935 in NIH3T3 cells. This confirms previous findings that LRRK2 kinase inhibition with H-1152 abolishes binding to 14-3-3 proteins, resulting in de-phosphorylation of LRRK2 at Ser910 and Ser935 (Dzamko et al., 2010). Based on these data, phosphorylation at Ser935 has been proposed as a readout of LRRK2 kinase activity (Dzamko et al., 2010) although this phosphorylation is not the direct consequence of autophosphorylation but is possibly controlled by a LRRK2-activated kinase/phosphatase and, therefore, does not always correlate with kinase activity (Dzamko et al., 2010). In our hands, Nov-LRRK2-11 reversed the phenotype of G2019S KI mice and inhibited LRRK2 phosphorylation at 10 mg/kg, confirming ex vivo pulldown experiments showing that Nov-LRRK2-11 penetrates into the brain (Troxler et al., 2013). Behavioral data were in agreement with PK data after 3 mg/kg oral dose, and with the apparent terminal half-life of Nov-LRRK2-11 in blood after i.v. dosing of 1 mg/kg (0.4 h) (Herzig et al., 2011; Troxler et al., 2013). Interestingly, the same behavioral effect was observed at ten-fold lower doses of H-1152, suggesting significant brain penetration also for H-1152, for which, however, no published pharmacokinetic are available. Further validation of this motor reversal phenotype with additional compounds inhibiting LRRK2

is of course desirable and necessary. The present study shows a clear dissociation between motor changes and in vivo LRRK2 phosphorylation. Indeed, Nov-LRRK2-11 inhibited motor activity in G2019S KI mice causing only minimal effects (on rotarod performance) in WT mice, in face of a marked inhibition of LRRK2 phosphorylation in the striatum and cerebral cortex of both genotypes. Moreover, although H-1152 consistently inhibited motor activity and LRRK2 phosphorylation in G2019S KI but not WT mice, its motor effects far exceeded those on LRRK2 phosphorylation. The most parsimonious way to explain this discrepancy is that LRRK2 de-phosphorylation at Ser935 is a marker for in vivo target engagement of LRRK2 kinase inhibitors, but does not follow their motor effects. Perhaps, other phosphorylation, or autophosphorylation (Sheng et al., 2012), site(s) on LRRK2 should be monitored. In fact, we should recall that both inhibitors target other kinases beyond LRRK2, which may act upstream and downstream of LRRK2. For instance, PKA has been shown to crosstalk with LRRK2 (Li et al., 2011; Muda et al., 2014; Parisiadou et al., 2014), whereas ROCK/MLCK are involved in actin cytoskeleton remodeling pathways, in which activity they could crosstalk with LRRK2. On the other hand, given the parallel (albeit temporally-dissociated) inhibition of motor activity and striatal LRRK2 phosphorylation induced by H-1152, we might speculate that striatal LRRK2 is a key regulator of motor activity. In this case, if higher LRRK2 kinase activity is present in the striatum of G2019S KI mice compared to WT mice, as predicted, normalization of these levels by LRRK2 kinase inhibitors might represent the trigger of a cascade of events leading to sustained motor inhibition. Moreover, the different patterns of LRRK2 de-phosphorylation of Nov-LRRK2-11 and H-1152 in G2019S KI and WT mice suggest a higher LRRK2 selectivity and/or brain exposure/free fraction of Nov-LRRK2-11. For further confirmation, additional information on earlier times-points (< 20 min) of Nov-LRRK2-11 effects as well as higher doses of H-1152 would be desirable. In addition, the finding that Nov-LRRK2-11 reduces LRRK2 levels in the cortex but not striatum indicates different properties of the LRRK2 system in these two areas.

The identification of a hyperkinetic phenotype in G2019S KI mice, causally linked to an increase of LRRK2 kinase activity, led us to investigate the underlying biochemical and neurochemical dopaminergic mechanisms. It is known that there is a preclinical stage in which patients with familial PD are asymptomatic, despite alterations of DA homeostasis start emerging (Adams et al., 2005; Nandhagopal et al., 2008; Sossi et al., 2010). We therefore attempted to unravel a relationship between dysregulation of motor activity and dopaminergic transmission in G2019S KI mice. Dopaminergic transmission comprises DA synthesis, the packaging of DA into synaptic vesicles by VMAT2, the release of DA into

the synaptic cleft, the interaction of DA with presynaptic and postsynaptic DA receptors, the reuptake of DA into presynaptic DA nerve terminals via the plasma membrane DAT, and the degradation of intra/extracellular DA by monoamine oxidases (MAO) and catechol-O-methyltransferases (COMT) .

We first analyzed the responsiveness to dopaminergic drugs, in behavioral pharmacology experiments. The cataleptic response to haloperidol observed in G2019S KI but not WT mice suggests dysregulation of DA transmission at striato-pallidal MSNs. In fact, a negative interaction between D2 and A2A receptors on PKA activity and cAMP level production occurs in striato-pallidal MSNs (Ferre et al., 1994; Ferre et al., 1991). Thus, a greater cataleptic response might correlate with greater activity at A2A receptors. In fact, blockade of postsynaptic D2 receptors on striato-pallidal MSNs favors the action of A2A receptors (Tozzi et al., 2011). A greater activity at A2A receptors, in turn, might reflect greater G_{olf} levels, since striatal A2A receptors are coupled to Golf (Hervè, 2011). The possibility of a greater signaling through G_{olf} is also corroborated by the finding that the blockade of D1/D5 receptors, which signal through G_{olf}, with SCH23390 worsens motor performance in G2019S KI mice but not WT controls.

In favor of an increased DA signaling, expression of G2019S LRRK2 in PC12 cells causes an increase in D1 receptor expression at cell membrane, possibly due to the LRRK2 interference with receptor turnover and endocytosis (Migheli et al., 2013). In addition, since LRRK2 interacts with PKARIIβ regulatory subunit (Parisiadou et al., 2014), which is abundant in striatal MSNs, changes in responsiveness of MSNs to DA might occur in G2019S KI mice, as demonstrated for R1441C KI mice (Parisiadou et al., 2014).

The different responsitivity of G2019S KI and WT mice to DA receptor selective antagonists, however, might also have a presynaptic origin, and be due to greater DA release and tonic activation (saturation) of DA receptors. We therefore investigated the behavioral outcome of D2 receptor activation. The D3/D2 receptor agonist PPX facilitated movement at low doses but was ineffective at higher ones in WT mice, providing a bell-shaped curve. Conversely, PPX was ineffective at low doses and inhibited motor function at higher ones, in G2019S KI mice. Motor impairment induced by DA agonists is known to be mediated by presynaptic D2/D3 autoreceptors (Maj et al., 1997; Mierau and Schingnitz, 1992; Siuciak and Fujiwara, 2004). Indeed, motor inhibition is the predominant action of D2 agonists in mice having intact DA transmission. Conversely, D2-mediated facilitation emerges in conditions where DA is reduced and D2 postsynaptic receptors upregulated, as in PD (Seeman, 2007). Considering that in WT mice DA transmission might be dysregulated do to the aging process, we speculate that low doses of PPX act on up-

regulated D2 postsynaptic receptors to promote movement whereas high doses of PPX recruit D2 presynaptic receptors, thus reversing motor facilitation. Conversely, in G2019S KI mice, PPX provided monophasic motor inhibition, likely acting on presynaptic D2 (auto)receptors. This indicates that, different from WT mice, DA transmission is intact and D2 postsynaptic receptors saturated in G2019S KI mice. In keeping with this view, no changes in striatal dopaminergic innervation or nigral DA cell number were found between genotypes. Moreover, microdialysis revealed no difference in extracellular DA levels between genotypes, suggesting that the hyperkinetic phenotype of G2019S mice does not rely on alterations of DA neuron activity. Indeed, previous microdialysis studies revealed that basal striatal extracellular DA levels reflect neuronal activity (for reviews see(Kehr, 1993; Westerink, 1995). Consistently, administration of a dose of Nov-LRRK2-11 that reduced motor activity did not affect striatal DA release. In light of these data, we can speculate that motor inhibition induced by Nov-LRRK2-11 is DA-independent and might occur either presynaptically, through inhibition of LRRK2 kinase activity regulating exocytosis at non-DA nerve terminals, or postsynaptically, through inhibition of LRRK2 kinase activity regulating DA signaling at MSNs.

Despite enhanced DA levels were not associated with the hyperkinetic phenotype of G2019S mice, signs of dysregulated presynaptic DA release machinery were evident in this genotype. First, G2019S KI mice showed a significantly lower metabolite/DA ratio, suggesting reduced DA turnover. It appears worth investigating, in future experiments, the enzymatic activity of COMT and/or MAO. Moreover, and perhaps more relevant, dysfunction of DAT was found in G2019S KI mice. Indeed, the DAT inhibitor GBR-12783 induced motor facilitation in WT mice, as expected, but was ineffective in G2019S KI mice. This lack of behavioral response might be due to the greater saturation of postsynaptic DA receptors, insensitive to further increases in DA levels, or be directly related to altered DAT function/expression. In favor of the latter, in vivo microdialysis showed a blunted DA response to acute DAT blockade with GBR-12783 in G2019S KI mice. Moreover, despite no difference in maximal WIN-35,428 binding to DAT was found between genotypes, reduced DAT protein levels and greater maximal transport rate (V_{max}) were found in G2019S mice. Increase in V_{max} might represent an attempt to compensate for the lower intracellular expression of DAT, suggesting a probable adaptation process within the presynaptic molecular machinery.

Of note, DAT function and trafficking are modulated by D2 autoreceptors via Gi/Go-dependent manner and require ERK1/2 activation. In particular, DAT is regulated by D2 autoreceptors through a direct physical interaction, and disruption of this interaction in the

mouse brain in vivo results in decreased striatal synaptosomal DA uptake and increased locomotor activity. On the other hand, DAT regulation is DA-dependent and is modulated by numerous signal transduction mechanisms, including a palette of protein kinases such as Ca^{2+}/calmodulin-dependent protein kinase II (CaMKII) and PKC. Numerous studies have demonstrated that direct activation of PKC leads to downregulation of DAT activity with an accompanying redistribution of DAT from the membrane. Likewise, there is some evidence that PKC may mediate DAT substrate-stimulated downregulation of DAT activity (Chen et al., 2010). In addition, increase of surface DAT expression is dependent on soluble N-ethylmaleimide-sensitive factor attachment protein receptor (SNARE) proteins such as syntaxin 1A and the vesicle-associated membrane protein (VAMP)/synaptobrevin which participate in the process of membrane fusion and exocytosis (Furman et al., 2009). Moreover, since DA release at the nerve terminal is mediated by the SNARE complex-dependent fusion of SVs, and is triggered by Ca^{2+} binding to synaptotagmins, we are tempting to speculate that G2019S LRRK2 might affect presynaptic machinery at different levels, modulating DAT trafficking/function by interacting with different kinases (i.e. ERK) and /or mobilizing SVs by acting on syntaxin 1A via its kinase activity.

To support the cross-talk between G2019S LRRK2 and DAT-mediated motor behavior, we show that the impaired motor behavior caused by blockade of LRRK2 kinase activity with Nov-LRRK2-11 was reversed upon GBR-12783 administration To possibly reinforce this view, the inducible temporal expression of G2019S LRRK2 in adult rats was associated with an increase of extracellular DA levels and a consequent enhancement of locomotor activity through gradual damage to DAT-mediated DA reuptake (Zhou et al., 2011). Supporting clinical evidence obtained by in vivo PET (positron emission tomographic) scanning in mutant LRRK2 carriers at asymptomatic stages reveals reduced DAT and VMAT2 binding even in the absence of clinically evident parkinsonism (Adams et al., 2005; Nandhagopal et al., 2008).

Concluding remarks

The present longitudinal phenotypic study provides genetic evidence that expression of the G2019S mutation under the endogenous promoter confers mice with better motor performances and preserves their age-related motor decline in tests specific for akinesia/bradykinesia. Enhancement of LRRK2 kinase activity likely underlies this phenotype since D1994S KD mice do not display motor abnormalities, and ATP-competitive LRRK2 inhibitors reversed motor phenotype in G2019S KI mice.

In particular, a correlation between in vivo motor effects of LRRK2 inhibitors and their ability to de-phosphorylate LRRK2 at Ser935 was shown for the first time. For these reasons, the present thesis work proposes G2019S KI mice as a valuable in vivo model to investigate the effects of LRRK2 inhibitors.

Moreover, we pointed out a correlation between hyperkinetic phenotype and an altered dopaminergic transmission, even though no changes in nigral DA cell counts or dopaminergic striatal nerve terminal density were observed in G2019S KI mice. However, the overall pattern of responses to a D2/D3 receptor agonist or antagonists, and to D1/D5 receptor antagonist suggested an elevated tonic activation of DA receptors in G2019S KI mice. Moreover, a cross-talk between the G2019S LRRK2 mutation and DAT-mediated motor behavior was unraveled, suggesting that G2019S LRRK2 might affect presynaptic dopaminergic machinery.

This study challenges the idea that G2019S is detrimental for motor activity in rodents, suggesting that other factors might be involved in inducing a PD-like phenotype, such alpha-synuclein (for reviews see (Greggio et al., 2011; Taymans and Cookson, 2010), or parkin (Smith et al., 2005).

Nonetheless, in G2019S KI mice, the reduced DA turnover together with loss of synaptic VMAT2, might result in accumulation of DA within the synapse, making it available to oxidation and leading to the formation of reactive byproducts (es DOPAL) which ultimately might damage dopaminergic neurites (Bisaglia et al., 2013; Marchitti et al., 2007).

REFERENCES

Abeliovich A, Schmitz Y, Farinas I, Choi-Lundberg D, Ho WH, Castillo PE, Shinsky N, Verdugo JM, Armanini M, Ryan A, Hynes M, Phillips H, Sulzer D and Rosenthal A (2000) Mice lacking alpha-synuclein display functional deficits in the nigrostriatal dopamine system. *Neuron* **25**:239-252.

Adams JR, van Netten H, Schulzer M, Mak E, McKenzie J, Strongosky A, Sossi V, Ruth TJ, Lee CS, Farrer M, Gasser T, Uitti RJ, Calne DB, Wszolek ZK and Stoessl AJ (2005) PET in LRRK2 mutations: comparison to sporadic Parkinson's disease and evidence for presymptomatic compensation. *Brain : a journal of neurology* **128**:2777-2785.

Alcalay RN, Caccappolo E, Mejia-Santana H, Tang MX, Rosado L, Ross BM, Verbitsky M, Kisselev S, Louis ED, Comella C, Colcher A, Jennings D, Nance MA, Bressman SB, Scott WK, Tanner C, Mickel S, Andrews H, Waters C, Fahn S, Cote L, Frucht S, Ford B, Rezak M, Novak K, Friedman JH, Pfeiffer R, Marsh L, Hiner B, Siderowf A, Ottman R, Marder K and Clark LN (2010) Frequency of known mutations in early-onset Parkinson disease: implication for genetic counseling: the consortium on risk for early onset Parkinson disease study. *Archives of neurology* **67**:1116-1122.

Alegre-Abarrategui J, Christian H, Lufino MM, Mutihac R, Venda LL, Ansorge O and Wade-Martins R (2009) LRRK2 regulates autophagic activity and localizes to specific membrane microdomains in a novel human genomic reporter cellular model. *Human molecular genetics* **18**:4022-4034.

Andres-Mateos E, Mejias R, Sasaki M, Li X, Lin BM, Biskup S, Zhang L, Banerjee R, Thomas B, Yang L, Liu G, Beal MF, Huso DL, Dawson TM and Dawson VL (2009) Unexpected lack of hypersensitivity in LRRK2 knock-out mice to MPTP (1-methyl-4-phenyl-1,2,3,6-tetrahydropyridine). *The Journal of neuroscience : the official journal of the Society for Neuroscience* **29**:15846-15850.

Auluck PK, Chan HY, Trojanowski JQ, Lee VM and Bonini NM (2002) Chaperone suppression of alpha-synuclein toxicity in a Drosophila model for Parkinson's disease. *Science* **295**:865-868.

Barrett JC, Hansoul S, Nicolae DL, Cho JH, Duerr RH, Rioux JD, Brant SR, Silverberg MS, Taylor KD, Barmada MM, Bitton A, Dassopoulos T, Datta LW, Green T, Griffiths AM, Kistner EO, Murtha MT, Regueiro MD, Rotter JI, Schumm LP, Steinhart AH, Targan SR, Xavier RJ, Consortium NIG, Libioulle C, Sandor C, Lathrop M, Belaiche J, Dewit O, Gut I, Heath S, Laukens D, Mni M, Rutgeerts P, Van Gossum A, Zelenika D, Franchimont D, Hugot JP, de Vos M, Vermeire S, Louis E, Belgian-French IBDC, Wellcome Trust Case Control C, Cardon LR, Anderson CA, Drummond H, Nimmo E, Ahmad T, Prescott NJ, Onnie CM, Fisher SA, Marchini J, Ghori J, Bumpstead S, Gwilliam R, Tremelling M, Deloukas P, Mansfield J, Jewell D, Satsangi J, Mathew CG, Parkes M, Georges M and Daly MJ (2008) Genome-wide association defines more than 30 distinct susceptibility loci for Crohn's disease. *Nature genetics* **40**:955-962.

Beal MF (2010) Parkinson's disease: a model dilemma. *Nature* **466**:S8-10.

Beilina A, Rudenko IN, Kaganovich A, Civiero L, Chau H, Kalia SK, Kalia LV, Lobbestael E, Chia R, Ndukwe K, Ding J, Nalls MA, International Parkinson's Disease Genomics C, North American Brain Expression C, Olszewski M, Hauser DN, Kumaran R, Lozano AM, Baekelandt V, Greene LE, Taymans JM, Greggio E and Cookson MR (2014) Unbiased screen for interactors of leucine-rich repeat kinase 2 supports a common pathway for sporadic and familial Parkinson disease. *Proceedings of the National Academy of Sciences of the United States of America* **111**:2626-2631.

Belluzzi E, Greggio E and Piccoli G (2012) Presynaptic dysfunction in Parkinson's disease: a focus on LRRK2. *Biochemical Society transactions* **40**:1111-1116.

Berger Z, Smith KA and Lavoie MJ (2010) Membrane localization of LRRK2 is associated with increased formation of the highly active LRRK2 dimer and changes in its phosphorylation. *Biochemistry* **49**:5511-5523.

Bido S, Marti M and Morari M (2011) Amantadine attenuates levodopa-induced dyskinesia in mice and rats preventing the accompanying rise in nigral GABA levels. *Journal of neurochemistry* **118**:1043-1055.

Bisaglia M, Greggio E, Beltramini M and Bubacco L (2013) Dysfunction of dopamine homeostasis: clues in the hunt for novel Parkinson's disease therapies. *FASEB journal : official publication of the Federation of American Societies for Experimental Biology* **27**:2101-2110.

Biskup S, Moore DJ, Celsi F, Higashi S, West AB, Andrabi SA, Kurkinen K, Yu SW, Savitt JM, Waldvogel HJ, Faull RL, Emson PC, Torp R, Ottersen OP, Dawson TM and Dawson VL (2006) Localization of LRRK2 to membranous and vesicular structures in mammalian brain. *Annals of neurology* **60**:557-569.

Bonifati V (2014) Genetics of Parkinson's disease--state of the art, 2013. *Parkinsonism & related disorders* **20 Suppl 1**:S23-28.

Canet-Aviles RM, Wilson MA, Miller DW, Ahmad R, McLendon C, Bandyopadhyay S, Baptista MJ, Ringe D, Petsko GA and Cookson MR (2004) The Parkinson's disease protein DJ-1 is neuroprotective due to cysteine-sulfinic acid-driven mitochondrial localization. *Proceedings of the National Academy of Sciences of the United States of America* **101**:9103-9108.

Carballo-Carbajal I, Weber-Endress S, Rovelli G, Chan D, Wolozin B, Klein CL, Patenge N, Gasser T and Kahle PJ (2010) Leucine-rich repeat kinase 2 induces alpha-synuclein expression via the extracellular signal-regulated kinase pathway. *Cellular signalling* **22**:821-827.

Cardona F, Tormos-Perez M and Perez-Tur J (2014) Structural and functional in silico analysis of LRRK2 missense substitutions. *Molecular biology reports* **41**:2529-2542.

Chan D, Citro A, Cordy JM, Shen GC and Wolozin B (2011) Rac1 protein rescues neurite retraction caused by G2019S leucine-rich repeat kinase 2 (LRRK2). *The Journal of biological chemistry* **286**:16140-16149.

Chang WP and Sudhof TC (2009) SV2 renders primed synaptic vesicles competent for Ca2+ -induced exocytosis. *The Journal of neuroscience : the official journal of the Society for Neuroscience* **29**:883-897.

Chartier-Harlin MC, Dachsel JC, Vilarino-Guell C, Lincoln SJ, Lepretre F, Hulihan MM, Kachergus J, Milnerwood AJ, Tapia L, Song MS, Le Rhun E, Mutez E, Larvor L, Duflot A, Vanbesien-Mailliot C, Kreisler A, Ross OA, Nishioka K, Soto-Ortolaza AI, Cobb SA, Melrose HL, Behrouz B, Keeling BH, Bacon JA, Hentati E, Williams L, Yanagiya A, Sonenberg N, Lockhart PJ, Zubair AC, Uitti RJ, Aasly JO, Krygowska-Wajs A, Opala G, Wszolek ZK, Frigerio R, Maraganore DM, Gosal D, Lynch T, Hutchinson M, Bentivoglio AR, Valente EM, Nichols WC, Pankratz N, Foroud T, Gibson RA, Hentati F, Dickson DW, Destee A and Farrer MJ (2011) Translation initiator EIF4G1 mutations in familial Parkinson disease. *American journal of human genetics* **89**:398-406.

Chaudhuri KR and Schapira AH (2009) Non-motor symptoms of Parkinson's disease: dopaminergic pathophysiology and treatment. *The Lancet Neurology* **8**:464-474.

Chen CY, Weng YH, Chien KY, Lin KJ, Yeh TH, Cheng YP, Lu CS and Wang HL (2012) (G2019S) LRRK2 activates MKK4-JNK pathway and causes degeneration of SN dopaminergic neurons in a transgenic mouse model of PD. *Cell death and differentiation* **19**:1623-1633.

Chen NH, Xu C, Coffey LL and Reith ME (1996) [3H]WIN 35,428 [2 beta-carbomethoxy-3 beta-(4-fluorophenyl)tropane] binding to rat brain membranes. Comparing dopamine cell body areas with nerve terminal regions. *Biochemical pharmacology* **51**:563-566.

Chen R, Furman CA and Gnegy ME (2010) Dopamine transporter trafficking: rapid response on demand. *Future neurology* **5**:123.

Cho HJ, Liu G, Jin SM, Parisiadou L, Xie C, Yu J, Sun L, Ma B, Ding J, Vancraenenbroeck R, Lobbestael E, Baekelandt V, Taymans JM, He P, Troncoso JC, Shen Y and Cai H (2013) MicroRNA-205 regulates the expression of Parkinson's disease-related leucine-rich repeat kinase 2 protein. *Human molecular genetics* **22**:608-620.

Cirnaru MD, Marte A, Belluzzi E, Russo I, Gabrielli M, Longo F, Arcuri L, Murru L, Bubacco L, Matteoli M, Fedele E, Sala C, Passafaro M, Morari M, Greggio E, Onofri F and Piccoli G (2014) LRRK2 kinase activity regulates synaptic vesicle trafficking and neurotransmitter release through modulation of LRRK2 macro-molecular complex. *Frontiers in molecular neuroscience* **7**:49.

Cookson MR (2009) alpha-Synuclein and neuronal cell death. *Molecular neurodegeneration* **4**:9.

Cookson MR (2010) The role of leucine-rich repeat kinase 2 (LRRK2) in Parkinson's disease. *Nature reviews Neuroscience* **11**:791-797.

Cotzias GC (1969) Parkinsoism anDopa. *Journal of chronic diseases* **22**:297-301.

Daniel G and Moore DJ (2014) Modeling LRRK2 Pathobiology in Parkinson's Disease: From Yeast to Rodents. *Current topics in behavioral neurosciences*.

Daniels V, Vancraenenbroeck R, Law BM, Greggio E, Lobbestael E, Gao F, De Maeyer M, Cookson MR, Harvey K, Baekelandt V and Taymans JM (2011) Insight into the mode of action of the LRRK2 Y1699C pathogenic mutant. *Journal of neurochemistry* **116**:304-315.

Dauer W and Przedborski S (2003) Parkinson's disease: mechanisms and models. *Neuron* **39**:889-909.

Davies P, Hinkle KM, Sukar NN, Sepulveda B, Mesias R, Serrano G, Alessi DR, Beach TG, Benson DL, White CL, Cowell RM, Das SS, West AB and Melrose HL (2013) Comprehensive characterization and optimization of anti-LRRK2 (leucine-rich repeat kinase 2) monoclonal antibodies. *The Biochemical journal* **453**:101-113.

Deng J, Lewis PA, Greggio E, Sluch E, Beilina A and Cookson MR (2008) Structure of the ROC domain from the Parkinson's disease-associated leucine-rich repeat kinase 2 reveals a dimeric GTPase. *Proceedings of the National Academy of Sciences of the United States of America* **105**:1499-1504.

Devi L, Raghavendran V, Prabhu BM, Avadhani NG and Anandatheerthavarada HK (2008) Mitochondrial import and accumulation of alpha-synuclein impair complex I in human dopaminergic neuronal cultures and Parkinson disease brain. *The Journal of biological chemistry* **283**:9089-9100.

Ding X and Goldberg MS (2009) Regulation of LRRK2 stability by the E3 ubiquitin ligase CHIP. *PloS one* **4**:e5949.

Dodson MW, Zhang T, Jiang C, Chen S and Guo M (2012) Roles of the Drosophila LRRK2 homolog in Rab7-dependent lysosomal positioning. *Human molecular genetics* **21**:1350-1363.

Donaldson JG and Radhakrishna H (2001) Expression and properties of ADP-ribosylation factor (ARF6) in endocytic pathways. *Methods in enzymology* **329**:247-256.

Dusonchet J, Kochubey O, Stafa K, Young SM, Jr., Zufferey R, Moore DJ, Schneider BL and Aebischer P (2011) A rat model of progressive nigral neurodegeneration induced by the Parkinson's disease-associated G2019S mutation in LRRK2. *The Journal of neuroscience : the official journal of the Society for Neuroscience* **31**:907-912.

Dzamko N, Deak M, Hentati F, Reith AD, Prescott AR, Alessi DR and Nichols RJ (2010) Inhibition of LRRK2 kinase activity leads to dephosphorylation of Ser(910)/Ser(935), disruption of 14-3-3 binding and altered cytoplasmic localization. *The Biochemical journal* **430**:405-413.

Fabbrini G, Brotchie JM, Grandas F, Nomoto M and Goetz CG (2007) Levodopa-induced dyskinesias. *Movement disorders : official journal of the Movement Disorder Society* **22**:1379-1389; quiz 1523.

Fahn S (2008) The history of dopamine and levodopa in the treatment of Parkinson's disease. *Movement disorders : official journal of the Movement Disorder Society* **23 Suppl 3**:S497-508.

Ferre S, O'Connor WT, Snaprud P, Ungerstedt U and Fuxe K (1994) Antagonistic interaction between adenosine A2A receptors and dopamine D2 receptors in the ventral striopallidal system. Implications for the treatment of schizophrenia. *Neuroscience* **63**:765-773.

Ferre S, von Euler G, Johansson B, Fredholm BB and Fuxe K (1991) Stimulation of high-affinity adenosine A2 receptors decreases the affinity of dopamine D2 receptors in rat striatal

membranes. *Proceedings of the National Academy of Sciences of the United States of America* **88**:7238-7241.

Fingerhut A, von Figura K and Honing S (2001) Binding of AP2 to sorting signals is modulated by AP2 phosphorylation. *The Journal of biological chemistry* **276**:5476-5482.

Follett J, Norwood SJ, Hamilton NA, Mohan M, Kovtun O, Tay S, Zhe Y, Wood SA, Mellick GD, Silburn PA, Collins BM, Bugarcic A and Teasdale RD (2014) The Vps35 D620N mutation linked to Parkinson's disease disrupts the cargo sorting function of retromer. *Traffic* **15**:230-244.

Fu H, Subramanian RR and Masters SC (2000) 14-3-3 proteins: structure, function, and regulation. *Annual review of pharmacology and toxicology* **40**:617-647.

Funayama M, Hasegawa K, Kowa H, Saito M, Tsuji S and Obata F (2002) A new locus for Parkinson's disease (PARK8) maps to chromosome 12p11.2-q13.1. *Annals of neurology* **51**:296-301.

Fung HC, Chen CM, Hardy J, Hernandez D, Singleton A and Wu YR (2006) Lack of G2019S LRRK2 mutation in a cohort of Taiwanese with sporadic Parkinson's disease. *Movement disorders : official journal of the Movement Disorder Society* **21**:880-881.

Furman CA, Chen R, Guptaroy B, Zhang M, Holz RW and Gnegy M (2009) Dopamine and amphetamine rapidly increase dopamine transporter trafficking to the surface: live-cell imaging using total internal reflection fluorescence microscopy. *The Journal of neuroscience : the official journal of the Society for Neuroscience* **29**:3328-3336.

Gaig C and Tolosa E (2009) When does Parkinson's disease begin? *Movement disorders : official journal of the Movement Disorder Society* **24 Suppl 2**:S656-664.

Galter D, Westerlund M, Carmine A, Lindqvist E, Sydow O and Olson L (2006) LRRK2 expression linked to dopamine-innervated areas. *Annals of neurology* **59**:714-719.

Gehrke S, Imai Y, Sokol N and Lu B (2010) Pathogenic LRRK2 negatively regulates microRNA-mediated translational repression. *Nature* **466**:637-641.

Giasson BI, Covy JP, Bonini NM, Hurtig HI, Farrer MJ, Trojanowski JQ and Van Deerlin VM (2006) Biochemical and pathological characterization of Lrrk2. *Annals of neurology* **59**:315-322.

Giesert F, Hofmann A, Burger A, Zerle J, Kloos K, Hafen U, Ernst L, Zhang J, Vogt-Weisenhorn DM and Wurst W (2013) Expression analysis of Lrrk1, Lrrk2 and Lrrk2 splice variants in mice. *PloS one* **8**:e63778.

Gillardon F (2009) Leucine-rich repeat kinase 2 phosphorylates brain tubulin-beta isoforms and modulates microtubule stability--a point of convergence in parkinsonian neurodegeneration? *Journal of neurochemistry* **110**:1514-1522.

Gilsbach BK, Ho FY, Vetter IR, van Haastert PJ, Wittinghofer A and Kortholt A (2012) Roco kinase structures give insights into the mechanism of Parkinson disease-related leucine-rich-repeat kinase 2 mutations. *Proceedings of the National Academy of Sciences of the United States of America* **109**:10322-10327.

Gloeckner CJ, Boldt K, von Zweydorf F, Helm S, Wiesent L, Sarioglu H and Ueffing M (2010) Phosphopeptide analysis reveals two discrete clusters of phosphorylation in the N-terminus and the Roc domain of the Parkinson-disease associated protein kinase LRRK2. *Journal of proteome research* **9**:1738-1745.

Gloeckner CJ, Kinkl N, Schumacher A, Braun RJ, O'Neill E, Meitinger T, Kolch W, Prokisch H and Ueffing M (2006) The Parkinson disease causing LRRK2 mutation I2020T is associated with increased kinase activity. *Human molecular genetics* **15**:223-232.

Goetz CG and Pal G (2014) Initial management of Parkinson's disease. *Bmj* **349**:g6258.

Goldwurm S, Di Fonzo A, Simons EJ, Rohe CF, Zini M, Canesi M, Tesei S, Zecchinelli A, Antonini A, Mariani C, Meucci N, Sacilotto G, Sironi F, Salani G, Ferreira J, Chien HF, Fabrizio E, Vanacore N, Dalla Libera A, Stocchi F, Diroma C, Lamberti P, Sampaio C, Meco G, Barbosa E, Bertoli-Avella AM, Breedveld GJ, Oostra BA, Pezzoli G and Bonifati V (2005) The G6055A (G2019S) mutation in LRRK2 is frequent in both early and late onset Parkinson's disease and originates from a common ancestor. *Journal of medical genetics* **42**:e65.

Gotthardt K, Weyand M, Kortholt A, Van Haastert PJ and Wittinghofer A (2008) Structure of the Roc-COR domain tandem of C. tepidum, a prokaryotic homologue of the human LRRK2 Parkinson kinase. *The EMBO journal* **27**:2239-2249.

Greggio E, Bisaglia M, Civiero L and Bubacco L (2011) Leucine-rich repeat kinase 2 and alpha-synuclein: intersecting pathways in the pathogenesis of Parkinson's disease? *Molecular neurodegeneration* **6**:6.

Greggio E, Jain S, Kingsbury A, Bandopadhyay R, Lewis P, Kaganovich A, van der Brug MP, Beilina A, Blackinton J, Thomas KJ, Ahmad R, Miller DW, Kesavapany S, Singleton A, Lees A, Harvey RJ, Harvey K and Cookson MR (2006) Kinase activity is required for the toxic effects of mutant LRRK2/dardarin. *Neurobiology of disease* **23**:329-341.

Greggio E, Taymans JM, Zhen EY, Ryder J, Vancraenenbroeck R, Beilina A, Sun P, Deng J, Jaffe H, Baekelandt V, Merchant K and Cookson MR (2009) The Parkinson's disease kinase LRRK2 autophosphorylates its GTPase domain at multiple sites. *Biochemical and biophysical research communications* **389**:449-454.

Greggio E, Zambrano I, Kaganovich A, Beilina A, Taymans JM, Daniels V, Lewis P, Jain S, Ding J, Syed A, Thomas KJ, Baekelandt V and Cookson MR (2008) The Parkinson disease-associated leucine-rich repeat kinase 2 (LRRK2) is a dimer that undergoes intramolecular autophosphorylation. *The Journal of biological chemistry* **283**:16906-16914.

Guardia-Laguarta C, Area-Gomez E, Rub C, Liu Y, Magrane J, Becker D, Voos W, Schon EA and Przedborski S (2014) alpha-Synuclein is localized to mitochondria-associated ER membranes. *The Journal of neuroscience : the official journal of the Society for Neuroscience* **34**:249-259.

Guerreiro PS, Huang Y, Gysbers A, Cheng D, Gai WP, Outeiro TF and Halliday GM (2013) LRRK2 interactions with alpha-synuclein in Parkinson's disease brains and in cell models. *Journal of molecular medicine* **91**:513-522.

Hakimi M, Selvanantham T, Swinton E, Padmore RF, Tong Y, Kabbach G, Venderova K, Girardin SE, Bulman DE, Scherzer CR, LaVoie MJ, Gris D, Park DS, Angel JB, Shen J, Philpott DJ and Schlossmacher MG (2011) Parkinson's disease-linked LRRK2 is expressed in circulating and tissue immune cells and upregulated following recognition of microbial structures. *Journal of neural transmission* **118**:795-808.

Hardy J, Lewis P, Revesz T, Lees A and Paisan-Ruiz C (2009) The genetics of Parkinson's syndromes: a critical review. *Current opinion in genetics & development* **19**:254-265.

Harraz MM, Dawson TM and Dawson VL (2011) MicroRNAs in Parkinson's disease. *Journal of chemical neuroanatomy* **42**:127-130.

Hassin-Baer S, Laitman Y, Azizi E, Molchadski I, Galore-Haskel G, Barak F, Cohen OS and Friedman E (2009) The leucine rich repeat kinase 2 (LRRK2) G2019S substitution mutation. Association with Parkinson disease, malignant melanoma and prevalence in ethnic groups in Israel. *Journal of neurology* **256**:483-487.

Haugarvoll K, Rademakers R, Kachergus JM, Nuytemans K, Ross OA, Gibson JM, Tan EK, Gaig C, Tolosa E, Goldwurm S, Guidi M, Riboldazzi G, Brown L, Walter U, Benecke R, Berg D, Gasser T, Theuns J, Pals P, Cras P, De Deyn PP, Engelborghs S, Pickut B, Uitti RJ, Foroud T, Nichols WC, Hagenah J, Klein C, Samii A, Zabetian CP, Bonifati V, Van Broeckhoven C, Farrer MJ and Wszolek ZK (2008) Lrrk2 R1441C parkinsonism is clinically similar to sporadic Parkinson disease. *Neurology* **70**:1456-1460.

Healy DG, Falchi M, O'Sullivan SS, Bonifati V, Durr A, Bressman S, Brice A, Aasly J, Zabetian CP, Goldwurm S, Ferreira JJ, Tolosa E, Kay DM, Klein C, Williams DR, Marras C, Lang AE, Wszolek ZK, Berciano J, Schapira AH, Lynch T, Bhatia KP, Gasser T, Lees AJ, Wood NW and International LC (2008) Phenotype, genotype, and worldwide genetic penetrance of LRRK2-associated Parkinson's disease: a case-control study. *The Lancet Neurology* **7**:583-590.

Hebert SS and De Strooper B (2009) Alterations of the microRNA network cause neurodegenerative disease. *Trends in neurosciences* **32**:199-206.

Hennis MR, Marvin MA, Taylor CM, 2nd and Goldberg MS (2014) Surprising behavioral and neurochemical enhancements in mice with combined mutations linked to Parkinson's disease. *Neurobiology of disease* **62**:113-123.

Herzig MC, Kolly C, Persohn E, Theil D, Schweizer T, Hafner T, Stemmelen C, Troxler TJ, Schmid P, Danner S, Schnell CR, Mueller M, Kinzel B, Grevot A, Bolognani F, Stirn M, Kuhn RR, Kaupmann K, van der Putten PH, Rovelli G and Shimshek DR (2011) LRRK2 protein levels are determined by kinase function and are crucial for kidney and lung homeostasis in mice. *Human molecular genetics* **20**:4209-4223.

Higashi S, Biskup S, West AB, Trinkaus D, Dawson VL, Faull RL, Waldvogel HJ, Arai H, Dawson TM, Moore DJ and Emson PC (2007) Localization of Parkinson's disease-associated LRRK2 in normal and pathological human brain. *Brain research* **1155**:208-219.

Hinkle KM, Yue M, Behrouz B, Dachsel JC, Lincoln SJ, Bowles EE, Beevers JE, Dugger B, Winner B, Prots I, Kent CB, Nishioka K, Lin WL, Dickson DW, Janus CJ, Farrer MJ and Melrose HL (2012) LRRK2 knockout mice have an intact dopaminergic system but display alterations in exploratory and motor co-ordination behaviors. *Molecular neurodegeneration* **7**:25.

Hulihan MM, Ishihara-Paul L, Kachergus J, Warren L, Amouri R, Elango R, Prinjha RK, Upmanyu R, Kefi M, Zouari M, Sassi SB, Yahmed SB, El Euch-Fayeche G, Matthews PM, Middleton LT, Gibson RA, Hentati F and Farrer MJ (2008) LRRK2 Gly2019Ser penetrance in Arab-Berber patients from Tunisia: a case-control genetic study. *The Lancet Neurology* **7**:591-594.

Iaccarino C, Crosio C, Vitale C, Sanna G, Carri MT and Barone P (2007) Apoptotic mechanisms in mutant LRRK2-mediated cell death. *Human molecular genetics* **16**:1319-1326.

Imai Y, Gehrke S, Wang HQ, Takahashi R, Hasegawa K, Oota E and Lu B (2008) Phosphorylation of 4E-BP by LRRK2 affects the maintenance of dopaminergic neurons in Drosophila. *The EMBO journal* **27**:2432-2443.

Jaleel M, Nichols RJ, Deak M, Campbell DG, Gillardon F, Knebel A and Alessi DR (2007) LRRK2 phosphorylates moesin at threonine-558: characterization of how Parkinson's disease mutants affect kinase activity. *The Biochemical journal* **405**:307-317.

Jameel NM, Thirunavukkarasu C, Wu T, Watkins SC, Friedman SL and Gandhi CR (2009) p38-MAPK- and caspase-3-mediated superoxide-induced apoptosis of rat hepatic stellate cells: reversal by retinoic acid. *Journal of cellular physiology* **218**:157-166.

Kachergus J, Mata IF, Hulihan M, Taylor JP, Lincoln S, Aasly J, Gibson JM, Ross OA, Lynch T, Wiley J, Payami H, Nutt J, Maraganore DM, Czyzewski K, Styczynska M, Wszolek ZK, Farrer MJ and Toft M (2005) Identification of a novel LRRK2 mutation linked to autosomal dominant parkinsonism: evidence of a common founder across European populations. *American journal of human genetics* **76**:672-680.

Kamikawaji S, Ito G and Iwatsubo T (2009) Identification of the autophosphorylation sites of LRRK2. *Biochemistry* **48**:10963-10975.

Kamikawaji S, Ito G, Sano T and Iwatsubo T (2013) Differential effects of familial parkinson mutations in LRRK2 revealed by a systematic analysis of autophosphorylation. *Biochemistry* **52**:6052-6062.

Kawakami F, Yabata T, Ohta E, Maekawa T, Shimada N, Suzuki M, Maruyama H, Ichikawa T and Obata F (2012) LRRK2 phosphorylates tubulin-associated tau but not the free molecule: LRRK2-mediated regulation of the tau-tubulin association and neurite outgrowth. *PloS one* **7**:e30834.

Kehr J (1993) A survey on quantitative microdialysis: theoretical models and practical implications. *Journal of neuroscience methods* **48**:251-261.

Kett LR, Boassa D, Ho CC, Rideout HJ, Hu J, Terada M, Ellisman M and Dauer WT (2012) LRRK2 Parkinson disease mutations enhance its microtubule association. *Human molecular genetics* **21**:890-899.

Kirik D, Rosenblad C and Bjorklund A (1998) Characterization of behavioral and neurodegenerative changes following partial lesions of the nigrostriatal dopamine system induced by intrastriatal 6-hydroxydopamine in the rat. *Experimental neurology* **152**:259-277.

Kordower JH (2015) Gene therapy for Parkinson's disease: still a hot topic? *Neuropsychopharmacology : official publication of the American College of Neuropsychopharmacology* **40**:255-256.

Kuschinsky K and Hornykiewicz O (1972) Morphine catalepsy in the rat: relation to striatal dopamine metabolism. *European journal of pharmacology* **19**:119-122.

Lam HA, Wu N, Cely I, Kelly RL, Hean S, Richter F, Magen I, Cepeda C, Ackerson LC, Walwyn W, Masliah E, Chesselet MF, Levine MS and Maidment NT (2011) Elevated tonic extracellular dopamine concentration and altered dopamine modulation of synaptic activity precede dopamine loss in the striatum of mice overexpressing human alpha-synuclein. *Journal of neuroscience research* **89**:1091-1102.

Langston JW and Ballard PA, Jr. (1983) Parkinson's disease in a chemist working with 1-methyl-4-phenyl-1,2,5,6-tetrahydropyridine. *The New England journal of medicine* **309**:310.

Law BM, Spain VA, Leinster VH, Chia R, Beilina A, Cho HJ, Taymans JM, Urban MK, Sancho RM, Blanca Ramirez M, Biskup S, Baekelandt V, Cai H, Cookson MR, Berwick DC and Harvey K (2014) A direct interaction between leucine-rich repeat kinase 2 and specific beta-tubulin isoforms regulates tubulin acetylation. *The Journal of biological chemistry* **289**:895-908.

Lee BD, Dawson VL and Dawson TM (2012a) Leucine-rich repeat kinase 2 (LRRK2) as a potential therapeutic target in Parkinson's disease. *Trends in pharmacological sciences* **33**:365-373.

Lee S, Imai Y, Gehrke S, Liu S and Lu B (2012b) The synaptic function of LRRK2. *Biochemical Society transactions* **40**:1047-1051.

Lees AJ (2009) The Parkinson chimera. *Neurology* **72**:S2-11.

Lesage S, Belarbi S, Troiano A, Condroyer C, Hecham N, Pollak P, Lohman E, Benhassine T, Ysmail-Dahlouk F, Durr A, Tazir M, Brice A and French Parkinson's Disease Genetics Study G (2008) Is the common LRRK2 G2019S mutation related to dyskinesias in North African Parkinson disease? *Neurology* **71**:1550-1552.

Lesage S and Brice A (2012) Role of mendelian genes in "sporadic" Parkinson's disease. *Parkinsonism & related disorders* **18 Suppl 1**:S66-70.

Leung IW and Lassam N (2001) The kinase activation loop is the key to mixed lineage kinase-3 activation via both autophosphorylation and hematopoietic progenitor kinase 1 phosphorylation. *The Journal of biological chemistry* **276**:1961-1967.

Lewis PA, Greggio E, Beilina A, Jain S, Baker A and Cookson MR (2007) The R1441C mutation of LRRK2 disrupts GTP hydrolysis. *Biochemical and biophysical research communications* **357**:668-671.

Li C and Beal MF (2005) Leucine-rich repeat kinase 2: a new player with a familiar theme for Parkinson's disease pathogenesis. *Proceedings of the National Academy of Sciences of the United States of America* **102**:16535-16536.

Li JQ, Tan L and Yu JT (2014) The role of the LRRK2 gene in Parkinsonism. *Molecular neurodegeneration* **9**:47.

Li X, Patel JC, Wang J, Avshalumov MV, Nicholson C, Buxbaum JD, Elder GA, Rice ME and Yue Z (2010) Enhanced striatal dopamine transmission and motor performance with LRRK2 overexpression in mice is eliminated by familial Parkinson's disease mutation G2019S. *The Journal of neuroscience : the official journal of the Society for Neuroscience* **30**:1788-1797.

Li X, Tan YC, Poulose S, Olanow CW, Huang XY and Yue Z (2007) Leucine-rich repeat kinase 2 (LRRK2)/PARK8 possesses GTPase activity that is altered in familial Parkinson's disease R1441C/G mutants. *Journal of neurochemistry* **103**:238-247.

Li X, Wang QJ, Pan N, Lee S, Zhao Y, Chait BT and Yue Z (2011) Phosphorylation-dependent 14-3-3 binding to LRRK2 is impaired by common mutations of familial Parkinson's disease. *PloS one* **6**:e17153.

Liao J, Wu CX, Burlak C, Zhang S, Sahm H, Wang M, Zhang ZY, Vogel KW, Federici M, Riddle SM, Nichols RJ, Liu D, Cookson MR, Stone TA and Hoang QQ (2014) Parkinson disease-associated mutation R1441H in LRRK2 prolongs the "active state" of its GTPase domain. *Proceedings of the National Academy of Sciences of the United States of America* **111**:4055-4060.

Lin X, Parisiadou L, Gu XL, Wang L, Shim H, Sun L, Xie C, Long CX, Yang WJ, Ding J, Chen ZZ, Gallant PE, Tao-Cheng JH, Rudow G, Troncoso JC, Liu Z, Li Z and Cai H (2009) Leucine-rich repeat kinase 2 regulates the progression of neuropathology induced by Parkinson's-disease-related mutant alpha-synuclein. *Neuron* **64**:807-827.

Liou AK, Leak RK, Li L and Zigmond MJ (2008) Wild-type LRRK2 but not its mutant attenuates stress-induced cell death via ERK pathway. *Neurobiology of disease* **32**:116-124.

Mabrouk OS, Marti M and Morari M (2010) Endogenous nociceptin/orphanin FQ (N/OFQ) contributes to haloperidol-induced changes of nigral amino acid transmission and parkinsonism: a combined microdialysis and behavioral study in naive and nociceptin/orphanin FQ receptor knockout mice. *Neuroscience* **166**:40-48.

Maekawa T, Mori S, Sasaki Y, Miyajima T, Azuma S, Ohta E and Obata F (2012) The I2020T Leucine-rich repeat kinase 2 transgenic mouse exhibits impaired locomotive ability accompanied by dopaminergic neuron abnormalities. *Molecular neurodegeneration* **7**:15.

Maj J, Rogoz Z, Skuza G and Kolodziejczyk K (1997) The behavioural effects of pramipexole, a novel dopamine receptor agonist. *European journal of pharmacology* **324**:31-37.

Mandemakers W, Snellinx A, O'Neill MJ and de Strooper B (2012) LRRK2 expression is enriched in the striosomal compartment of mouse striatum. *Neurobiology of disease* **48**:582-593.

Manning G, Plowman GD, Hunter T and Sudarsanam S (2002) Evolution of protein kinase signaling from yeast to man. *Trends in biochemical sciences* **27**:514-520.

Marchitti SA, Deitrich RA and Vasiliou V (2007) Neurotoxicity and metabolism of the catecholamine-derived 3,4-dihydroxyphenylacetaldehyde and 3,4-dihydroxyphenylglycolaldehyde: the role of aldehyde dehydrogenase. *Pharmacological reviews* **59**:125-150.

Marcotte EM, Pellegrini M, Ng HL, Rice DW, Yeates TO and Eisenberg D (1999) Detecting protein function and protein-protein interactions from genome sequences. *Science* **285**:751-753.

Marin I (2006) The Parkinson disease gene LRRK2: evolutionary and structural insights. *Molecular biology and evolution* **23**:2423-2433.

Marin I (2008) Ancient origin of the Parkinson disease gene LRRK2. *Journal of molecular evolution* **67**:41-50.

Marti-Masso JF, Ruiz-Martinez J, Bolano MJ, Ruiz I, Gorostidi A, Moreno F, Ferrer I and Lopez de Munain A (2009) Neuropathology of Parkinson's disease with the R1441G mutation in LRRK2. *Movement disorders : official journal of the Movement Disorder Society* **24**:1998-2001.

Marti M, Mela F, Fantin M, Zucchini S, Brown JM, Witta J, Di Benedetto M, Buzas B, Reinscheid RK, Salvadori S, Guerrini R, Romualdi P, Candeletti S, Simonato M, Cox BM and Morari M (2005) Blockade of nociceptin/orphanin FQ transmission attenuates symptoms and neurodegeneration associated with Parkinson's disease. *The Journal of neuroscience : the official journal of the Society for Neuroscience* **25**:9591-9601.

Marti M, Mela F, Veronesi C, Guerrini R, Salvadori S, Federici M, Mercuri NB, Rizzi A, Franchi G, Beani L, Bianchi C and Morari M (2004) Blockade of nociceptin/orphanin FQ receptor signaling in rat substantia nigra pars reticulata stimulates nigrostriatal dopaminergic transmission and motor behavior. *The Journal of neuroscience : the official journal of the Society for Neuroscience* **24**:6659-6666.

Mata IF, Ross OA, Kachergus J, Huerta C, Ribacoba R, Moris G, Blazquez M, Guisasola LM, Salvador C, Martinez C, Farrer M and Alvarez V (2006) LRRK2 mutations are a common cause of Parkinson's disease in Spain. *European journal of neurology : the official journal of the European Federation of Neurological Societies* **13**:391-394.

Matta S, Van Kolen K, da Cunha R, van den Bogaart G, Mandemakers W, Miskiewicz K, De Bock PJ, Morais VA, Vilain S, Haddad D, Delbroek L, Swerts J, Chavez-Gutierrez L, Esposito G, Daneels G, Karran E, Holt M, Gevaert K, Moechars DW, De Strooper B and Verstreken P (2012) LRRK2 controls an EndoA phosphorylation cycle in synaptic endocytosis. *Neuron* **75**:1008-1021.

McNaught KS and Olanow CW (2006) Protein aggregation in the pathogenesis of familial and sporadic Parkinson's disease. *Neurobiology of aging* **27**:530-545.

Meixner A, Boldt K, Van Troys M, Askenazi M, Gloeckner CJ, Bauer M, Marto JA, Ampe C, Kinkl N and Ueffing M (2011) A QUICK screen for Lrrk2 interaction partners--leucine-rich repeat kinase 2 is involved in actin cytoskeleton dynamics. *Molecular & cellular proteomics : MCP* **10**:M110 001172.

Melrose H, Lincoln S, Tyndall G, Dickson D and Farrer M (2006) Anatomical localization of leucine-rich repeat kinase 2 in mouse brain. *Neuroscience* **139**:791-794.

Melrose HL, Dachsel JC, Behrouz B, Lincoln SJ, Yue M, Hinkle KM, Kent CB, Korvatska E, Taylor JP, Witten L, Liang YQ, Beevers JE, Boules M, Dugger BN, Serna VA, Gaukhman A, Yu X, Castanedes-Casey M, Braithwaite AT, Ogholikhan S, Yu N, Bass D, Tyndall G, Schellenberg GD, Dickson DW, Janus C and Farrer MJ (2010) Impaired dopaminergic neurotransmission and microtubule-associated protein tau alterations in human LRRK2 transgenic mice. *Neurobiology of disease* **40**:503-517.

Melrose HL, Kent CB, Taylor JP, Dachsel JC, Hinkle KM, Lincoln SJ, Mok SS, Culvenor JG, Masters CL, Tyndall GM, Bass DI, Ahmed Z, Andorfer CA, Ross OA, Wszolek ZK, Delldonne A, Dickson DW and Farrer MJ (2007) A comparative analysis of leucine-rich repeat kinase 2 (Lrrk2) expression in mouse brain and Lewy body disease. *Neuroscience* **147**:1047-1058.

Mierau J and Schingnitz G (1992) Biochemical and pharmacological studies on pramipexole, a potent and selective dopamine D2 receptor agonist. *European journal of pharmacology* **215**:161-170.

Migheli R, Del Giudice MG, Spissu Y, Sanna G, Xiong Y, Dawson TM, Dawson VL, Galioto M, Rocchitta G, Biosa A, Serra PA, Carri MT, Crosio C and Iaccarino C (2013) LRRK2 affects vesicle trafficking, neurotransmitter extracellular level and membrane receptor localization. *PloS one* **8**:e77198.

Mills RD, Mulhern TD, Cheng HC and Culvenor JG (2012) Analysis of LRRK2 accessory repeat domains: prediction of repeat length, number and sites of Parkinson's disease mutations. *Biochemical Society transactions* **40**:1086-1089.

Mittermeyer G, Christine CW, Rosenbluth KH, Baker SL, Starr P, Larson P, Kaplan PL, Forsayeth J, Aminoff MJ and Bankiewicz KS (2012) Long-term evaluation of a phase 1 study of AADC gene therapy for Parkinson's disease. *Human gene therapy* **23**:377-381.

Moore DJ, Zhang L, Dawson TM and Dawson VL (2003) A missense mutation (L166P) in DJ-1, linked to familial Parkinson's disease, confers reduced protein stability and impairs homo-oligomerization. *Journal of neurochemistry* **87**:1558-1567.

Mortiboys H, Johansen KK, Aasly JO and Bandmann O (2010) Mitochondrial impairment in patients with Parkinson disease with the G2019S mutation in LRRK2. *Neurology* **75**:2017-2020.

Muda K, Bertinetti D, Gesellchen F, Hermann JS, von Zweydorf F, Geerlof A, Jacob A, Ueffing M, Gloeckner CJ and Herberg FW (2014) Parkinson-related LRRK2 mutation R1441C/G/H impairs PKA phosphorylation of LRRK2 and disrupts its interaction with 14-3-3. *Proceedings of the National Academy of Sciences of the United States of America* **111**:E34-43.

Muramatsu S (2010) [Gene therapy for Parkinson disease]. *Nihon rinsho Japanese journal of clinical medicine* **68 Suppl 8**:646-649.

Nandhagopal R, Mak E, Schulzer M, McKenzie J, McCormick S, Sossi V, Ruth TJ, Strongosky A, Farrer MJ, Wszolek ZK and Stoessl AJ (2008) Progression of dopaminergic dysfunction in a LRRK2 kindred: a multitracer PET study. *Neurology* **71**:1790-1795.

Ng CH, Mok SZ, Koh C, Ouyang X, Fivaz ML, Tan EK, Dawson VL, Dawson TM, Yu F and Lim KL (2009) Parkin protects against LRRK2 G2019S mutant-induced dopaminergic neurodegeneration in Drosophila. *The Journal of neuroscience : the official journal of the Society for Neuroscience* **29**:11257-11262.

Nichols RJ, Dzamko N, Hutti JE, Cantley LC, Deak M, Moran J, Bamborough P, Reith AD and Alessi DR (2009) Substrate specificity and inhibitors of LRRK2, a protein kinase mutated in Parkinson's disease. *The Biochemical journal* **424**:47-60.

Nichols RJ, Dzamko N, Morrice NA, Campbell DG, Deak M, Ordureau A, Macartney T, Tong Y, Shen J, Prescott AR and Alessi DR (2010) 14-3-3 binding to LRRK2 is disrupted by multiple Parkinson's disease-associated mutations and regulates cytoplasmic localization. *The Biochemical journal* **430**:393-404.

Nijhawan SR, Banks SJ, Aziz TZ, Panourias I, Gregory R, Yianni J, Parkin S, Joint C and Scott RB (2009) Changes in cognition and health-related quality of life with unilateral thalamotomy for Parkinsonian tremor. *Journal of clinical neuroscience : official journal of the Neurosurgical Society of Australasia* **16**:44-50.

Niu J, Yu M, Wang C and Xu Z (2012) Leucine-rich repeat kinase 2 disturbs mitochondrial dynamics via Dynamin-like protein. *Journal of neurochemistry* **122**:650-658.

Odekerken VJ, van Laar T, Staal MJ, Mosch A, Hoffmann CF, Nijssen PC, Beute GN, van Vugt JP, Lenders MW, Contarino MF, Mink MS, Bour LJ, van den Munckhof P, Schmand BA, de Haan RJ, Schuurman PR and de Bie RM (2013) Subthalamic nucleus versus globus pallidus bilateral deep brain stimulation for advanced Parkinson's disease (NSTAPS study): a randomised controlled trial. *The Lancet Neurology* **12**:37-44.

Ohren JF, Chen H, Pavlovsky A, Whitehead C, Zhang E, Kuffa P, Yan C, McConnell P, Spessard C, Banotai C, Mueller WT, Delaney A, Omer C, Sebolt-Leopold J, Dudley DT, Leung IK, Flamme C, Warmus J, Kaufman M, Barrett S, Tecle H and Hasemann CA (2004) Structures of human MAP kinase kinase 1 (MEK1) and MEK2 describe novel noncompetitive kinase inhibition. *Nature structural & molecular biology* **11**:1192-1197.

Okun MS and Vitek JL (2004) Lesion therapy for Parkinson's disease and other movement disorders: update and controversies. *Movement disorders : official journal of the Movement Disorder Society* **19**:375-389.

Olanow CW and Brundin P (2013) Parkinson's disease and alpha synuclein: is Parkinson's disease a prion-like disorder? *Movement disorders : official journal of the Movement Disorder Society* **28**:31-40.

Paisan-Ruiz C (2009) LRRK2 gene variation and its contribution to Parkinson disease. *Human mutation* **30**:1153-1160.

Paisan-Ruiz C, Jain S, Evans EW, Gilks WP, Simon J, van der Brug M, Lopez de Munain A, Aparicio S, Gil AM, Khan N, Johnson J, Martinez JR, Nicholl D, Carrera IM, Pena AS, de Silva R, Lees A, Marti-Masso JF, Perez-Tur J, Wood NW and Singleton AB (2004) Cloning of the gene containing mutations that cause PARK8-linked Parkinson's disease. *Neuron* **44**:595-600.

Paisan-Ruiz C, Lewis PA and Singleton AB (2013) LRRK2: cause, risk, and mechanism. *Journal of Parkinson's disease* **3**:85-103.

Paisan-Ruiz C, Nath P, Wood NW, Singleton A and Houlden H (2008) Clinical heterogeneity and genotype-phenotype correlations in hereditary spastic paraplegia because of Spatacsin mutations (SPG11). *European journal of neurology : the official journal of the European Federation of Neurological Societies* **15**:1065-1070.

Palfi S, Gurruchaga JM, Ralph GS, Lepetit H, Lavisse S, Buttery PC, Watts C, Miskin J, Kelleher M, Deeley S, Iwamuro H, Lefaucheur JP, Thiriez C, Fenelon G, Lucas C, Brugieres P, Gabriel I, Abhay K, Drouot X, Tani N, Kas A, Ghaleb B, Le Corvoisier P, Dolphin P, Breen DP, Mason S, Guzman NV, Mazarakis ND, Radcliffe PA, Harrop R, Kingsman SM, Rascol O, Naylor S, Barker RA, Hantraye P, Remy P, Cesaro P and Mitrophanous KA (2014) Long-term safety and tolerability of ProSavin, a lentiviral vector-based gene therapy for Parkinson's disease: a dose escalation, open-label, phase 1/2 trial. *Lancet* **383**:1138-1146.

Papkovskaia TD, Chau KY, Inesta-Vaquera F, Papkovsky DB, Healy DG, Nishio K, Staddon J, Duchen MR, Hardy J, Schapira AH and Cooper JM (2012) G2019S leucine-rich repeat kinase 2 causes uncoupling protein-mediated mitochondrial depolarization. *Human molecular genetics* **21**:4201-4213.

Parisiadou L, Xie C, Cho HJ, Lin X, Gu XL, Long CX, Lobbestael E, Baekelandt V, Taymans JM, Sun L and Cai H (2009) Phosphorylation of ezrin/radixin/moesin proteins by LRRK2 promotes the rearrangement of actin cytoskeleton in neuronal morphogenesis. *The Journal of neuroscience : the official journal of the Society for Neuroscience* **29**:13971-13980.

Parisiadou L, Yu J, Sgobio C, Xie C, Liu G, Sun L, Gu XL, Lin X, Crowley NA, Lovinger DM and Cai H (2014) LRRK2 regulates synaptogenesis and dopamine receptor activation through modulation of PKA activity. *Nature neuroscience* **17**:367-376.

Park J, Lee G and Chung J (2009) The PINK1-Parkin pathway is involved in the regulation of mitochondrial remodeling process. *Biochemical and biophysical research communications* **378**:518-523.

Paus M, Kohl Z, Ben Abdallah NM, Galter D, Gillardon F and Winkler J (2013) Enhanced dendritogenesis and axogenesis in hippocampal neuroblasts of LRRK2 knockout mice. *Brain research* **1497**:85-100.

Periquet M, Lucking C, Vaughan J, Bonifati V, Durr A, De Michele G, Horstink M, Farrer M, Illarioshkin SN, Pollak P, Borg M, Brefel-Courbon C, Denefle P, Meco G, Gasser T, Breteler MM, Wood N, Agid Y, Brice A and French Parkinson's Disease Genetics Study Group. The European Consortium on Genetic Susceptibility in Parkinson's D (2001) Origin of the mutations in the parkin gene in Europe: exon rearrangements are independent recurrent events, whereas point mutations may result from Founder effects. *American journal of human genetics* **68**:617-626.

Piccoli G, Condliffe SB, Bauer M, Giesert F, Boldt K, De Astis S, Meixner A, Sarioglu H, Vogt-Weisenhorn DM, Wurst W, Gloeckner CJ, Matteoli M, Sala C and Ueffing M (2011) LRRK2 controls synaptic vesicle storage and mobilization within the recycling pool. *The Journal of neuroscience : the official journal of the Society for Neuroscience* **31**:2225-2237.

Polymeropoulos MH, Lavedan C, Leroy E, Ide SE, Dehejia A, Dutra A, Pike B, Root H, Rubenstein J, Boyer R, Stenroos ES, Chandrasekharappa S, Athanassiadou A, Papapetropoulos T, Johnson WG, Lazzarini AM, Duvoisin RC, Di Iorio G, Golbe LI and Nussbaum RL (1997) Mutation in the alpha-synuclein gene identified in families with Parkinson's disease. *Science* **276**:2045-2047.

Pountney DL, Voelcker NH and Gai WP (2005) Annular alpha-synuclein oligomers are potentially toxic agents in alpha-synucleinopathy. Hypothesis. *Neurotoxicity research* **7**:59-67.

Pungaliya PP, Bai Y, Lipinski K, Anand VS, Sen S, Brown EL, Bates B, Reinhart PH, West AB, Hirst WD and Braithwaite SP (2010) Identification and characterization of a leucine-rich repeat kinase 2 (LRRK2) consensus phosphorylation motif. *PloS one* **5**:e13672.

Rajput A, Dickson DW, Robinson CA, Ross OA, Dachsel JC, Lincoln SJ, Cobb SA, Rajput ML and Farrer MJ (2006) Parkinsonism, Lrrk2 G2019S, and tau neuropathology. *Neurology* **67**:1506-1508.

Ramirez-Valle F, Braunstein S, Zavadil J, Formenti SC and Schneider RJ (2008) eIF4GI links nutrient sensing by mTOR to cell proliferation and inhibition of autophagy. *The Journal of cell biology* **181**:293-307.

Ramonet D, Daher JP, Lin BM, Stafa K, Kim J, Banerjee R, Westerlund M, Pletnikova O, Glauser L, Yang L, Liu Y, Swing DA, Beal MF, Troncoso JC, McCaffery JM, Jenkins NA, Copeland NG, Galter D, Thomas B, Lee MK, Dawson TM, Dawson VL and Moore DJ (2011) Dopaminergic neuronal loss, reduced neurite complexity and autophagic abnormalities in transgenic mice expressing G2019S mutant LRRK2. *PloS one* **6**:e18568.

Rascol O, Brooks DJ, Melamed E, Oertel W, Poewe W, Stocchi F, Tolosa E and group Ls (2005) Rasagiline as an adjunct to levodopa in patients with Parkinson's disease and motor fluctuations (LARGO, Lasting effect in Adjunct therapy with Rasagiline Given Once daily, study): a randomised, double-blind, parallel-group trial. *Lancet* **365**:947-954.

Rizzi A, Vergura R, Marzola G, Ruzza C, Guerrini R, Salvadori S, Regoli D and Calo G (2008) Neuropeptide S is a stimulatory anxiolytic agent: a behavioural study in mice. *British journal of pharmacology* **154**:471-479.

Ross OA, Cook C and Petrucelli L (2015) Linking the VPS35 and EIF4G1 Pathways in Parkinson's Disease. *Neuron* **85**:1-3.

Rozas G, Guerra MJ and Labandeira-Garcia JL (1997) An automated rotarod method for quantitative drug-free evaluation of overall motor deficits in rat models of parkinsonism. *Brain research Brain research protocols* **2**:75-84.

Rubio JP, Topp S, Warren L, St Jean PL, Wegmann D, Kessner D, Novembre J, Shen J, Fraser D, Aponte J, Nangle K, Cardon LR, Ehm MG, Chissoe SL, Whittaker JC, Nelson MR and Mooser VE (2012) Deep sequencing of the LRRK2 gene in 14,002 individuals reveals evidence of purifying selection and independent origin of the p.Arg1628Pro mutation in Europe. *Human mutation* **33**:1087-1098.

Rudenko IN, Chia R and Cookson MR (2012) Is inhibition of kinase activity the only therapeutic strategy for LRRK2-associated Parkinson's disease? *BMC medicine* **10**:20.

Ruffmann C, Giaccone G, Canesi M, Bramerio M, Goldwurm S, Gambacorta M, Rossi G, Tagliavini F and Pezzoli G (2012) Atypical tauopathy in a patient with LRRK2-G2019S mutation and tremor-dominant Parkinsonism. *Neuropathology and applied neurobiology* **38**:382-386.

San Luciano M, Lipton RB, Wang C, Katz M, Zimmerman ME, Sanders AE, Ozelius LJ, Bressman SB and Saunders-Pullman R (2010) Clinical expression of LRRK2 G2019S mutations in the elderly. *Movement disorders : official journal of the Movement Disorder Society* **25**:2571-2576.

Sanberg PR, Bunsey MD, Giordano M and Norman AB (1988) The catalepsy test: its ups and downs. *Behavioral neuroscience* **102**:748-759.

Sancho RM, Law BM and Harvey K (2009) Mutations in the LRRK2 Roc-COR tandem domain link Parkinson's disease to Wnt signalling pathways. *Human molecular genetics* **18**:3955-3968.

Santini E, Heiman M, Greengard P, Valjent E and Fisone G (2009) Inhibition of mTOR signaling in Parkinson's disease prevents L-DOPA-induced dyskinesia. *Science signaling* **2**:ra36.

Sasaki Y, Suzuki M and Hidaka H (2002) The novel and specific Rho-kinase inhibitor (S)-(+)-2-methyl-1-[(4-methyl-5-isoquinoline)sulfonyl]-homopiperazine as a probing molecule for Rho-kinase-involved pathway. *Pharmacology & therapeutics* **93**:225-232.

Satake W, Nakabayashi Y, Mizuta I, Hirota Y, Ito C, Kubo M, Kawaguchi T, Tsunoda T, Watanabe M, Takeda A, Tomiyama H, Nakashima K, Hasegawa K, Obata F, Yoshikawa T, Kawakami H, Sakoda S, Yamamoto M, Hattori N, Murata M, Nakamura Y and Toda T (2009) Genome-wide association study identifies common variants at four loci as genetic risk factors for Parkinson's disease. *Nature genetics* **41**:1303-1307.

Schallert T, De Ryck M, Whishaw IQ, Ramirez VD and Teitelbaum P (1979) Excessive bracing reactions and their control by atropine and L-DOPA in an animal analog of Parkinsonism. *Experimental neurology* **64**:33-43.

Seeman P (2007) Antiparkinson therapeutic potencies correlate with their affinities at dopamine D2(High) receptors. *Synapse* **61**:1013-1018.

Sharma S, Bandopadhyay R, Lashley T, Renton AE, Kingsbury AE, Kumaran R, Kallis C, Vilarino-Guell C, O'Sullivan SS, Lees AJ, Revesz T, Wood NW and Holton JL (2011) LRRK2 expression in idiopathic and G2019S positive Parkinson's disease subjects: a morphological and quantitative study. *Neuropathology and applied neurobiology* **37**:777-790.

Sheng Z, Zhang S, Bustos D, Kleinheinz T, Le Pichon CE, Dominguez SL, Solanoy HO, Drummond J, Zhang X, Ding X, Cai F, Song Q, Li X, Yue Z, van der Brug MP, Burdick DJ, Gunzner-Toste J, Chen H, Liu X, Estrada AA, Sweeney ZK, Scearce-Levie K, Moffat JG, Kirkpatrick DS and Zhu H (2012) Ser1292 autophosphorylation is an indicator of LRRK2 kinase activity and contributes to the cellular effects of PD mutations. *Science translational medicine* **4**:164ra161.

Shimura H, Hattori N, Kubo S, Mizuno Y, Asakawa S, Minoshima S, Shimizu N, Iwai K, Chiba T, Tanaka K and Suzuki T (2000) Familial Parkinson disease gene product, parkin, is a ubiquitin-protein ligase. *Nature genetics* **25**:302-305.

Shin N, Jeong H, Kwon J, Heo HY, Kwon JJ, Yun HJ, Kim CH, Han BS, Tong Y, Shen J, Hatano T, Hattori N, Kim KS, Chang S and Seol W (2008) LRRK2 regulates synaptic vesicle endocytosis. *Experimental cell research* **314**:2055-2065.

Siuciak JA and Fujiwara RA (2004) The activity of pramipexole in the mouse forced swim test is mediated by D2 rather than D3 receptors. *Psychopharmacology* **175**:163-169.

Skibinski G, Nakamura K, Cookson MR and Finkbeiner S (2014) Mutant LRRK2 toxicity in neurons depends on LRRK2 levels and synuclein but not kinase activity or inclusion bodies. *The Journal of neuroscience : the official journal of the Society for Neuroscience* **34**:418-433.

Smith WW, Pei Z, Jiang H, Moore DJ, Liang Y, West AB, Dawson VL, Dawson TM and Ross CA (2005) Leucine-rich repeat kinase 2 (LRRK2) interacts with parkin, and mutant LRRK2 induces neuronal degeneration. *Proceedings of the National Academy of Sciences of the United States of America* **102**:18676-18681.

Snead D and Eliezer D (2014) Alpha-synuclein function and dysfunction on cellular membranes. *Experimental neurobiology* **23**:292-313.

Song P, Mabrouk OS, Hershey ND and Kennedy RT (2012) In vivo neurochemical monitoring using benzoyl chloride derivatization and liquid chromatography-mass spectrometry. *Analytical chemistry* **84**:412-419.

Sossi V, de la Fuente-Fernandez R, Nandhagopal R, Schulzer M, McKenzie J, Ruth TJ, Aasly JO, Farrer MJ, Wszolek ZK and Stoessl JA (2010) Dopamine turnover increases in asymptomatic LRRK2 mutations carriers. *Movement disorders : official journal of the Movement Disorder Society* **25**:2717-2723.

Spillantini MG, Schmidt ML, Lee VM, Trojanowski JQ, Jakes R and Goedert M (1997) Alpha-synuclein in Lewy bodies. *Nature* **388**:839-840.

Tain LS, Chowdhury RB, Tao RN, Plun-Favreau H, Moisoi N, Martins LM, Downward J, Whitworth AJ and Tapon N (2009) Drosophila HtrA2 is dispensable for apoptosis but acts downstream of PINK1 independently from Parkin. *Cell death and differentiation* **16**:1118-1125.

Tamura M, Nakao H, Yoshizaki H, Shiratsuchi M, Shigyo H, Yamada H, Ozawa T, Totsuka J and Hidaka H (2005) Development of specific Rho-kinase inhibitors and their clinical application. *Biochimica et biophysica acta* **1754**:245-252.

Tan EK, Zhao Y, Skipper L, Tan MG, Di Fonzo A, Sun L, Fook-Chong S, Tang S, Chua E, Yuen Y, Tan L, Pavanni R, Wong MC, Kolatkar P, Lu CS, Bonifati V and Liu JJ (2007) The LRRK2 Gly2385Arg variant is associated with Parkinson's disease: genetic and functional evidence. *Human genetics* **120**:857-863.

Taymans JM and Cookson MR (2010) Mechanisms in dominant parkinsonism: The toxic triangle of LRRK2, alpha-synuclein, and tau. *BioEssays : news and reviews in molecular, cellular and developmental biology* **32**:227-235.

Thaler A, Posen J, Giladi N, Manor Y, Mayanz C, Mirelman A and Gurevich T (2012) Appreciation of humor is decreased among patients with Parkinson's disease. *Parkinsonism & related disorders* **18**:144-148.

Tong Y, Giaime E, Yamaguchi H, Ichimura T, Liu Y, Si H, Cai H, Bonventre JV and Shen J (2012) Loss of leucine-rich repeat kinase 2 causes age-dependent bi-phasic alterations of the autophagy pathway. *Molecular neurodegeneration* **7**:2.

Tong Y, Pisani A, Martella G, Karouani M, Yamaguchi H, Pothos EN and Shen J (2009) R1441C mutation in LRRK2 impairs dopaminergic neurotransmission in mice. *Proceedings of the National Academy of Sciences of the United States of America* **106**:14622-14627.

Tong Y, Yamaguchi H, Giaime E, Boyle S, Kopan R, Kelleher RJ, 3rd and Shen J (2010) Loss of leucine-rich repeat kinase 2 causes impairment of protein degradation pathways, accumulation of alpha-synuclein, and apoptotic cell death in aged mice. *Proceedings of the National Academy of Sciences of the United States of America* **107**:9879-9884.

Tozzi A, de Iure A, Di Filippo M, Tantucci M, Costa C, Borsini F, Ghiglieri V, Giampa C, Fusco FR, Picconi B and Calabresi P (2011) The distinct role of medium spiny neurons and cholinergic interneurons in the D(2)/A(2)A receptor interaction in the striatum:

implications for Parkinson's disease. *The Journal of neuroscience : the official journal of the Society for Neuroscience* **31**:1850-1862.

Trinh J and Farrer M (2013) Advances in the genetics of Parkinson disease. *Nature reviews Neurology* **9**:445-454.

Trinh J, Guella I and Farrer MJ (2014) Disease Penetrance of Late-Onset Parkinsonism: A Meta-analysis. *JAMA neurology* **71**:1535-1539.

Troxler T, Greenidge P, Zimmermann K, Desrayaud S, Druckes P, Schweizer T, Stauffer D, Rovelli G and Shimshek DR (2013) Discovery of novel indolinone-based, potent, selective and brain penetrant inhibitors of LRRK2. *Bioorganic & medicinal chemistry letters* **23**:4085-4090.

Ujiie S, Hatano T, Kubo S, Imai S, Sato S, Uchihara T, Yagishita S, Hasegawa K, Kowa H, Sakai F and Hattori N (2012) LRRK2 I2020T mutation is associated with tau pathology. *Parkinsonism & related disorders* **18**:819-823.

Ungerstedt U, Ljungberg T and Steg G (1974) Behavioral, physiological, and neurochemical changes after 6-hydroxydopamine-induced degeneration of the nigro-striatal dopamine neurons. *Advances in neurology* **5**:421-426.

Valente EM, Abou-Sleiman PM, Caputo V, Muqit MM, Harvey K, Gispert S, Ali Z, Del Turco D, Bentivoglio AR, Healy DG, Albanese A, Nussbaum R, Gonzalez-Maldonado R, Deller T, Salvi S, Cortelli P, Gilks WP, Latchman DS, Harvey RJ, Dallapiccola B, Auburger G and Wood NW (2004a) Hereditary early-onset Parkinson's disease caused by mutations in PINK1. *Science* **304**:1158-1160.

Valente EM, Salvi S, Ialongo T, Marongiu R, Elia AE, Caputo V, Romito L, Albanese A, Dallapiccola B and Bentivoglio AR (2004b) PINK1 mutations are associated with sporadic early-onset parkinsonism. *Annals of neurology* **56**:336-341.

Viaro R, Calcagno M, Marti M, Borrelli E and Morari M (2013) Pharmacological and genetic evidence for pre- and postsynaptic D2 receptor involvement in motor responses to nociceptin/orphanin FQ receptor ligands. *Neuropharmacology* **72**:126-138.

Viaro R, Sanchez-Pernaute R, Marti M, Trapella C, Isacson O and Morari M (2008) Nociceptin/orphanin FQ receptor blockade attenuates MPTP-induced parkinsonism. *Neurobiology of disease* **30**:430-438.

Volta M, Mabrouk OS, Bido S, Marti M and Morari M (2010) Further evidence for an involvement of nociceptin/orphanin FQ in the pathophysiology of Parkinson's disease: a behavioral and neurochemical study in reserpinized mice. *Journal of neurochemistry* **115**:1543-1555.

Wang L, Xie C, Greggio E, Parisiadou L, Shim H, Sun L, Chandran J, Lin X, Lai C, Yang WJ, Moore DJ, Dawson TM, Dawson VL, Chiosis G, Cookson MR and Cai H (2008) The chaperone activity of heat shock protein 90 is critical for maintaining the stability of leucine-rich repeat kinase 2. *The Journal of neuroscience : the official journal of the Society for Neuroscience* **28**:3384-3391.

Weintraub D, Comella CL and Horn S (2008) Parkinson's disease--Part 1: Pathophysiology, symptoms, burden, diagnosis, and assessment. *The American journal of managed care* **14**:S40-48.

Weiss HD, Hirsch ES, Williams JR, Swearengin L and Marsh L (2010) Detection of impulse control disorders in Parkinson disease patients. *The neurologist* **16**:406-407.

West AB, Cowell RM, Daher JP, Moehle MS, Hinkle KM, Melrose HL, Standaert DG and Volpicelli-Daley LA (2014) Differential LRRK2 expression in the cortex, striatum, and substantia nigra in transgenic and nontransgenic rodents. *The Journal of comparative neurology* **522**:2465-2480.

West AB, Moore DJ, Biskup S, Bugayenko A, Smith WW, Ross CA, Dawson VL and Dawson TM (2005) Parkinson's disease-associated mutations in leucine-rich repeat kinase 2 augment kinase activity. *Proceedings of the National Academy of Sciences of the United States of America* **102**:16842-16847.

West AB, Moore DJ, Choi C, Andrabi SA, Li X, Dikeman D, Biskup S, Zhang Z, Lim KL, Dawson VL and Dawson TM (2007) Parkinson's disease-associated mutations in LRRK2 link enhanced GTP-binding and kinase activities to neuronal toxicity. *Human molecular genetics* **16**:223-232.

Westerink BH (1995) Brain microdialysis and its application for the study of animal behaviour. *Behavioural brain research* **70**:103-124.

Wider C, Dickson DW and Wszolek ZK (2010) Leucine-rich repeat kinase 2 gene-associated disease: redefining genotype-phenotype correlation. *Neuro-degenerative diseases* **7**:175-179.

Winner B, Melrose HL, Zhao C, Hinkle KM, Yue M, Kent C, Braithwaite AT, Ogholikhan S, Aigner R, Winkler J, Farrer MJ and Gage FH (2011) Adult neurogenesis and neurite outgrowth are impaired in LRRK2 G2019S mice. *Neurobiology of disease* **41**:706-716.

Wszolek ZK, Vieregge P, Uitti RJ, Gasser T, Yasuhara O, McGeer P, Berry K, Calne DB, Vingerhoets FJ, Klein C and Pfeiffer RF (1997) German-Canadian family (family A) with parkinsonism, amyotrophy, and dementia - Longitudinal observations. *Parkinsonism & related disorders* **3**:125-139.

Xiong Y, Dawson VL and Dawson TM (2012) LRRK2 GTPase dysfunction in the pathogenesis of Parkinson's disease. *Biochemical Society transactions* **40**:1074-1079.

Zhang Z, Burgunder JM, An X, Wu Y, Chen W, Zhang J, Wang Y, Xu Y, Gou Y, Yuan G, Mao X and Peng R (2009) LRRK2 R1628P variant is a risk factor of Parkinson's disease among Han-Chinese from mainland China. *Movement disorders : official journal of the Movement Disorder Society* **24**:1902-1905.

Zhou H, Huang C, Tong J, Hong WC, Liu YJ and Xia XG (2011) Temporal expression of mutant LRRK2 in adult rats impairs dopamine reuptake. *International journal of biological sciences* **7**:753-761.

Zhu J, Mactutus CF, Wallace DR and Booze RM (2009) HIV-1 Tat protein-induced rapid and reversible decrease in [3H]dopamine uptake: dissociation of [3H]dopamine uptake and [3H]2beta-carbomethoxy-3-beta-(4-fluorophenyl)tropane (WIN 35,428) binding in rat striatal synaptosomes. *The Journal of pharmacology and experimental therapeutics* **329**:1071-1083.

Zimprich A, Biskup S, Leitner P, Lichtner P, Farrer M, Lincoln S, Kachergus J, Hulihan M, Uitti RJ, Calne DB, Stoessl AJ, Pfeiffer RF, Patenge N, Carbajal IC, Vieregge P, Asmus F, Muller-Myhsok B, Dickson DW, Meitinger T, Strom TM, Wszolek ZK and Gasser T (2004) Mutations in LRRK2 cause autosomal-dominant parkinsonism with pleomorphic pathology. *Neuron* **44**:601-607.

ORIGINAL PAPERS

- Cristino L, Luongo L, Squillace M, Paolone G, Mango D, Piccinin S, Zianni E, Imperatore R, Iannotta M, **Longo F**, Errico F, Vescovi AL, Morari M, Maione S, Gardoni F, Nistico R, Usiello A. D-Aspartate-Oxidase influences glutamatergic system homeostasis in mammalian brain. Neurobiology of Aging 2015. *In Press, Accepted Manuscript*

- Ravani L, Sarpietro MG, Esposito E, Di Stefano A, Sozio P, Calcagno M, Drechsler M, Contado C, **Longo F**, Giuffrida MC, Castelli F, Morari M, Cortesi R. Lipid nanocarriers containing a levodopa prodrug with a potential antiparkinsonian activity. Mater Sci Eng C Mater Biol Appl. 2015 Mar;48:294-300.

- **Longo F**, Russo I, Shimshek DR, Greggio E, Morari M. Genetic and pharmacologicalevidence that G2019S LRRK2 confers a hyperkinetic phenotype, resistant to motor decline associated with aging. Neurobiol Dis. 2014 Aug 6; 71C:62-73.

- Cirnaru MD, Marte A, Belluzzi E, Russo I, Gabrielli M, **Longo F**, Arcuri L, Murru L, Bubacco L, Matteoli M, Fedele E, Sala C, Passafaro M, Morari M, Greggio E, Onofri F and Piccoli G. LRRK2 kinase activity regulates synaptic vesicle trafficking and neurotransmitter release through modulation of LRRK2 macro-molecular complex. Front Mol Neurosci. 2014 May 27; 7:49.

- Bonito-Oliva A, Pignatelli M, Spigolon G, Yoshitake T, Seiler S, **Longo F**, Piccinin S, Kehr J, Mercuri NB, Nisticò R, Fisone G. Cognitive Impairment and Dentate Gyrus Synaptic Dysfunction in Experimental Parkinsonism. Biol Psychiatry. 2013 Mar 28. PII: S0006-3223(13)00183-2. DOI: 10.1016/J.BIOPSYCH.2013.02.015.